FR 14744
JULY 1981

MECHANICAL PROPERTIES OF TURBINE BLADE ALLOYS IN HYDROGEN AT ELEVATED TEMPERATURES

FINAL REPORT

Contract NAS8-33561

Prepared for
National Aeronautics and Space Administration
George C. Marshall Space Flight Center
Huntsville, Alabama 35812

UNITED TECHNOLOGIES
PRATT & WHITNEY AIRCRAFT

GOVERNMENT PRODUCTS DIVISION
P.O. Box 2691
West Palm Beach, Florida 33402

Printed in the United States of America

FR 14844
JULY 1981

MECHANICAL PROPERTIES OF TURBINE BLADE ALLOYS IN HYDROGEN AT ELEVATED TEMPERATURES

FINAL REPORT

Contract NAS8-33561

Prepared for
National Aeronautics and Space Administration
George C. Marshall Space Flight Center
Huntsville, Alabama 35812

D. P. DeLuca
Principal Investigator

J. R. Warren
Responsible Engineer

B. A. Cowles
Program Manager

M. C. VanWanderham
Supervisor, Mechanics of
Materials and Structures

UNITED TECHNOLOGIES
PRATT&WHITNEY
AIRCRAFT

GOVERNMENT PRODUCTS DIVISION
P.O. Box 2691
West Palm Beach, Florida 33402

Printed in the United States of America

FOREWORD

This program was conducted using the Program Manager — Project Group System by the Pratt & Whitney Aircraft Group, Government Products Division, Materials and Mechanics Technology Laboratory, under the cognizance of Mr. W.B. McPherson, Metallurgy Branch, Materials & Process Laboratory, Marshall Space Flight Center. B.A. Cowles was the Pratt & Whitney Program Manager for the effort.

Acknowledgement is given to the following personnel of the Project Group.

D.P. Deluca — Principal Investigator
J.R. Warren — Responsible Engineer
B.A. Cowles — Program Manager
D.P. Shoemaker — Fatigue and Crack Growth Tests
J.R. Teel, Jr. — Tensile and Creep Rupture Tests
D.L. Pearson — Test Stand Operations
C.G. Annis, Jr. — Crack Growth Consultation
D.A. Wilson — Crack Growth Specimen Precrack
B.J. Schwartz — Crack Growth Data Assistance

CONTENTS

TABLES

TABLES (Continued)

ILLUSTRATIONS

ILLUSTRATIONS (Continued)

ILLUSTRATIONS (Continued)

ILLUSTRATIONS (Continued)

ILLUSTRATIONS (Continued)

ILLUSTRATIONS (Continued)

SECTION I
INTRODUCTION

The objective of this program was to determine the mechanical properties of single crystal (SC) MAR-M-246+Hf and single crystal PWA 1480 in a gaseous hydrogen environment at 760°C (1400°F) and 871°C (1600°F), and to complete the evaluation of directionally solidified (DS) MAR-M-246+Hf initiated under previous, related contracts (NAS8-30744, NAS8-33109). These alloys have been proposed for use in space propulsion systems in pure or partial high-pressure hydrogen environments at elevated temperatures.

Mechanical property tests included tensile, creep, low cycle fatigue (LCF), and crack growth. Specimens were oriented in both transverse and longitudinal directions relative to the casting solidification direction. All testing was conducted on solid specimens exposed to externally pressurized environments of gaseous hydrogen and hydrogen-enriched steam at a pressure of 34.5 MPa (5000 psig).

Tensile and creep rupture properties were determined using standard ASTM techniques. Low cycle fatigue behavior was established using axially-loaded strain control tests. Currently there are no industry wide accepted ASTM procedures for strain control LCF testing at elevated temperatures. The techniques for LCF data generation and analysis appear in Section VI, "Low Cycle Fatigue," Crack growth rate behavior was obtained using specimen configuration and testing techniques, where applicable, according to ASTM E399-74.

This report is arranged in sections that cover the program conclusions, material tested, and results and conclusions of the individual property tests. It includes information covered in the monthly progress reports previously issued under this contract, and pertinent test results from previous contract work.

The International System of Units (SI) is used as the primary system of units for reporting test parameters and results. Customary English units are included in parenthesis following the SI units, or in separate columns in data tables. The customary system of units was used for the principal measurements and calculations and results converted to SI units for reporting purposes.

SECTION II
RESULTS AND CONCLUSIONS

A. GENERAL

Efforts in this program consisted of testing to determine the mechanical properties of three cast nickel-base alloys. The alloys were tested in forms that are proposed for use in a high-pressure hydrogen or hydrogen-water vapor environment. The effect of loading direction (longitudinal or transverse) on the anisotropic material mechanical behavior was evaluated. Environmental degradation of properties could not be established due to the absence of comparable testing in an inert atmosphere. However, some general conclusions can be made by comparing the results of tests in the hydrogen environment with those in the hydrogen water-vapor environment.

Detailed conclusions are presented in the various sections pertaining to types of tests. General results and conclusions are presented below. Based upon limited testing and the anisotropic nature of the materials studied, these conclusions are tentative and could not be statistically substantiated.

B. TENSILE PROPERTIES

Orientation of the test specimen with respect to the solidification or primary crystal axis direction had a large effect on the tensile properties for all the alloys.

Tensile strengths were superior in the longitudinal direction, with ductility and modulus of elasticity greater in the transverse direction.

At the temperatures examined, tensile strengths were generally at a maximum at 760°C (1400°F), and ductilities were greatest at 871°C (1600°F).

The general rank order (best to worst) in tensile strength of the materials tested was PWA 1480, then directionally solidified (DS) MAR-M-246+Hf followed by single crystal (SC) MAR-M-246+Hf.

C. CREEP RUPTURE

At both 760°C (1400°F) and 871°C (1600°F), PWA 1480 was superior in creep-rupture properties followed by DS MAR-M-246+Hf and then SC MAR-M-246+Hf.

The presence of water vapor (50% by weight) in the hydrogen environment had no effect on the creep-rupture properties of PWA 1480,but a significant degradation was noted for SC MAR-M-246+Hf.

D. LOW CYCLE FATIGUE

At 760°C (1400°F) and $\Delta\epsilon_{total}$ above 1.5% the rank order of the fatigue capabilities is: PWA 1480 longitudinal, SC MAR-M-246+Hf transverse*, PWA 1480 transverse, SC MAR-M-246+Hf transverse and DS MAR-M-246+Hf transverse. At lower strain ranges (approximately 1.0%) the rank order is: SC MAR-M-246+Hf transverse*, PWA 1480 longitudinal, PWA 1480 transverse, SC MAR-M-246+Hf and DS MAR-M-246+Hf transverse.

*This material more closely resembles longitudinal data due to the transverse orientation actually being on a principal system axis. This data comes from earlier contract testing (NAS8-33109, FR-11852).

At 871°C (1600°F) and $\Delta\epsilon_{total}$ above 1.3% the rank order of the fatigue capabilities is: PWA 1480 longitudinal, PWA 1480 transverse, DS MAR-M-246+Hf transverse, and SC MAR-M-246+Hf transverse, with PWA 1480 longitudinal having the fatigue capability approximately one order of magnitude greater than the other alloys and little difference between PWA 1480, DS MAR-M-246+Hf and SC MAR-M-246+Hf in the transverse direction. At the lower strain ranges the rank order is: SC MAR-M-246+Hf transverse, PWA 1480 longitudinal, PWA 1480 transverse, and DS MAR-M-246+Hf transverse.

The addition of steam had little effect on PWA 1480 and SC MAR-M-246+Hf, but degraded DS MAR-M-246+Hf by an order of magnitude.

These conclusions are based on very limited testing and extrapolation of the data curves. Further testing could change the results presented here.

E. CRACK GROWTH

Results of crack growth testing of PWA 1480 revealed no significant difference in growth rate with increase of temperature from 760°C (1400°F) to 871°C (1600°F) nor with the addition of steam.

Results of SC MAR-M-246+Hf testing revealed an increase in crack growth rate with increasing temperature but not with the addition of steam.

The testing of DS MAR-M-246+Hf did not show a significant change in crack growth rate due to the presence of steam.

SECTION III
MATERIALS AND SPECIMENS

A. TEST MATERIAL

The purpose of this program was to determine the mechanical properties of three cast nickel-base alloys in high-pressure hydrogen environments. Testing evaluated these materials in two orientations, longitudinal and transverse, and in two forms, single crystal (SC) or directionally solidified (DS), according to the test matrix in table 1.

Table 1. Test Outline

Material	*Specimen Orientation*[1]	*Test Temperature °C(°F)*	*Test Environment*[2]	*Number of Tests*			
				Tensile	*LCF*[4]	*Creep Rupture*	*da/DN*[3]
MAR-M-246+Hf DS	Long	24(77)	H_2	2			
	Trans	25(77)	H_2	2			
	Long	760(1400)	H_2	3			
	Trans	760(1400)	H_2	3			
	Long	871(1600)	H_2	3			
	Trans	871(1600)	H_2	3	4		3
	Trans	871(1600)	H_2+H_2O		1		1
MAR-M-246+Hf SC	Long	25(77)	H_2	2			
	Trans	25(77)	H_2	2			
	Long	760(1400)	H_2	3		3	
	Trans	760(1400)	H_2	3			3
	Long	871(1600)	H_2	3		3	
	Trans	871(1600)	H_2	3	4		3
	Long	871(1600)	H_2+H_2O			1	
	Trans	871(1600)	H_2+H_2O		1		1
PW 1480	Long	25(77)	H_2	2			
	Trans	24(77)	H_2	2			
	Long	760(1400)	H_2	3	4	3	
	Trans	760(1400)	H_2	2	3		3
	Long	871(1600)	H_2	2	4	3	
	Trans	871(1600)	H_2	3	3		3
	Long	871(1600)	H_2+H_2O		1		
	Trans	871(1600)	H_2+H_2O		1		1
Total				47	26	14	18

[1]Specimen Orientation: Trans. — (Transverse) Perpendicular to or across the grain or solidification direction.
Long. — (Longitudinal) Parallel to or in the same direction as the grain or solidification direction.

[2]Test Environment: H_2 — Gaseous hydrogen with oxygen less than 1 ppm. 34.5 MPa (5000 psig)
H_2+H_2O — 50 gaseous hydrogen, 50 water vapor by weight, 34.5 MPa (5000 psia)

[3]da/dN: Crack Growth Rate
Trans — Transverse in this case means the crack will cross the grain or solidification direction.
Apply 480-sec dwell at maximum load.

[4]LCF Cyclic, nondwell strain control tests.

All test material was furnished by the NASA Marshall Space Flight Center (MSFC). The DS MAR-M-246+Hf material was supplied in the as-cast condition in the form of 10 rectangular castings, 1.25 cm × 3.8 cm × 14.0 cm (0.5 × 1.5 × 5.5 inches) with solidification axis in the 14 cm direction. The SC MAR-M-246+Hf material, also as-cast, was supplied as 20 rectangular blocks, 1.25 cm × 3.8 cm × 10.2 cm (0.5 × 1.5 × 4 inches) with the primary crystal axis in the 10.2 cm direction. The single crystal PWA 1480 material was provided in a fully heat treated condition in several forms:

— 4 pieces, 1.25 cm × 7.6 cm × 7.6 cm (0.5 × 3 × 3 inches) with primary crystal axis in one of the 7.6 cm directions

— 7 pieces, 1.6 cm × 4.4 cm at 5.7 cm (0.625 × 1.75 × 3.25 inches) with primary crystal axis in the 4.4 cm direction

— 24 round bars, 1.25 cm dia × 8 cm long (0.5 in. dia × 3.125 in. long) with primary crystal axis in 8 cm direction.

The PWA 1480 and the DS and SC MAR-M-246+Hf material underwent metallographic examination in order to determine alloy thermal history and document microstructure prior to heat treatment. The MAR-M-246+Hf DS and SC material was supplied in the as cast condition and required solution and precipitation heat treatment.

The MAR-M-246 material which was needed for transverse property test specimens required TLP[8] bonding to obtain material of sufficient length for specimen fabrication. The TLP bond cycle was then followed by the standard MAR-M-246 heat treatment cycle.

The complete heat treatment for the TLP bonded MAR-M-246+Hf material was as follows:

1. 1196°C (2185°F) ±8°C (15°F)/22 hr in vacuum (TLP bond), heat to 1221°C (2230°F).

2. 1221°C (2230°F) ±8°C (15°F)/2 hr in vacuum. Cool to room temperature (Solution HT).

3. 871°C (1600°F) ±8°C (15°F)/24 hr in vacuum. Cool to room temperature (Precipitation HT).

The MAR-M-246+Hf material which did not require TLP bonding was only heat treated per steps 2 and 3 above. Microstructure of the SC and DS MAR-M-246+Hf before and after heat treatment is presented in figures 1 through 4. Microstructure is shown for both longitudinal and transverse directions.

The PWA 1480 material was supplied in the fully heat-treated condition although the cooling rate appeared to have been slower than optimum. Microstructural examination of a test piece cut from an unusable portion of the supplied material, and tensile test results indicated that the material required re-heat treatment. The PWA 1480 heat treatment was applied as follows:

1. 1288°C (2350°F) ±8°C (15°F)/4 hr in protective atmosphere/Cool at 139°C/min (250°F/min) to 871°C (1600°F)/AC (Solution HT)

2. 1079°C (1975°F) ±14°C (25°F)/4 hr in protective atmosphere/Cool at 33°C/min (60°F/min) to 871°C (1600°F)/AC (Coating HT)

3. 871°C (1600°F) ±14°C (25°F)/32 hr in air/AC (Precipitation HT).

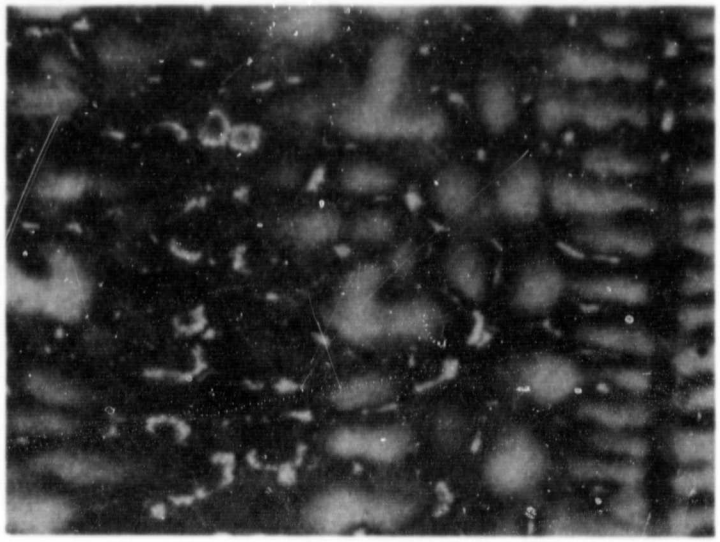

Longitudinal Section Glyceregia Mag: 100X

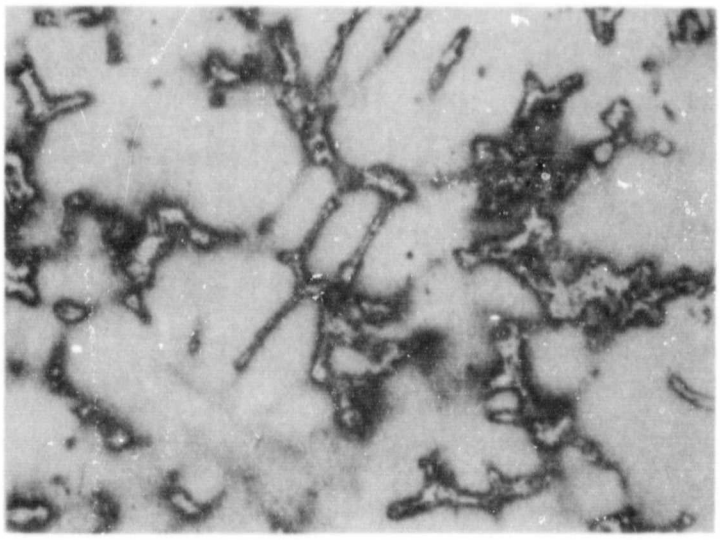

Transverse Section Glyceregia Mag: 100X

FD 191803

Figure 1. Typical Microstructure of As-Cast Single Crystal MAR-M-246 + Hf

Longitudinal Section Glyceregia Mag: 100X

Transverse Section Glyceregia Mag: 100X

FD 191804

Figure 2. Typical Microstructure of As-Cast Directionally Solidified MAR-M-246 + Hf

Sample C16, Glyceregia Mag: 100X

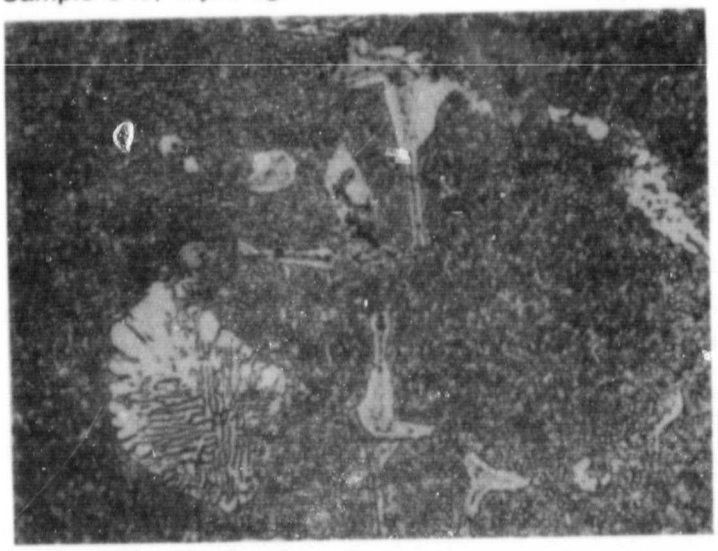

Sample C16, Glyceregia Mag: 500X

FD 191806

Figure 3. Typical Microstructure of TLP Bonded and Heat Treated Directionally Solidified MAR-M-246 + Hf

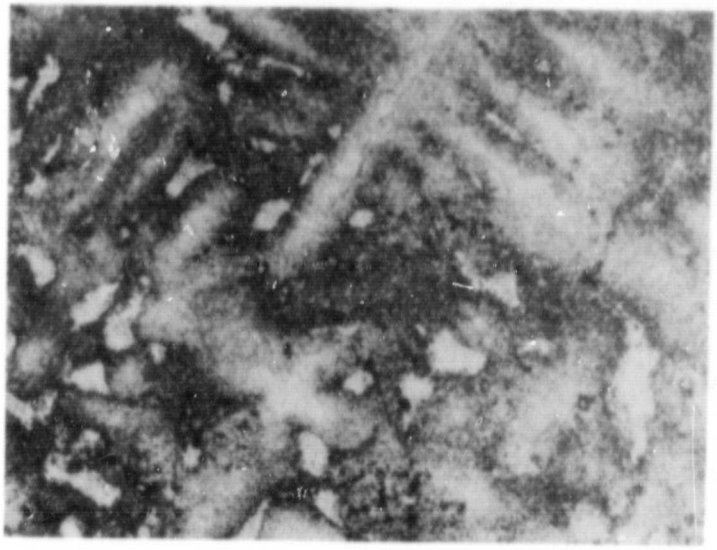

Sample N7, Glyceregia, Electropolished Mag: 100X

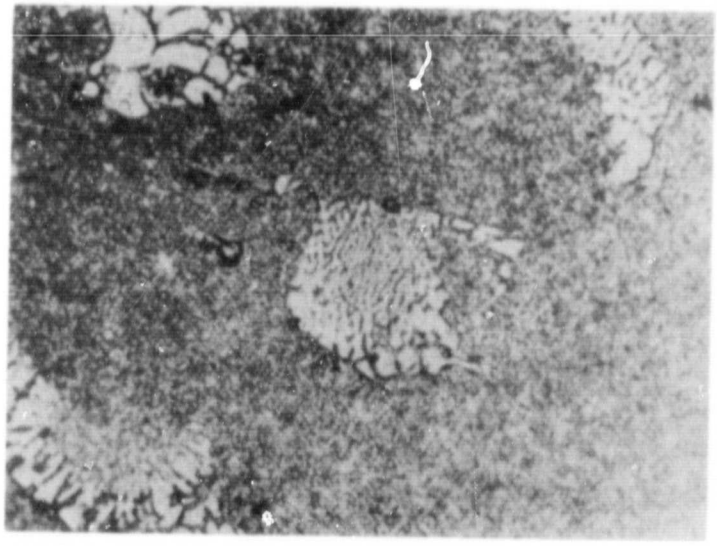

Sample N7, Glyceregia, Electropolished Mag: 500X

FD 191809

Figure 4. Typical Microstructure of Heat Treated Single Crystal MAR-M-246 + Hf

After heat treatment, microstructure and tensile properties were checked and found to meet PWA 1480 specification. Microstructure is shown in figure 5 for heat treated PWA 1480 in both longitudinal and transverse directions.

An assessment of ultrasonic C-scans of the 7.6 cm square PWA 1480 blocks was made. Shrinkage porosity had been observed in three of the four blocks supplied. These blocks were to furnish material for the transverse LCF and tensile tests; however, insufficient material due to porosity necessitated a reduction in the number of transverse tests planned.

Table 2 summarizes the alloys studied in this program, including form, heat treatments, and associated information, and table 3 lists the chemical compositions.

B. TEST GASES

Hydrogen and hydrogen-water vapor were used during the testing of specimens, and nitrogen was used as a preliminary purge gas. Propellant grade hydrogen was provided under Military Specification P-27201, which requires the gas to have an oxygen content of less than 1 part per million. Analysis verified the gas to be of this purity. The hydrogen gas was used to provide the test environment. The hydrogen and water vapor environment was obtained by utilizing triple distilled water and a retort system so the water was vaporized by furnace heat while maintaining the specified pressure. The hydrogen-water vapor atmosphere was 50% water-vapor and 50% hydrogen by weight.

Gas handling systems supplying the test vessels were equipped to enable sampling before and after specimen tests. The hydrogen was sampled extensively, both dry and saturated with water vapor (wet hydrogen was dried prior to analysis). Samples were analyzed with a gas chromatograph with accuracy in the parts per billion range.

Analysis verified that the gas was of the required purity (1 ppm O_2). Hydrogen environment pressure was maintained at 34.5 MPa (5000 psig) during testing.

C. TEST SPECIMENS

Test specimens were fabricated in both the transverse (perpendicular) and longitudinal (parallel) directions relative to the solidification direction of the castings. Since standard tensile, creep, and LCF test specimens are longer than 3.8 cm (1.5 in.), additional material had to be bonded to each side of the cast MAR-M-246+Hf blocks for fabrication of these transverse test specimens.

Bonding of additional material to the test blocks was accomplished using the transient-liquid-phase (TLP®) diffusion brazing process. (TLP is a registered trademark for the transient liquid phase bonding process patented by Pratt & Whitney Aircraft Group) In this process, a bonding alloy foil is placed between the bonding surfaces. Pressure is utilized to cause intimate contact between the mating surfaces. The bonding alloy foil melts and solidifies isothermally at the bonding temperature. Bond joint mechanical properties approaching those of the base metal are obtained by proper selection of the bonding alloys composition, time, temperature and pressure. The bonding alloy used was PWA 1182, which has a composition similar to MAR-M-200+Hf. This bonding alloy was successfully used to TLP bond single crystal and directionally solidified MAR-M-246+Hf under a previous NASA program, NAS8-33109. Bonding of extensions to the test material is illustrated schematically in figure 6. Transverse crack growth specimens were obtained without the need for TLP bonding as shown in figure 7. Transverse for crack growth specimens means orientation such that crack growth properties perpendicular to the primary grain direction would be determined. The transverse-oriented PWA 1480 tensile, creep, and LCF specimens were machined from the 7.6 cm (1.25 in.) square blocks and did not require TLP bonding of additional material.

Table 2. Turbine Blade Alloys Evaluated for Mechanical Properties in High Pressure Hydrogen Environments

Material	*Form*	*Vendor*	*Heat No.*	*As-Tested Condition (Heat Treatment*
MAR-M-246 (Hf Modified)	Directionally Solidified	Howmet	DE-008	TLP Bond Cycle*: 1196°C/22 hr in vacuum/Heat to 1221°C Solution HT: 1221°C/2 hr in vacuum/Cool to room temp Precipitation HT: 871°C/24 hr in vacuum/Cool to room temp
MAR-M-246 (Hf Modified)	Single Crystal	Howmet	DE-008	TLP Bond Cycle*: 1196°C/22 hr in heat to 1221°C Solution HT: 1221°C/2 hr in vacuum/Cool to room temp Precipitation HT: 871°C/24 hr in vacuum/Cool to room temp
PW 1480	Single Crystal	Howmet	P.O.'s 298577, 298578, 298759	Solution HT: 1288°C/4 hr in protective atmos/Cool at 139°C/min to 871°C/AC Coating HT: 1079°C/4 hr in protective atmos/Cool at 33°C/min to 871°C/AC Precipitation HT: 871°C/32 hr in air/AC

*Only transverse oriented LCF, Creep, and Tensile specimen material received this TLP Bond cycle to obtain sufficient length of raw material in transverse direction to fabricate specimens.

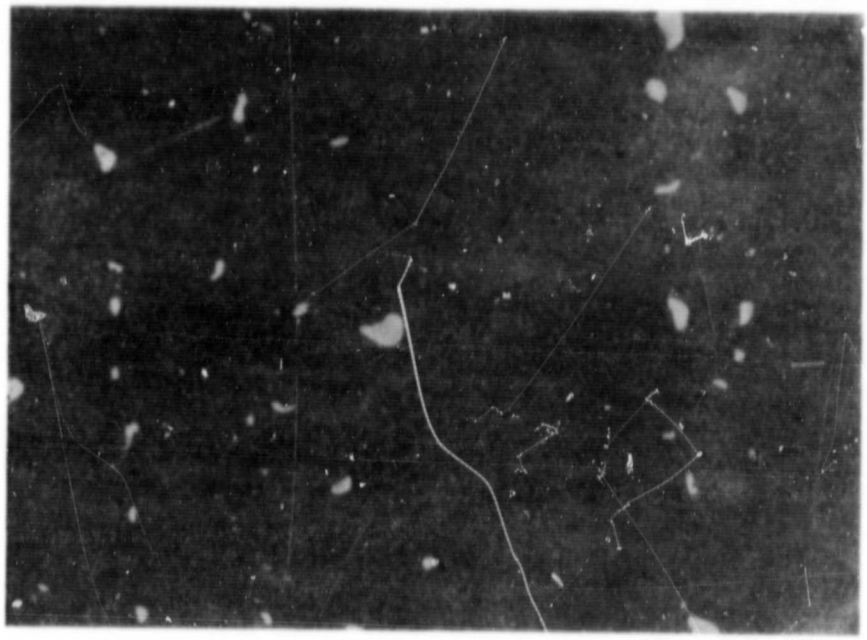

Longitudinal Section Mag: 100X

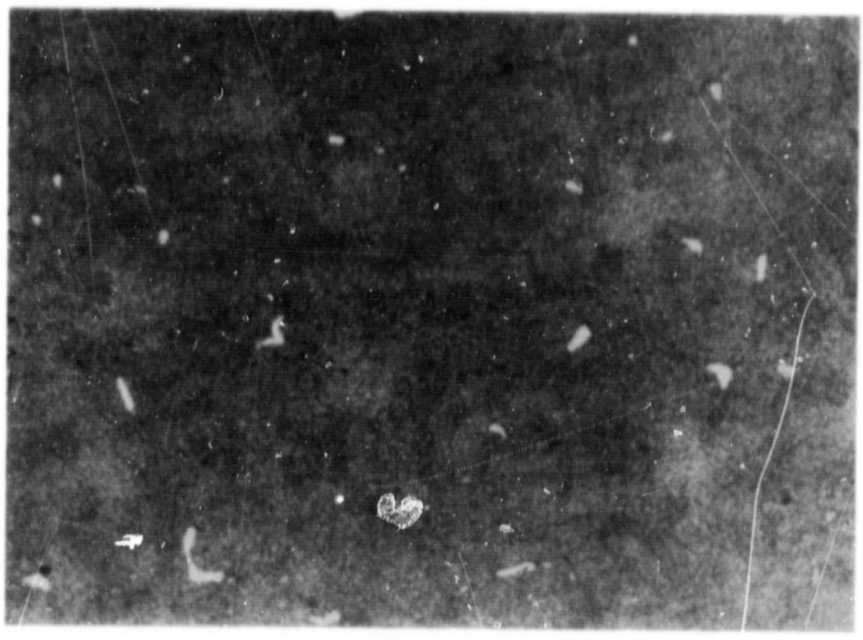

Transverse Section Mag: 100X

FD 223717

Figure 5. Typical Microstructure of Heat Treated Single Crystal PWA 1480

Table 3. Chemical Composition of Turbine Blade Alloys Used for Mechanical Properties Investigation

Material	*Form*	*Heat No.*	*C*	*Si*	*Mn*	*P*	*S*	*Cr*	*Ni*	*Mo*	*Al*	*Ti*
MAR-M-246 (Hf Modified)	Directionally Solidified and Single Crystal	DE-008	0.14	0.06	<0.10		6 ppm	8.85	Bal	2.70	5.50	1.55
PWA 1480	Single Crystal	P.O. 298577 298578 298579	40 ppm	0.03	0.01	0.005	0.004	10.18	Bal		5.12	1.38

Material	*Form*	*Heat No.*	*Cu*	*Fe*	*Mg*	*Ta*	*Co*	*W*	*Zr*	*B*	*Hf*
MAR-M-246 (Hf Modified)	Directionally Solidified and Single Crystal	DE-008	<0.10	0.19	6 ppm	1.51	10.20	10.10	0.04	0.014	1.85
PWA 1480	Single Crystal	P.O. 298577 298578 298579	0.01	0.05		12.07	4.78	3.94	70 ppm	10 ppm	50 ppm

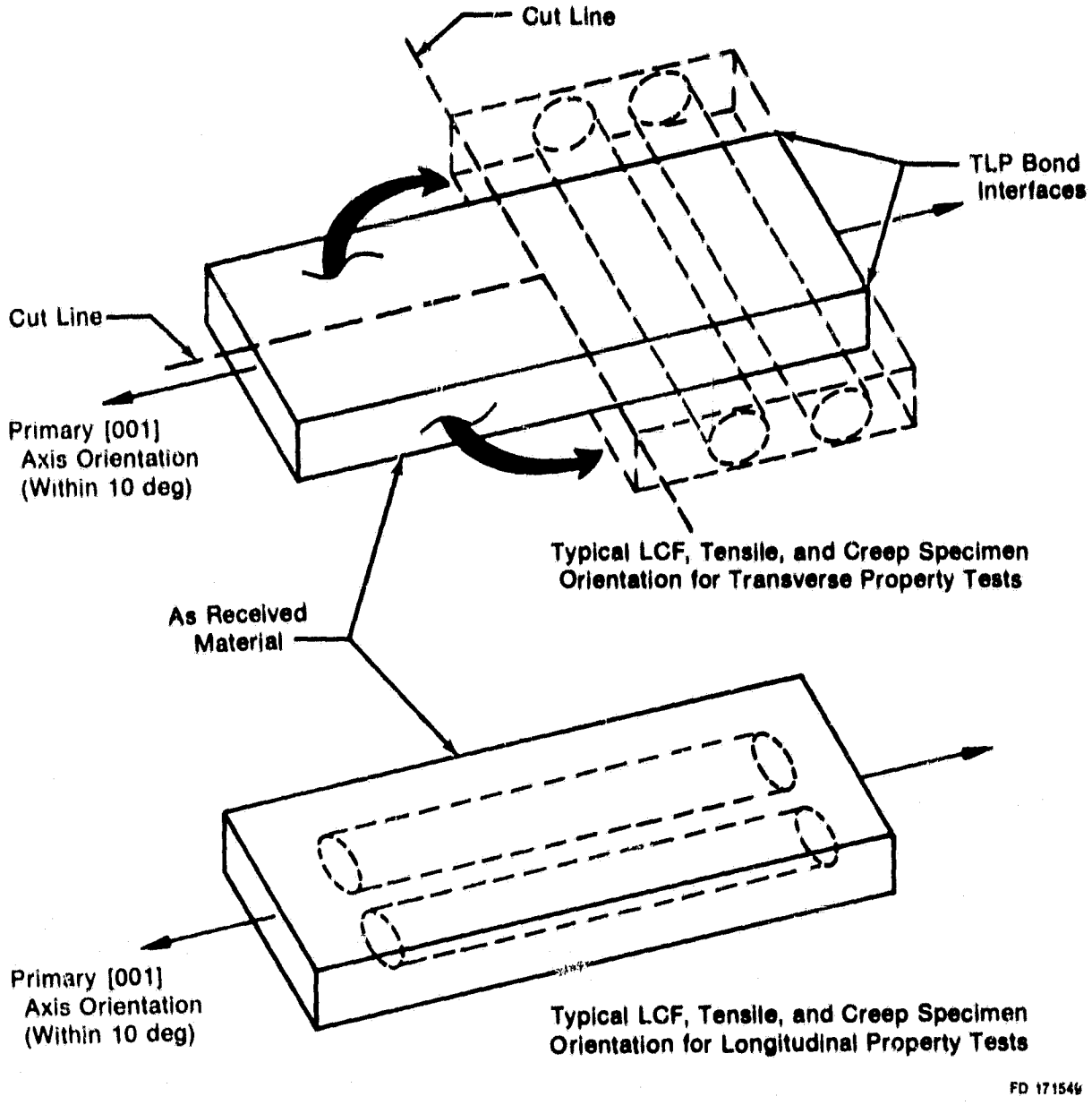

Figure 6. Typical Test Blank Fabrication for LCF, Tensile, and Creep MAR-M-246 + Hf Specimens

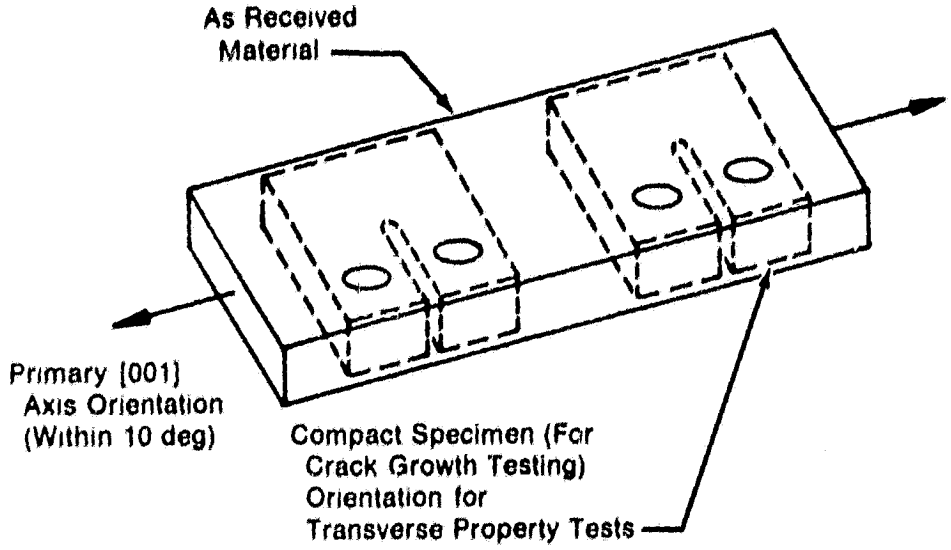

Figure 7. Typical Test Blank Layout for Compact (Crack Growth) MAR-M-246 + Hf Specimens

After bonding and heat treatment, microstructure and crystal orientation were examined for most of the cast test blocks. Crystallographic orientation of the single crystal material was determined by the Laue back reflection technique. Transverse direction single crystal specimen orientations could vary from the [010] to the [110] direction. Since the [010] direction is a primary cubic crystal axis direction, properties of transverse-oriented test specimens with axes along the [010] direction were expected to be very similar to those of longitudinal specimens (oriented along the [001] direction). Consequently, where sufficient test material was available, cast bars with orientations near the [110] direction were preferentially selected for transverse property testing.

Standard tensile, creep-rupture, Low and crack growth specimens were machined according to prints presented in figures 8 through 11. (Note: all dimensions on specimen prints are in inches). The standard tensile specimen (figure 8) was too long to be made from the TLP bonded transverse raw material, hence a smaller version (figure 9) was used in those cases. Figure 12 depicts the orientation of finish-machined test specimens relative to the MAR-M-246+Hf (DS and SC) cast bars.

Results of the orientation analysis appear in figures 13 and 14 and tables 4 through 7.

Failed crack growth specimens of each alloy were etched to better illustrate the crack propagation path relative to the solidification direction (figure 15).

All specimens were machined by the Pratt & Whitney Aircraft Group, Materials Control Laboratory Machine Shop and finished to an average roughness of 8 μ-in. rms or less.

All test specimens were visually examined prior to testing in normal light and with fluorescent penetrant to screen for machining anomalies or surface discontinuities. Additional specimens were randomly selected for thorough dimensional inspection to ensure conformance to print requirements.

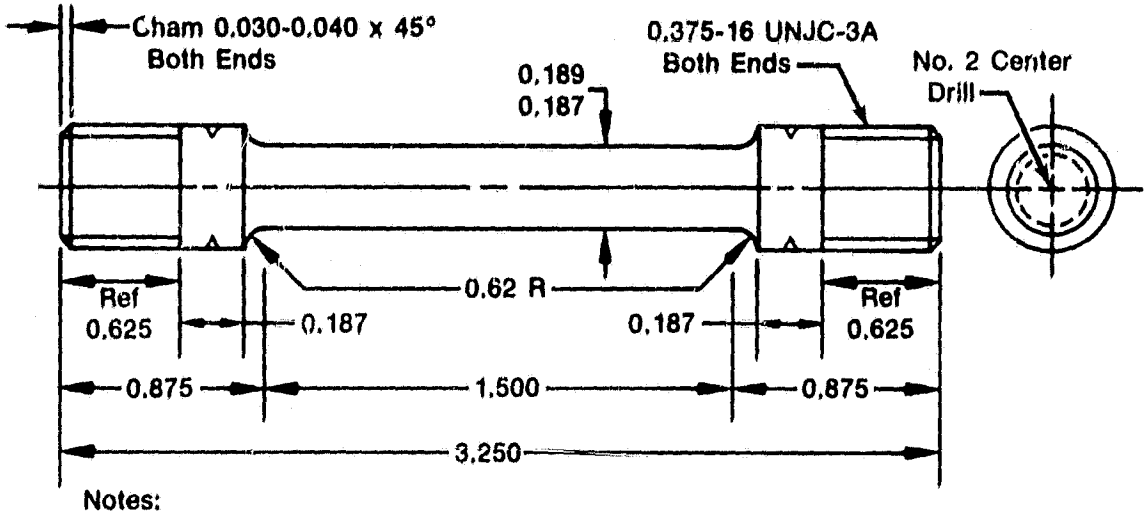

Notes:

1. All Dimensions in Inches
2. All Dia Must Be Concentric Within 0.001 FIR
3. Gage Section To Be 8 ± 3 Microinches AA Grind Finish
4. All Dim + 0.003 Unless Noted
5. Dia of Gage Section To Be Slightly Smaller at Center (Approx 0.0015)

FD 223718

Figure 8. Standard Tensile Specimen

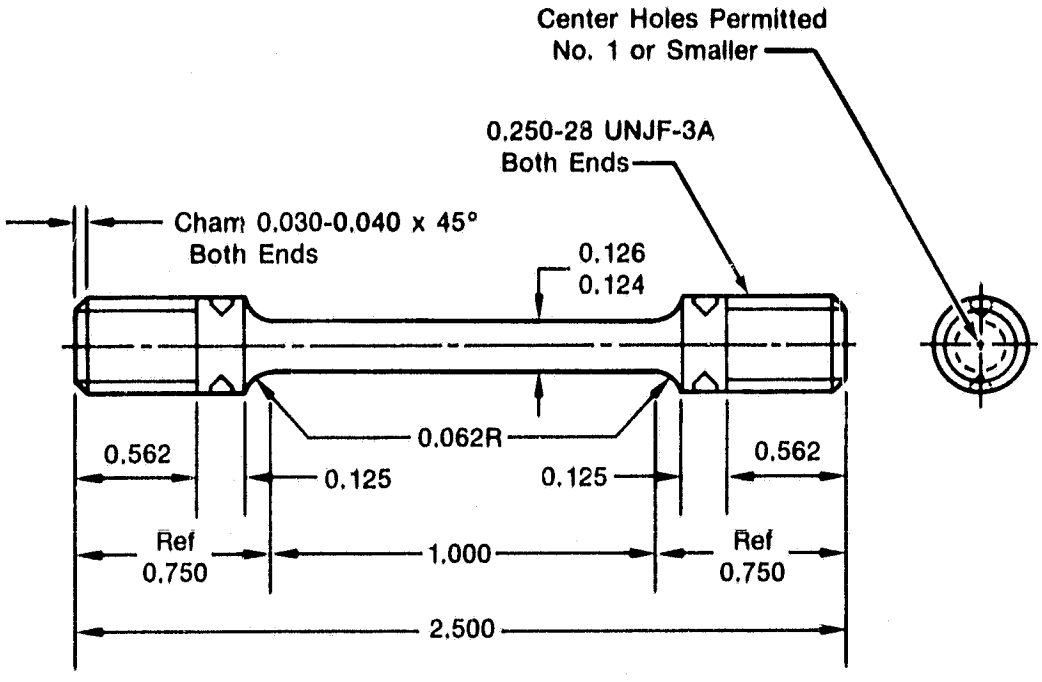

Notes:

1. All Dimensions in Inches
2. All Dia Must Be Concentric Within 0.001 FIR
3. Gage Section To Be 8 ± 3 Microinches AA Grind Finish
4. All Dim ± 0.003 Unless Noted
5. Dia of Gage Section To Be Slightly Smaller At Center (0.0015)

FD 223719

Figure 9. Standard Creep-Rupture (or Alternate Tensile) Specimen

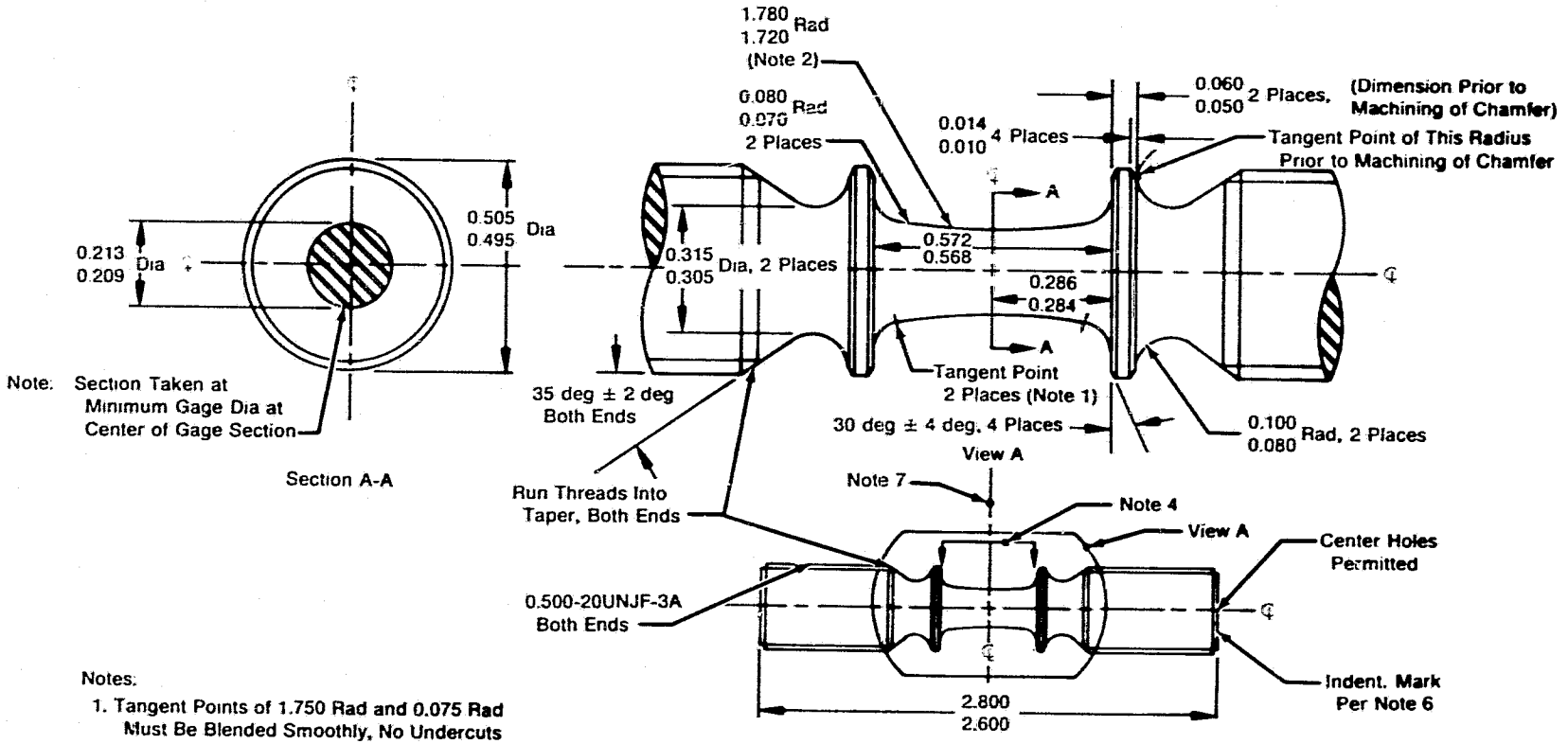

Notes:

1. Tangent Points of 1.750 Rad and 0.075 Rad Must Be Blended Smoothly, No Undercuts or Ridges Permitted
2. Center of 1.750 Rad Must Be Located Within 0.004 of Transverse ℄ of Gage
3. All Diameters To Be Concentric Within 0.002 FIR
4. Gage Section To Be 8 ± 3 μ AA Grind Finish, Including Inboard Collar Faces
5. Work to Dimensions, Do Not Scale
6. Identification Markings Permitted Only On Ends of Specimen
7. Locate ℄ Within 0.010 of Overall Specimen Length. Refer to View A for All Other References to This ℄

All Dimensions Are in Inches

FD 173403

Figure 10. Strain Control LCF Specimens

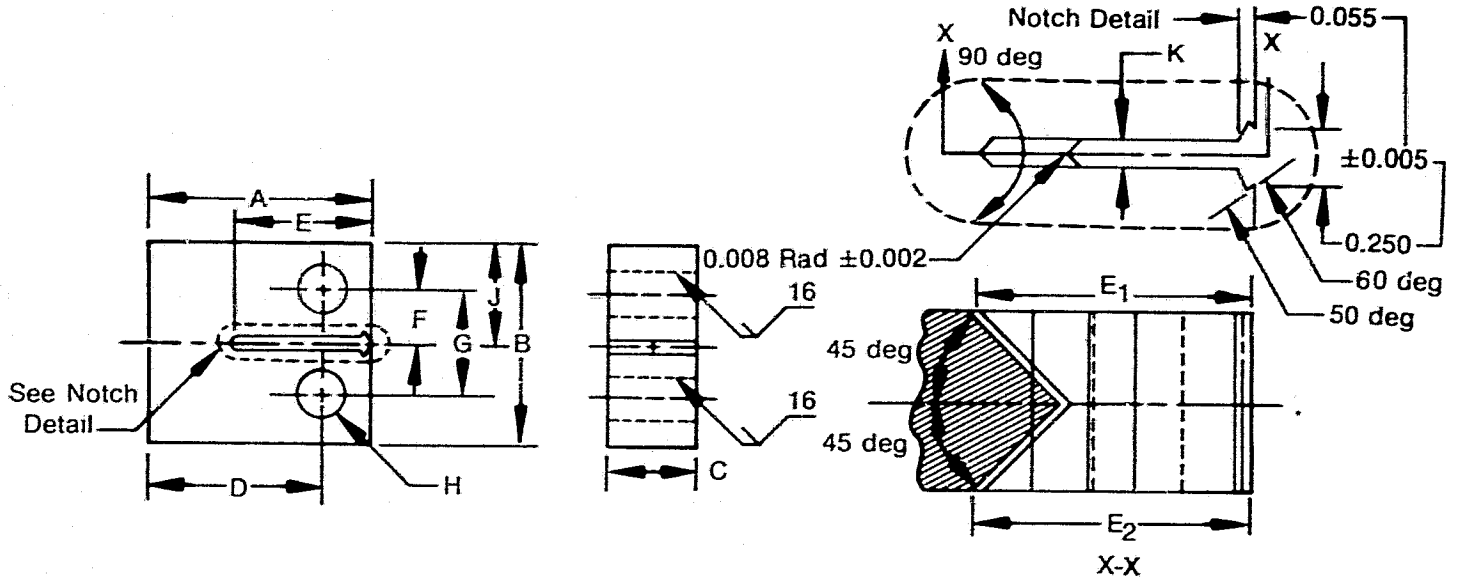

NOTES: 1. All Dimensions in Inches.

2. All External Surfaces Must Be Perpendicular and Parallel to Within 0.002
3. Finish Surfaces to Within 32 rms or Smoother Per PWA 362 UOS
4. $E_1 = E_2$ to Within 0.0025
5. Indicated ℄ Must Be Within 0.0015 of True Position

Specimen Number	A ± 0.005	B ± 0.005	C ± 0.005	D ± 0.002	E ± 0.005	F ± 0.002	G ± 0.002	H + 0.001 − 0.000	J ± 0.002	K ± 0.005
1	0.625	0.600	0.250	0.500	0.325	0.137	0.275	0.125	0.300	0.031
2	0.937	0.900	0.375	0.750	0.512	0.206	0.412	0.187	0.450	0.046
3	1.250	1.200	0.500	1.000	0.700	0.275	0.550	0.250	0.600	0.062
4	1.875	1.800	0.750	1.500	1.075	0.412	0.825	0.375	0.900	0.094
5	2.500	2.400	1.000	2.000	1.450	0.550	1.100	0.500	1.200	0.125
6	3.125	3.000	1.250	2.500	1.825	0.687	1.375	0.625	1.500	0.156
7	3.750	3.600	1.500	3.000	2.200	0.825	1.650	0.750	1.800	0.187

FD 173404

Figure 11. Crack Growth Rate Specimen (Compact)

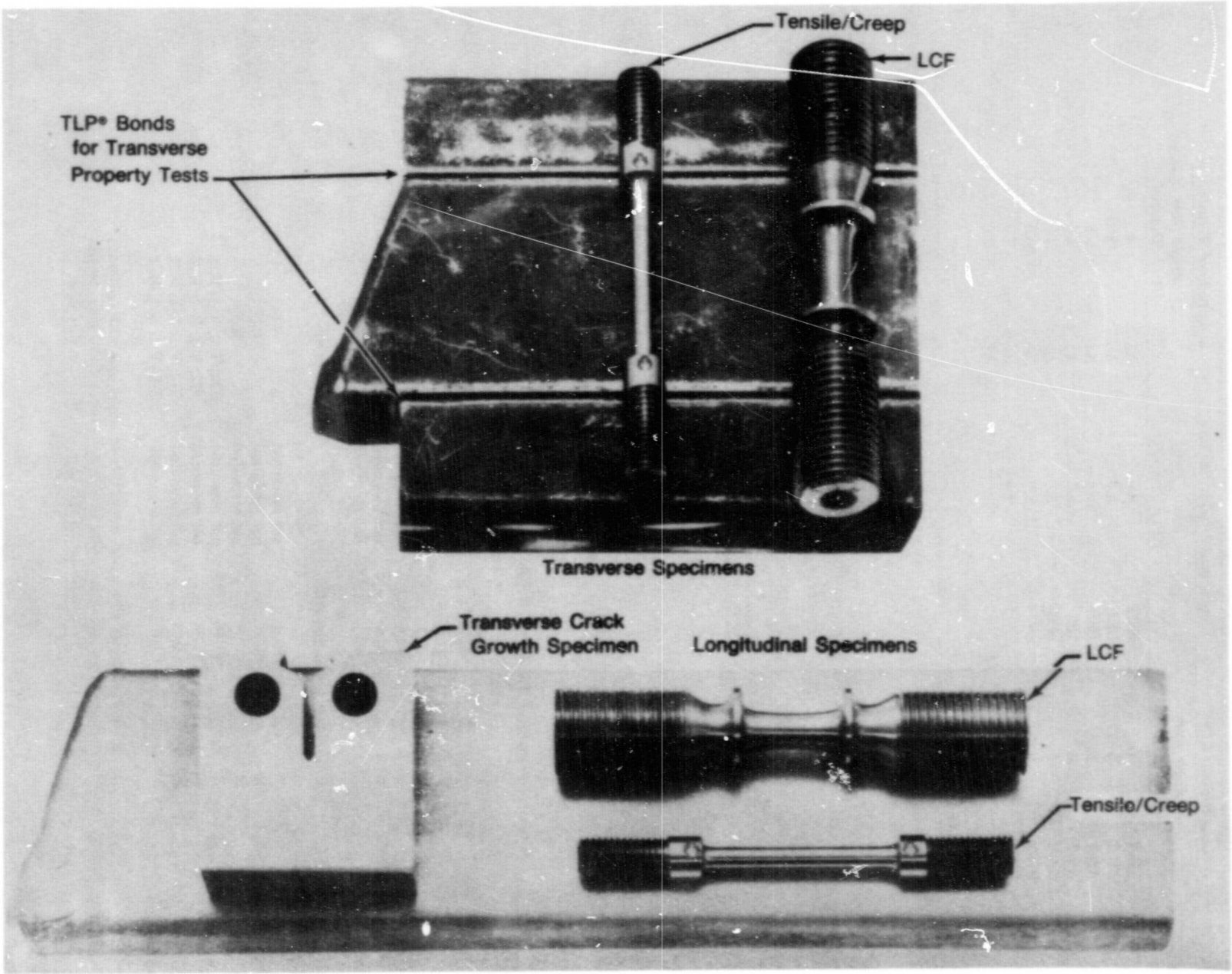

Figure 12. Orientation of Tensile/Creep Rupture, Crack Growth, and Strain Control of LCF Specimens With Respect to Cast Bars

Table 4. Specimen Orientations for Longitudinal PWA 1480 Testing

Longitudinal LCF		Longitudinal Creep Rupture		Longitudinal Tensile	
S/N	Angle from [001] (Degrees)	S/N	Angle from [001] (Degrees)	S/N	Angle from [001] (Degrees)
AE-2	4	2E12	9.0	AF-2	4
AR-2	5	LE1	5.0	AG-1	2
AZ-2	5	1E10	8.5	AJ-1	1.5
AS-2	5	1E3	8.5	AY-2	7.5
BA-2	5	1F8	6.5	AN-2	7.0
BB-2	5	2E16	9.0	BA-1	10.0
F-1	4.5	2E11	1.5	AJ-2	7.0
K-2	5			AF-1	2.0*

*649°C (1200°F) air tensile test

Table 5. Specimen Orientations for Transverse PWA 1480 Testing

S/N	Angle from [001] (Degrees)	Angle from [110]	Slab
Transverse LCF			
4L	81.5	not measured*	B-2
5L	81.5	not measured*	B-2
6L	81	not measured*	C-1
7L	81	not measured*	C-1
8L	81	not measured*	C-1
9L	81	not measured*	C-1
13L	84.5	not measured*	B-1
Transverse Tensile			
1-T	81.5	not measured*	B-2
2-T	81.5	not measured*	B-2
10-T	81.5	not measured*	B-1
11-T	81.5	not measured*	B-1
16-T	85.5	not measured*	T-1
17-T	85.5	not measured*	T-1
18-T	85.5	not measured*	T-1
Transverse Crack Growth			
W-2	83.5	not measured	W-2
R-3	84.0	not measured	R-3
E-3	87.5	not measured	E-3
A	85-88	not measured	G2, V-2, X-1, K-2
B	85-88	not measured	G2, V-2, X-1, K-2
MC1	85-88	not measured	G2, V-2, X-1, K-2
MC2	85-88	not measured	G2, V-2, X-1, K-2

*Insufficient material eliminated the ability to select bars with optimum crystallographic [110] orientation in the x-y plane of the bars. Specimens were taken perpendicular to the bars solidification direction.

Table 6. Transverse Specimen Orientations for Single Crystal MAR-M-246 + Hf Testing

S/N	Bar	β Angle from [001] (Degrees)	Angle from [110] (Degrees)
Transverse LCF			
TS-11	I-7	4	4
TS-12	I-7	4	4
TS-13	I-7	4	4
TS-14	L-2	14	4
TS-15	L-2	14	4
TS-16	L-2	14	4
TS-17	C-6	6	25
TS-18	C-6	6	25
Transverse Tensile			
TS-1	H-7	5	20
TS-2	H-7	5	20
TS-3	H-7	5	20
TS-4	H-7	5	20
TS-5	H-7	5	20
TS-6	J-2	5	0
TS-7	J-2	5	0
TS-8	J-2	5	0
Transverse Crack Growth			
S-19	O-6	not measured*	not measured
S-20	N-6	not measured*	not measured
S-21	M-1	not measured*	not measured
S-22	N-1	not measured*	not measured
S-23	O-7	not measured*	not measured
S-24	N-7	not measured*	not measured
S-25	K-2	6	38

*Not measured on these bars.
21 bars were measured.
One bar exceeded 10 deg.

Table 7. Specimen Orientations for Longitudinal Single Crystal MAR-M-246 + Hf Testing

S/N	*Bar*	*Angle from [001]*
Longitudinal Tensile		
S1	O6	Not measured, specimens taken parallel to solidification direction of bar. 21 candidate bars for transverse property testing were measured. One bar exceeded 10 deg.
S2	O6	
S3	O6	
S4	N6	
S5	N6	
S6	N6	
S7	M1	
S8	M1	
Longitudinal Creep Rupture		
S11	N1	Angle from [001] not measured. Specimens taken parallel to solidification direction of bar.
S12	N1	
S13	O7	
S14	O7	
S15	O7	
S16	N7	
S17	N7	

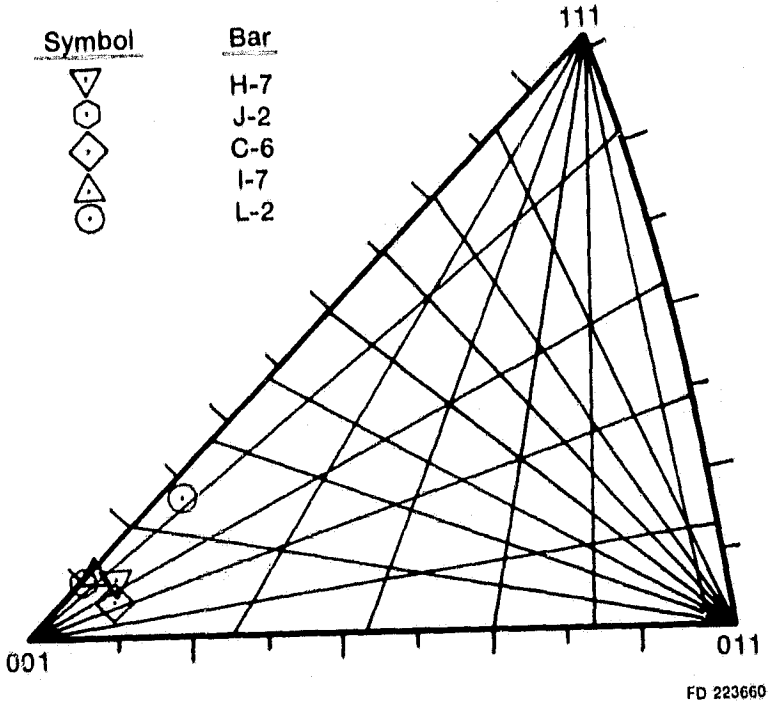

Figure 13. Unit Stereographic Triangle (Inverse Pole Figure) for Crystallographic Axes Orientation of Cast Blank Single Crystal MAR-M-246 + Hf Test Material

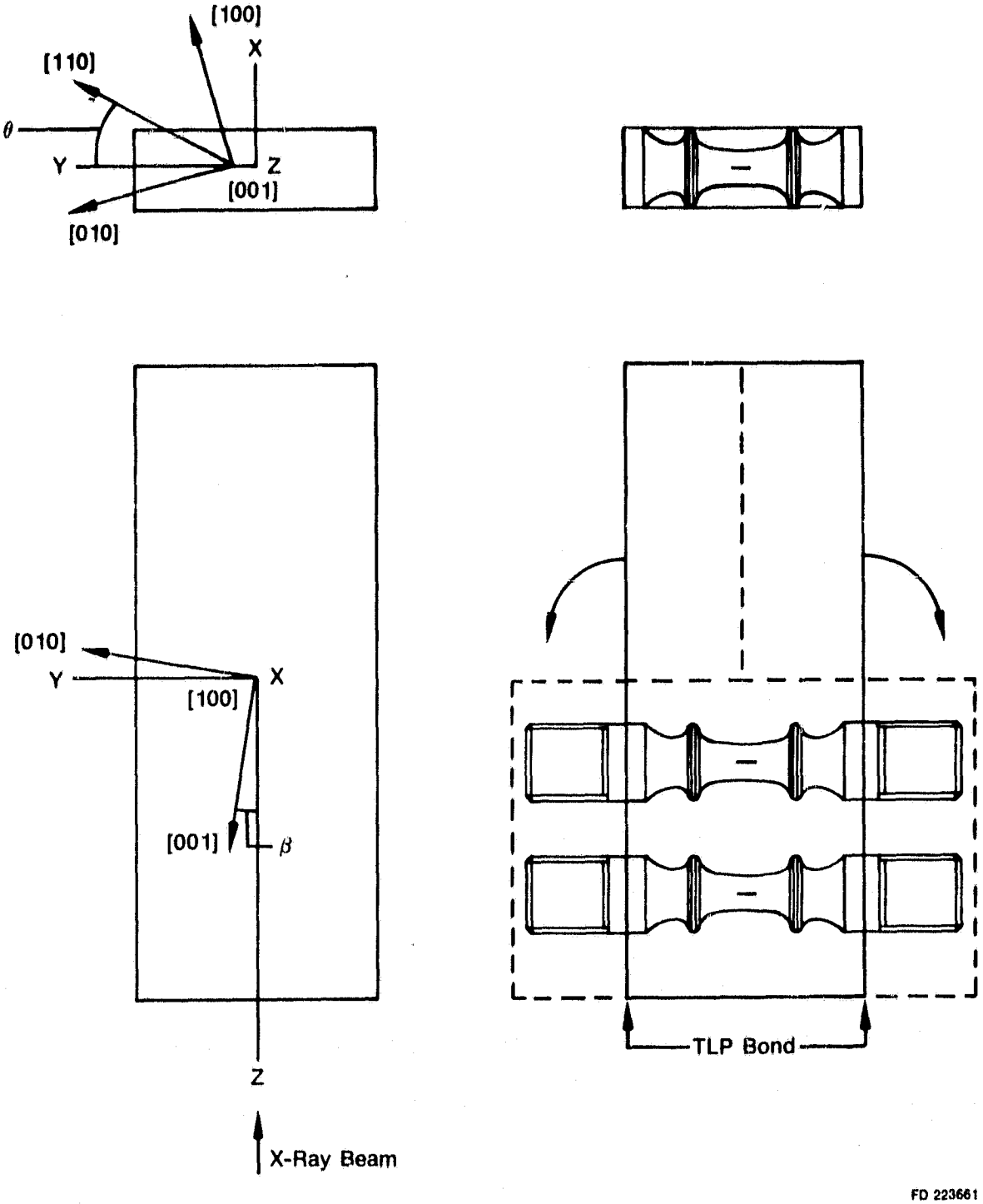

Figure 14. Crystallographic Analysis and Specimen Orientation for Single Crystal MAR-M-246 + Hf

FAL 63897

DS Mar-M-246 Hf Mag: 1.5X

FAL 63896

SC Mar-M-246 Hf Mag: 1.5X

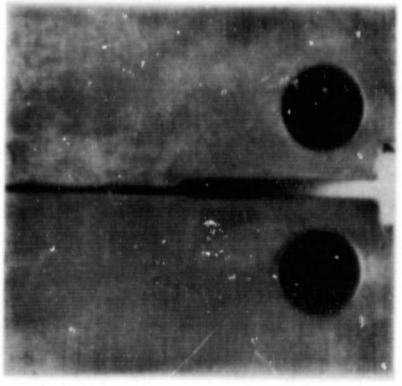

FAL 63978

PWA 1480 (SC) Mag: 1.5X

FD 223259

Figure 15. Crack Growth Specimen Orientation (for Crack Growth Perpendicular to Solidification or Primary Crystal Axis)

SECTION IV
TENSILE PROPERTIES

A. INTRODUCTION

The smooth tensile properties of three nickel-base alloys were investigated in a 34.5 MPa (5000 psig) hydrogen environment. Temperature ranged from 25°C (77°F) to 871°C (1600°F). Tensile tests established ultimate and 0.2% yield strengths, elongation, reduction of area, and modulus of elasticity. These properties are compared in two orientations, longitudinal and transverse to the solidification direction, for MAR-M-246+Hf in the directionally solidified and single crystal forms, and for single crystal PWA 1480.

B. RESULTS AND CONCLUSIONS

The effects of temperature and orientation upon the tensile properties of the alloys tested under this contract appear in figures 16 through 18. Results are also presented for previous contract testing (NAS8-30744 Report FR-7746) of DS MAR-M-246+Hf in figure 19. The mean values for the repeated tests at each temperature are plotted.

The tensile strengths were generally at a maximum for the alloys at 760°C (1400°F) based on comparing the results at 25, 760, and 871°C (77, 1400 and 1600°F). Ductilities were greatest at the maximum test temperature of 871°C (1600°F). Significant differences in tensile properties occurred due to specimen orientation. The strengths were approximately 10% higher in the longitudinal direction than in the transverse direction for all alloys. Ductilities were generally higher in the transverse direction.

The effect of temperature and orientation upon the moduli of elasticity for the alloys is shown in figure 20. As with the other tensile properties, specimen orientation had a large effect. The transverse moduli were from 30-100% greater than the longitudinal moduli.

The rank order of both ultimate and yield strengths (best to worst) for the materials tested at room temperature is:

1. PWA 1480 longitudinal (L)
2. DS MAR-M-246+Hf longitudinal (L)
3. PWA 1480 transverse (T)
4. SC MAR-M-246+Hf longitudinal (L)
5. DS MAR-M-246+Hf transverse (T)
6. SC MAR-M-246+Hf transverse (T)

At 760C (1400°F) the ranking is slightly reordered:

	Ultimate Strength	*0.2% Yield*
1.	PWA 1480 (L)	PWA 1480 (L)
2.	DS MAR-M-246+Hf (L)	DS MAR-M-246+Hf (L)
3.	SC MAR-M-246+Hf (L)	PWA 1480 (T)
4.	PWA 1480 (T)	SC MAR-M-246+Hf (L)
5.	SC MAR-M-246+Hf (T)	SC MAR-M-246+Hf (T)
6.	DS MAR-M-246+Hf (T)	DS MAR-M-246+Hf (T)

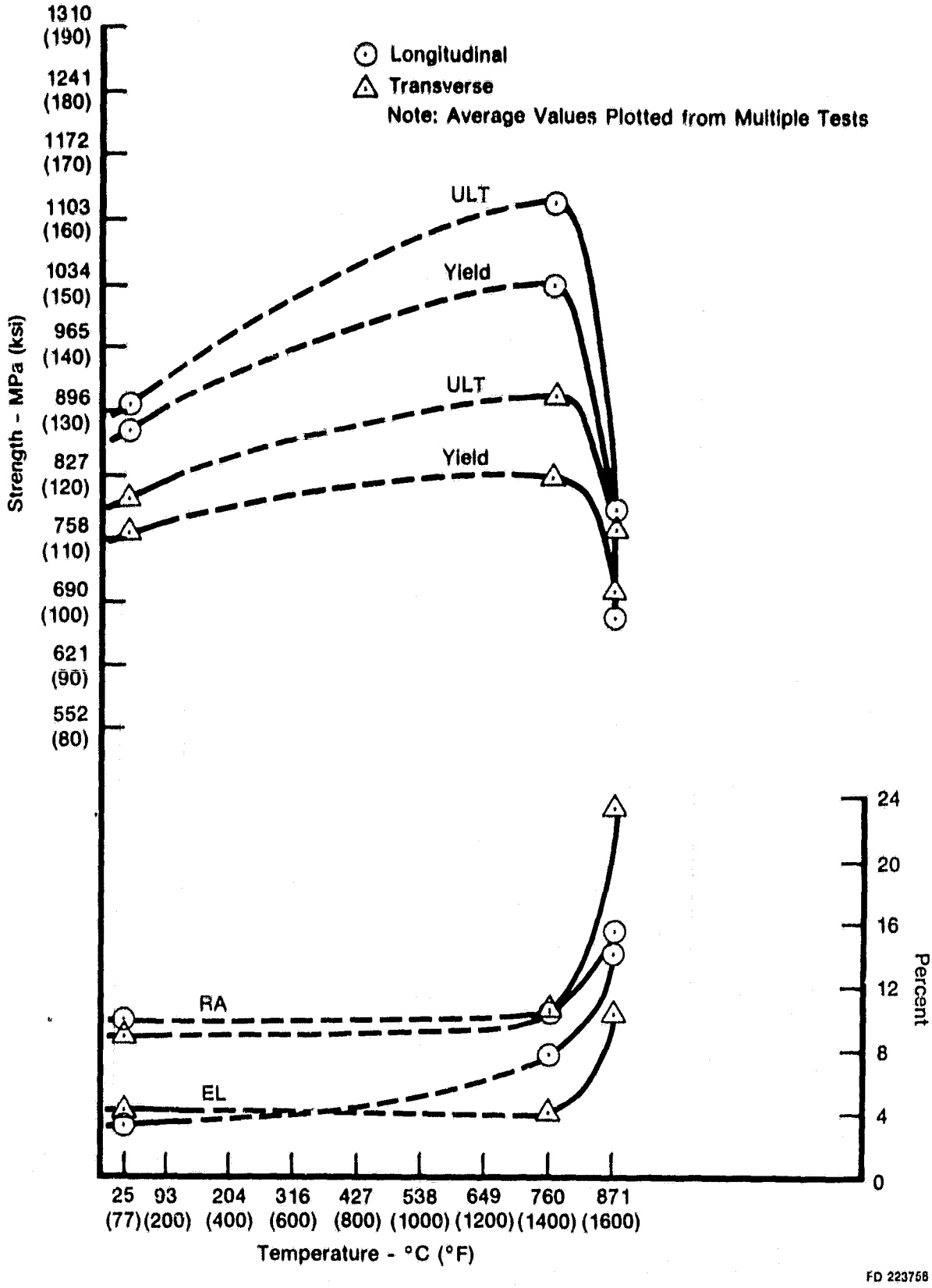

Figure 16. Effect of Temperature on Tensile Properties of Directionally Solidified MAR-M-246 + Hf (in Hydrogen at 34.5 MPa (5000 psig))

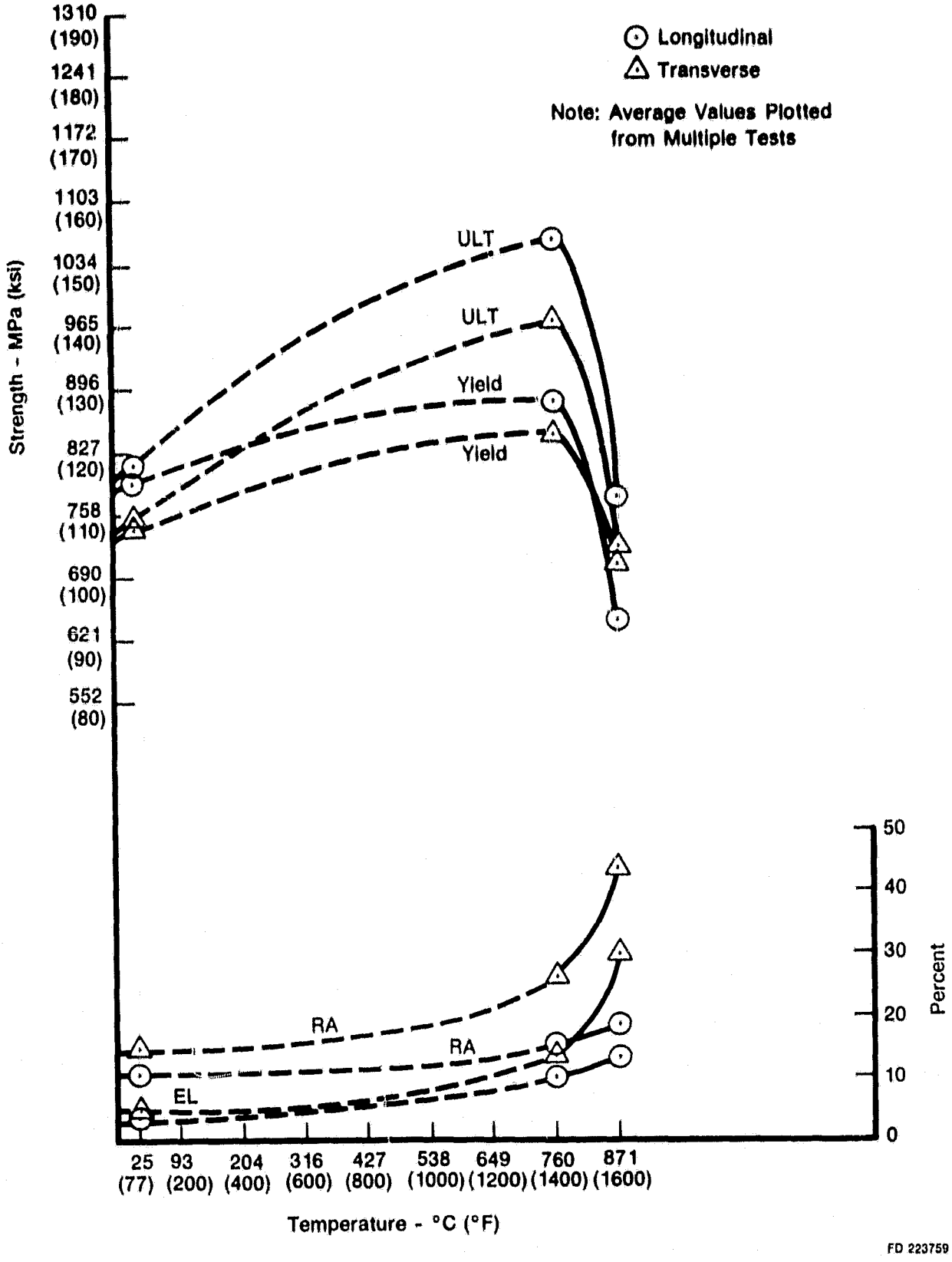

Figure 17. Effect of Temperature on Tensile Properties of Single Crystal MAR-M-246 + Hf (in Hydrogen at 34.5 MPa (5000 psig))

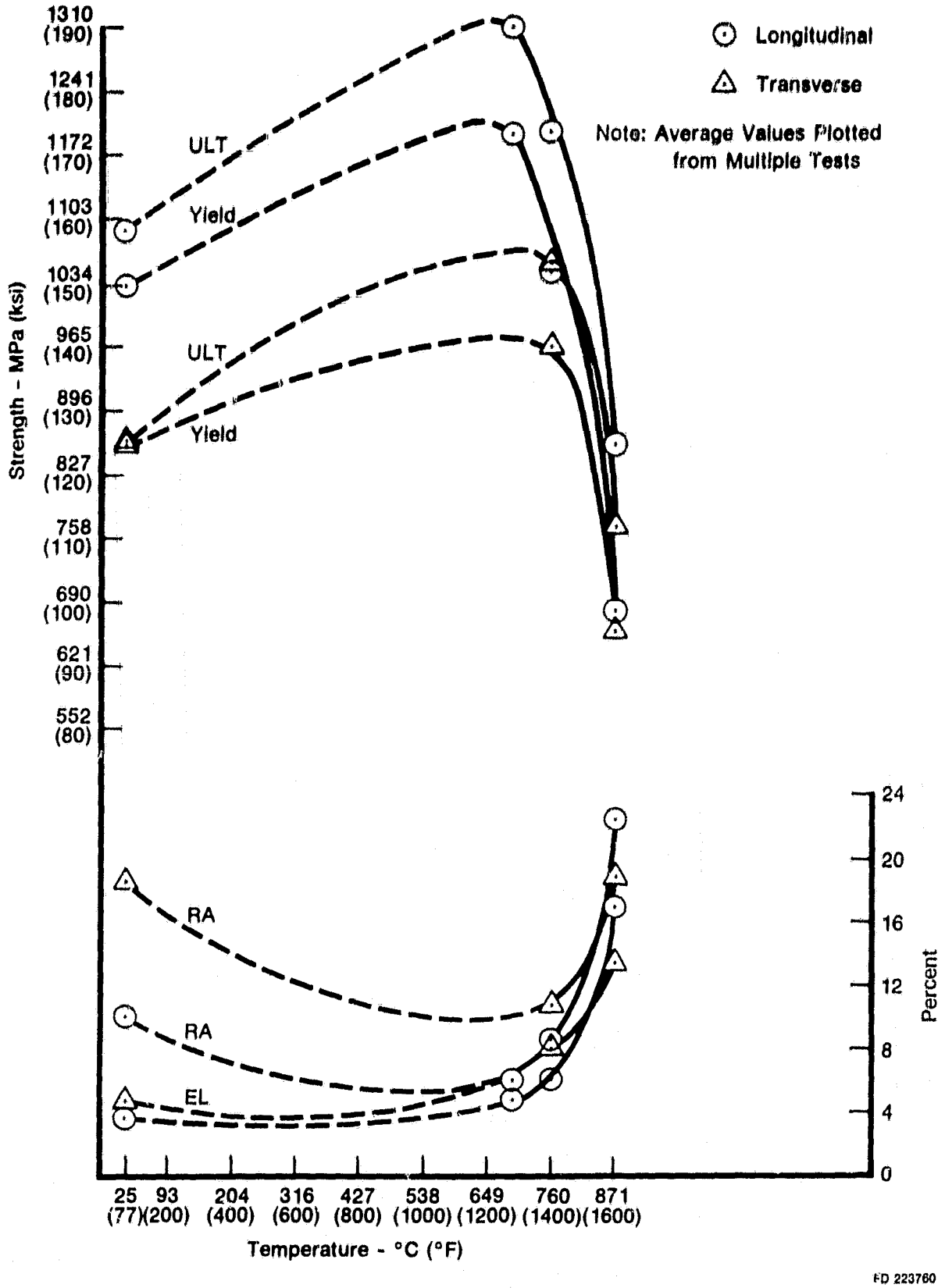

Figure 18. Effect of Temperature on Tensile Properties of PWA 1480 (in Hydrogen at 34.5 MPa (5000 psig))

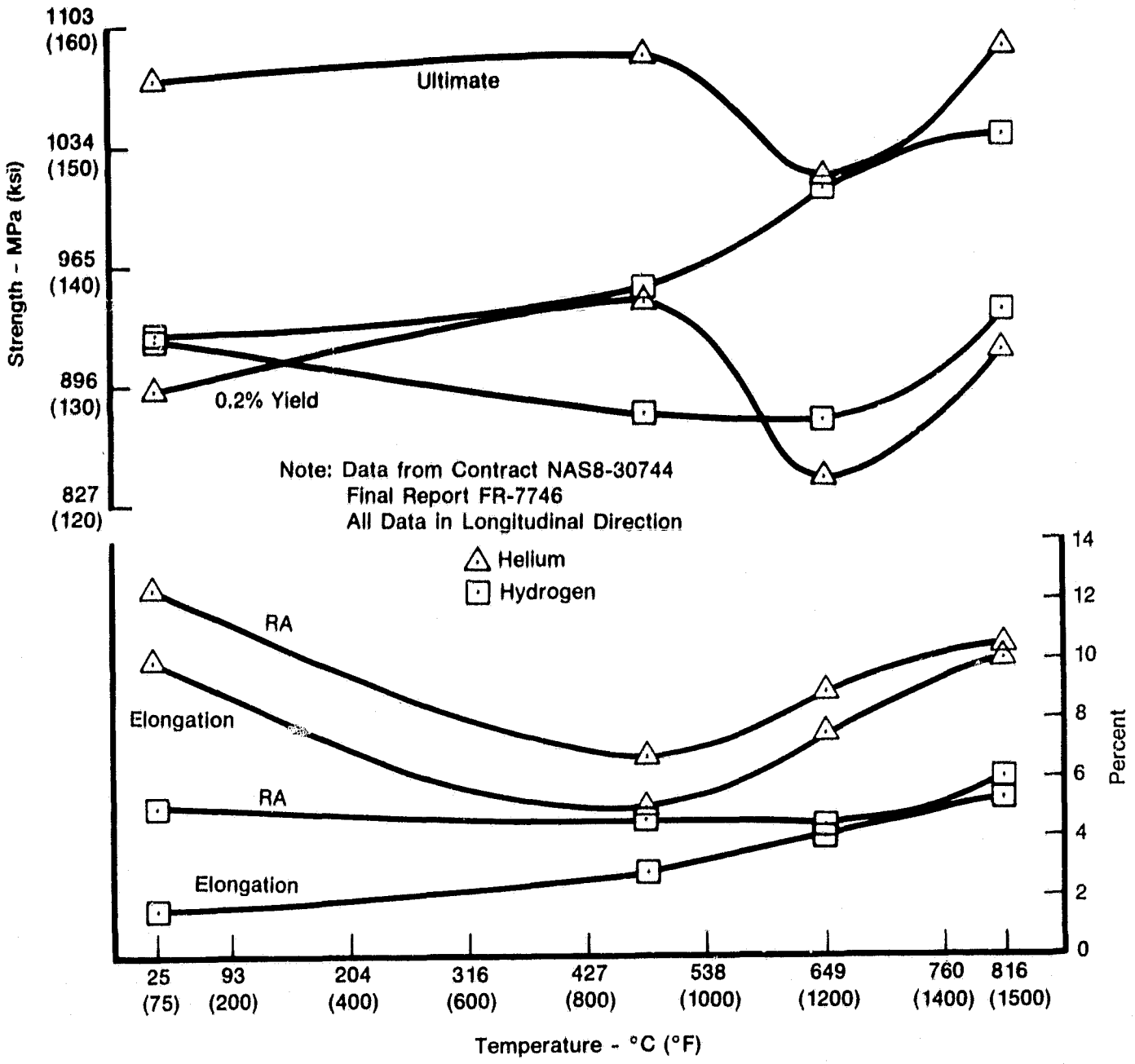

Figure 19. Effect of Temperature and Environment on the Longitudinal Tensile Properties of Directionally Solidified (DS) MAR-M-246 (Hf Modified) at 34.5 MPa (5000 psig)

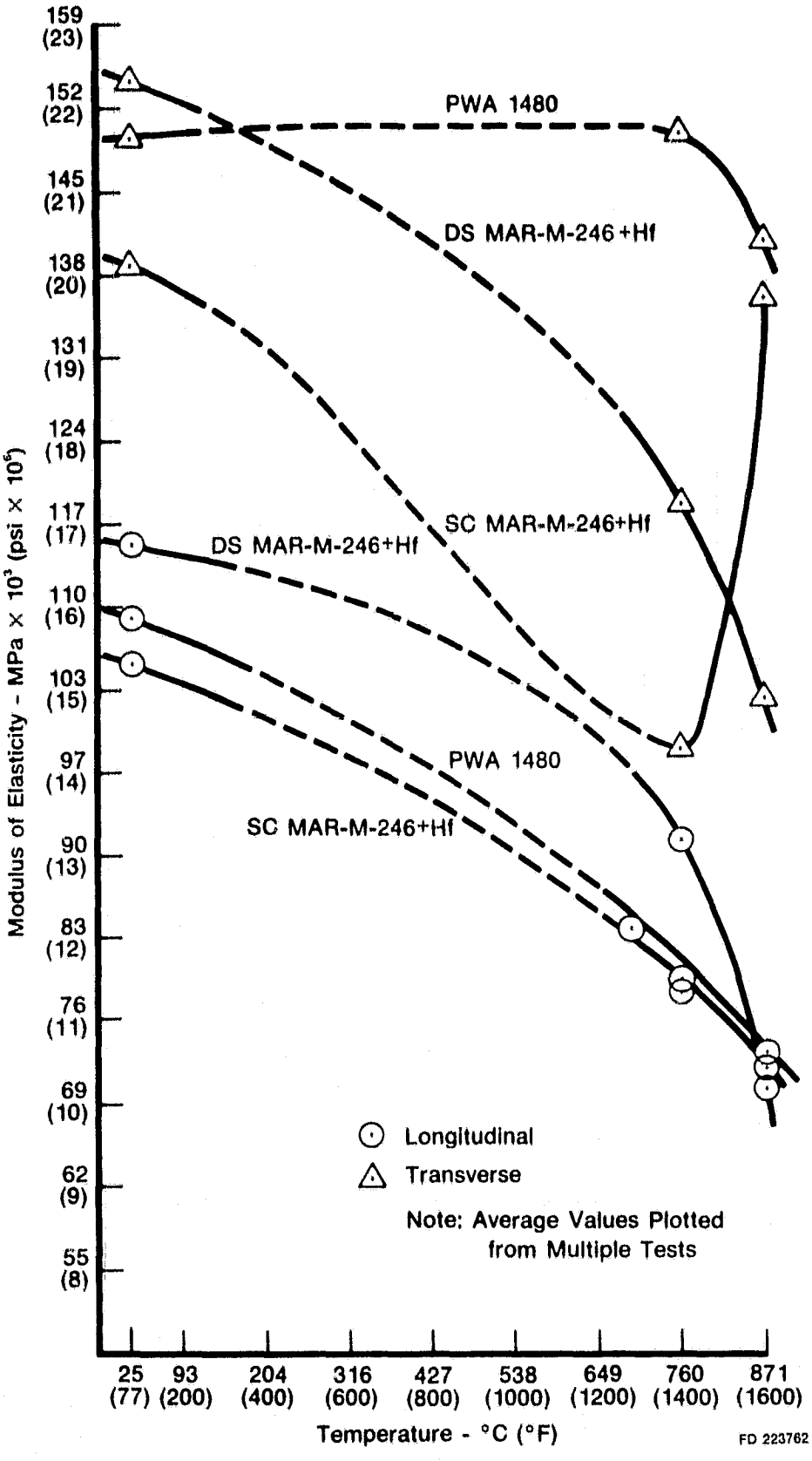

Figure 20. Effect of Temperature on Modulus of Elasticity for Turbine Blade Alloys (in Hydrogen at 34.5 MPa (5000 psig))

At 871°C (1600°F) the rank order again changes:

Ultimate Strength	*0.2% Yield*
1. PWA 1480 (L)	SC MAR-M-246+Hf (T)
2. DS MAR-M-246+Hf (L)	DS MAR-M-246+Hf (T)
3. SC MAR-M-246+Hf (L)	PWA 1480 (L)
4. PWA 1480 (T)	DS MAR-M-246+Hf (L)
5. DS MAR-M-246+Hf (T)	PWA 1480 (T)
6. SC MAR-M-246+Hf (T)	SC MAR-M-246+Hf (L)

These conclusions are tentative, being based upon very limited testing and the inherent variability in properties of anisotropic materials. Some data scatter may also be attributed to primary crystal axis [001] orientation for the longitudinal tests, and transverse axis [110] misalignment among the transverse tests.

Test results are listed in tables 8 through 13.

Table 8. Longitudinal Tensile Results for Directionally Solidified MAR-M-246 + Hf in Hydrogen at 34.5 MPa (5000 psig)

Spec	*Temperature*		*Strength*				*Ductility*		*Modulus of Elasticity*
			0.2% Yield		*Ultimate*		*EL*	*RA*	
S/N	*°C*	*°F*	*MPa*	*ksi*	*MPa*	*ksi*	*%*	*%*	*MPa × 10³ (psi × 10⁶)*
D-1	RT	RT	879.8	127.6	906.7	131.5	3.0	10.8	113.1 (16.4)
D-2	RT	RT	867.4	125.8	900.5	130.6	3.0	8.6	117.9 (17.1)
D-3	760	1400	1088.0	157.8	1099.7	159.5	10.0	11.7	106.9 (15.5)
D-4	760	1400	1000.5	145.1	1172.2	170.0	6.0	7.7	82.7 (12.0)
D-5	760	1400	1017.7	147.6	1106.6	160.5	7.0	11.6	82.7 (12.0)
D-7	871	1600	616.4	89.4	732.2	106.2	14.0	15.2	64.8 (9.4)
D-8	871	1600	696.4	101.0	806.7	117.0	16.0	15.8	68.3 (9.9)
D34	871	1600	710.9	103.1	843.2	122.3	12.0	15.3	77.2 (11.2)

Table 9. Transverse Tensile Results for Directionally Solidified MAR-M-246 + Hf in Hydrogen at 34.5 MPa (5000 psig)

Spec	Temperature		Strength				Ductility		Modulus of Elasticity
			0.2% Yield		Ultimate		EL	RA	MPa × 10^3
S/N	°C	°F	MPa	ksi	MPa	ksi	%	%	(psi × 10^6)
D-9	RT	RT	766.0	111.1	805.3	116.8	4.0	10.7	152.4 (22.1)
D-10	RT	RT	760.5	110.3	799.8	116.0	4.0	6.9	155.8 (22.6)
D-11	760	1400	824.6	119.6	930.8	135.0	4.0	6.2	117.9 (17.1)
D-12	760	1400	823.9	119.5	905.3	131.3	4.0	13.2	114.5 (16.6)
D-13	760	1400	831.5	120.6	910.1	132.0	4.0	12.3	124.8 (18.1)
D-19	871	1600	702.6	101.9	774.3	112.3	9.6	31.8	102.7 (14.9)
D-20	871	1600	734.3	106.5	799.8	116.0	13.0	24.1	111.7 (16.2)
D-21	871	1600	672.3	97.5	744.0	107.9	8.0	14.4	93.8 (13.6)

Table 10. Longitudinal Tensile Results for Single Crystal MAR-M-246 + Hf in Hydrogen at 34.5 MPa (5000 psig)

Spec	Temperature		Strength				Ductility		Modulus of Elasticity
			0.2% Yield		Ultimate		EL	RA	MPa × 10^3
S/N	°C	°F	MPa	ksi	MPa	ksi	%	%	(psi × 10^6)
S-1	RT	RT	792.9	115.0	808.8	117.3	2.0	10.0	103.4 (15.0)
S-2	RT	RT	792.9	115.0	815.7	118.3	4.0	11.4	107.6 (15.6)
S-3	760	1400	881.9	127.9	1063.9	154.3	10.0	15.9	76.5 (11.1)
S-4	760	1400	881.9	127.2	1056.3	153.2	11.0	14.7	77.9 (11.3)
S-5	760	1400	886.7	128.6	1072.2	155.5	10.0	15.2	83.4 (12.1)
S-6	871	1600	647.4	93.9	785.3	113.9	10.0	16.8	69.0 (10.0)
S-7	871	1600	632.3	91.7	788.1	114.3	15.0	20.9	74.5 (10.8)
S-8	871	1600	652.9	94.7	776.4	112.6	15.0	18.0	71.7 (10.4)

Table 11. Transverse Tensile Results for Single Crystal MAR-M-246 + Hf in Hydrogen at 34.5 MPa (5000 psig)

Spec	Temperature		Strength				Ductility		Modulus of Elasticity
			0.2% Yield		Ultimate		EL	RA	MPa × 10^3
S/N	°C	°F	MPa	ksi	MPa	ksi	%	%	(psi × 10^6)
TS-1	RT	RT	746.7	108.3	760.5	110.3	4.0	13.8	137.9 (20.0)
TS-2	RT	RT	751.6	109.0	763.9	110.8	5.1	16.1	139.3 (20.2)
TS-3	760	1400	848.1	123.0	973.6	141.2	14.0	27.9	110.3 (16.0)
TS-4	760	1400	827.4	120.0	965.3	140.0	14.0	27.9	98.6 (14.3)
TS-5	760	1400	861.9	125.0	968.7	140.5	12.0	22.2	86.9 (12.6)
TS-6	871	1600	693.6	100.6	726.0	105.3	33.0	41.7	144.8 (21.0)
TS-7	871	1600	710.2	103.0	732.2	106.2	29.0	43.6	133.8 (19.4)
TS-8	871	1600	710.2	103.0	726.0	105.3	27.0	44.8	130.3 (18.9)

Table 12. Longitudinal Tensile Results for PWA 1480 in Hydrogen at 34.5 MPA (5000 psig)

Spec	Temperature		Strength				Ductility		Modulus of Elasticity
			0.2% Yield		Ultimate		EL	RA	MPa × 10^3
S/N	°C	°F	MPa	ksi	MPa	ksi	%	%	(psi × 10^6)
AF-2	RT	RT	1050.8	152.4	1115.6	161.8	4.0	9.4	108.9 (15.8)
AG-1	RT	RT	1012.2	146.8	1063.9	154.3	3.3	10.4	109.6 (15.9)
AG-2	690*	1275	1197.0	173.6	1313.5	190.5	4.7	5.9	83.4 (12.1)
AJ-1	760	1400	1060.5	153.8	1214.2	176.1	5.3	7.6	78.6 (11.4)
AY-2	760	1400	1043.2	151.3	1186.6	172.1	6.7	9.9	77.9 (11.3)
AN-2	871	1600	644.7	93.5	838.4	121.6	24.0	26.2	75.2 (10.9)
BA-1	871	1600	677.1	98.2	881.2	127.8	17.3	23.0	75.2 (10.9)
AJ-2	871	1600	724.7	105.1	877.7	127.3	10.7	18.5	69.0 (10.0)

*Run at 690°C due to temperature cont. malfunction

Table 13. Transverse Tensile Results for PWA 1480 in Hydrogen at 34.5 MPA (5000 psig)

Spec	Temperature		Strength 0.2% Yield		Strength Ultimate		Ductility EL	Ductility RA	Modulus of Elasticity
S/N	°C	°F	MPa	ksi	MPa	ksi	%	%	MPa × 10^3 (psi × 10^6)
1-T	RT	RT	879.1	127.5	881.9	127.9	4.7	17.9	149.6 (21.7)
2-T	RT	RT	842.6	122.2	842.6	122.2	4.7	19.4	148.9 (21.6)
10-T	760	1400	972.2	141.0	1050.8	152.4	11.3	15.9	141.3 (20.5)
11-T	760	1400	968.1	140.4	1068.7	155.0	4.7	5.9	157.9 (22.9)*
16-T	871	1600	672.3	97.5	777.8	112.8	10.7	15.9	141.3 (20.5)
17-T	871	1600	624.7	90.6	731.6	106.1	16.7	24.5	137.2 (19.9)
18-T	871	1600	696.4	101.0	811.5	117.7	12.7	15.9	144.1 (20.9)

*Failed in radius

C. TEST PROCEDURE

All tensile tests were conducted per ASTM E8-69, "Tension Testing of Metallic Materials," using two smooth specimen designs. The test specimen used depended upon the size of the raw material and the specimen orientation. All longitudinal and transverse PWA 1480 tests used the longer tensile specimen shown in figure 8. The MAR-M-246+Hf longitudinal, and transverse tensile tests which required TLP bonding of the raw material, necessitated use of the smaller specimen shown in figure 9.

Smooth specimens were tested at a strain rate of 0.005 mm/mm/min (in./in./min) to yield and a crosshead speed of 1.27 mm/min (0.05 in./min) from yield to fracture.

All tensile testing was conducted on a Tinius Olsen 266.8-kN (60,000-lb) capacity tensile machine, equipped with a P&WA-designed and developed pressure vessel. All controls and instrumentation readout equipment are located inside an adjacent blockhouse. This equipment is shown in figures 21 and 22.

Various views of the pressure vessel showing specimen, extensometer, and furnace setup are presented in figure 22. The vessel is made of AISI 347 stainless steel and incorporates a high-pressure GrayLoc connector. A compensating device built into the base of the vessel eliminated the effect of loads resulting from differential specimen and adapter cross-sectional areas.

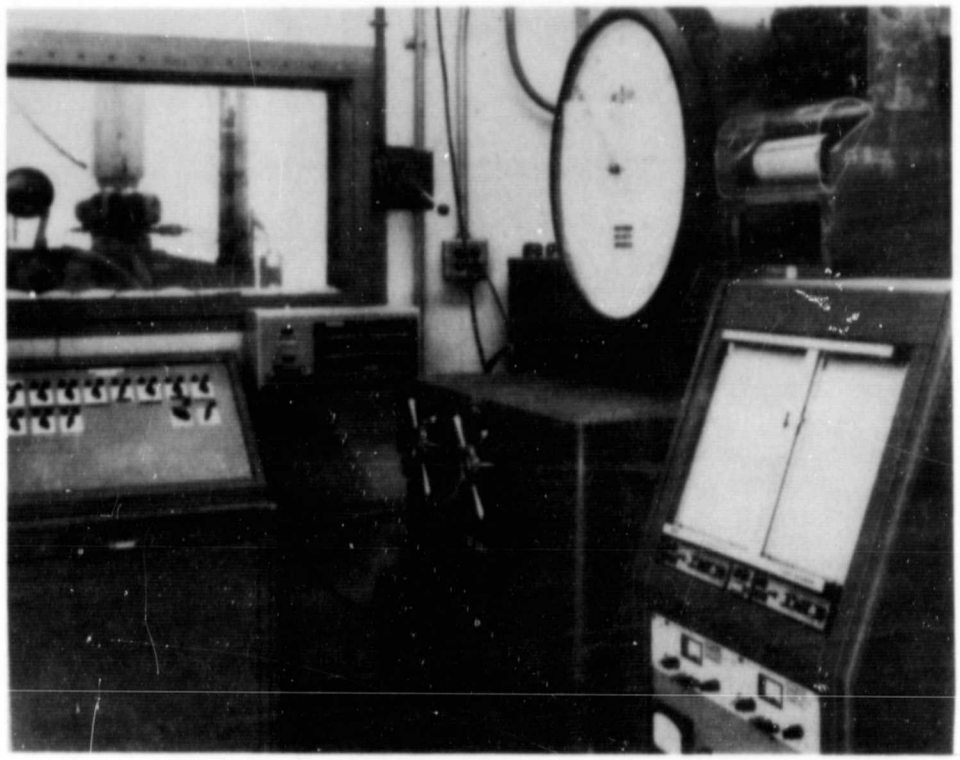

Figure 21. Tensile Machine, Test Environmental Control and Data Acquisition Equipment

To measure specimen strain for both room temperature and elevated temperature tests an averaging-type linear variable displacement transducer (LVDT) extensometer system was used (figure 23). Specimen load was determined by both the tensile machine load measuring system and an internal strain-gage-type load cell; thus, absolute specimen load was known and friction at the pressure vessel seals was of no consequence. Electrical connections to the internal load cell, extensometer, thermocouples, and furnace were made through the bottom of the pressure vessel via high-pressure bulkhead connectors.

For elevated temperature testing, a two-zone resistance furnace with separate control systems for each zone was used. The furnace surrounds the specimen and fits within the frame of the pressure vessel. Thermocouples attached to the specimen gage section were used to monitor and control temperature during test. Temperature was controlled uniformly over the specimen gage section for all tests using calibrated thermocouple, temperature readout, and control instrumentation.

Prior to test, specimens were rinsed with trichlorethylene, wiped dry, rinsed with acetone, wiped dry, and inserted into the test fixture. All handling of specimens was done with clean gloves.

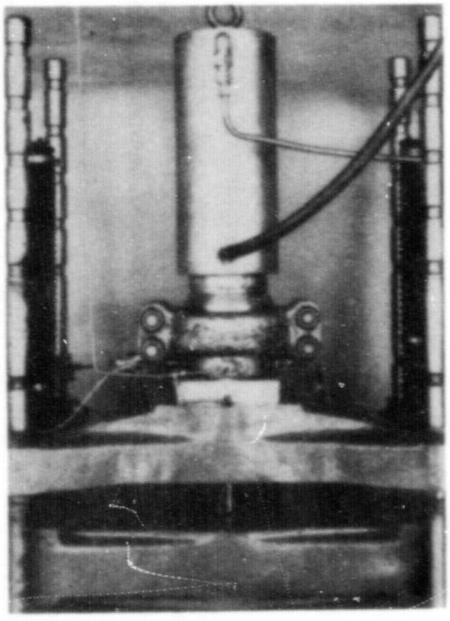

a) Test Vessel Installed on Tensile Machine Located in Remote Test Cell

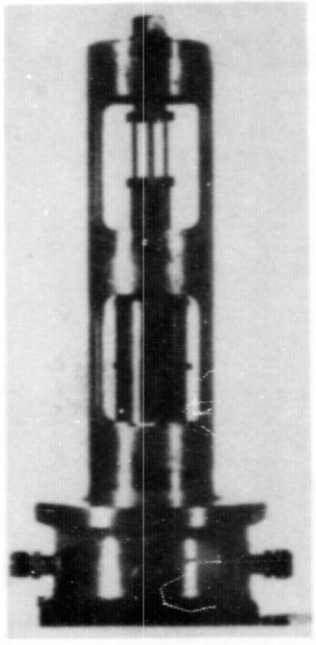

b) Test Vessel Open with Smooth Specimen in Place and Extensometer Attached

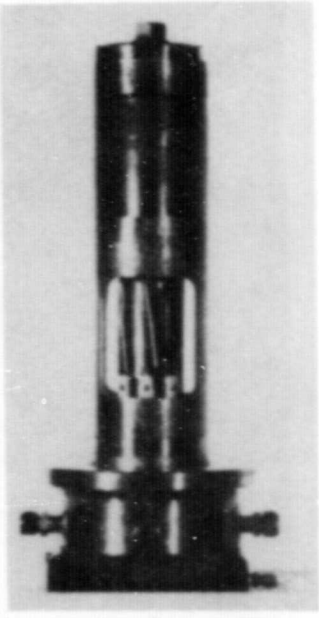

c) Test Vessel Open with Furnace Attached

FD 223764

Figure 22. Views of Tensile Test Vessel

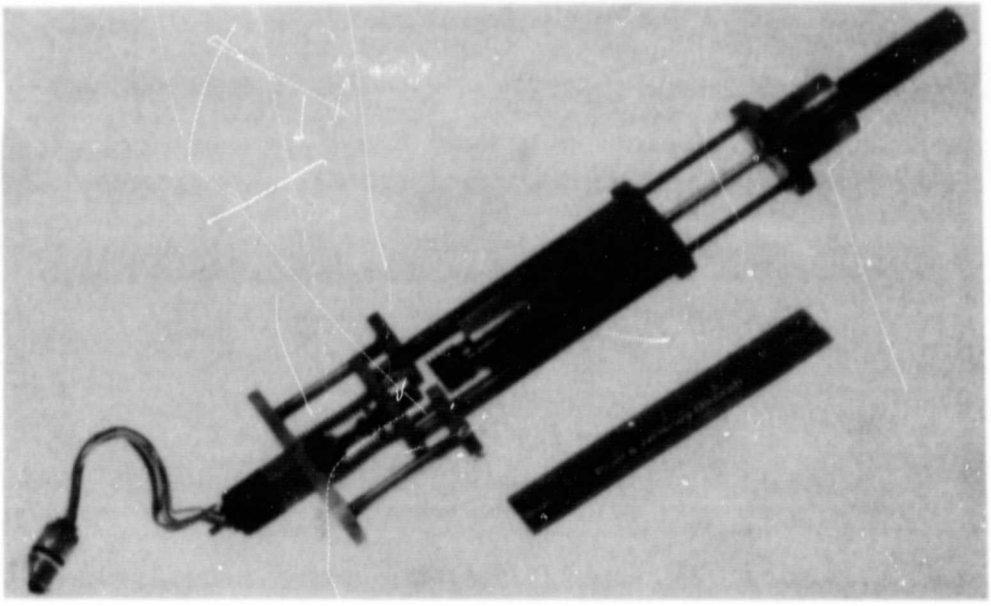

Figure 23. Averaging Type LVDT Extensometer System

Periodic checks of hydrogen test environments revealed oxygen levels less than 1 ppm. This purity level was obtained using the following test procedure:

1. Secure pressure vessel
2. Pressurize to 0.345 MPa (50 psig) with nitrogen gas and leak check
3. Vent system to 0.0345 MPa (5 psig)
4. Repressurize and vent with nitrogen gas (steps 2 and 3) two additional times
5. Pressure purge to 3.45 MPa (500 psig) with hydrogen gas
6. Evacuate pressure vessel, gas supply, and sampling system to an indicated absolute pressure of 0.00007 MPa (0.0096 psia, 500 microns)
7. Repressurize and evacuate system (steps 5 and 6) two additional times
8. Pressurize system to 3.45 MPa (500 psig) with hydrogen gas and obtain gas sample
9. Pressurize to 34.5 MPa (5,000 psig) with hydrogen gas and conduct test
10. Vent to atmospheric pressure, flow and pressure purge with nitrogen gas, open pressure vessel and remove failed specimen.

Tensile properties, including 0.2% offset yield strength, ultimate strength, percent elongation, reduction of area, and modulus of elasticity were obtained for all specimen tests from the load-deflection X-Y plotter curves.

SECTION V
CREEP-RUPTURE

A. INTRODUCTION

The creep-rupture properties of two single crystal nickel-base alloys were determined in 34.5 MPa (5000 psig) hydrogen and hydrogensteam environments at 760°C (1400°F) and 871°C (1600°F). Testing established creep rate, rupture life, elongation, and reduction of area in the longitudinal direction for single crystal MAR-M-246+Hf and PWA 1480. Data from previously tested Directionally Solidified MAR-M-246+Hf (from NAS8-30744, FR-7746) is presented for comparison.

B. RESULTS AND CONCLUSIONS

Creep stress vs time curves for SC MAR-M-246+Hf and PWA 1480 are presented in figures 24 through 27. Time to creep 0.5%, 1.0% 2.0%, and rupture are given for the alloys at 760°C (1400°F) and 871°C (1600°F) in both hydrogen and hydrogen-water vapor environments. Figure 28 depicts stress-rupture properties of DS MAR-M-246+Hf from earlier contract work.

At 760°C (1400°F), PWA 1480 was superior in stress rupture to SC and DS MAR-M-246+Hf by approximately one half to one order of magnitude (figures 27 and 28). The DS MAR-M-246+Hf was generally superior to the SC MAR-M-246+Hf by between 10% and nearly an order of magnitude. This wide variation may be attributed to single crystal orientation angle and/or data scatter with limited testing.

At 871°C (1600°F) the same rank order exists for the stress rupture properties of the alloys, i.e., PWA 1480 followed by DS MAR-M-246+Hf, then SC MAR-M-246+Hf. The PWA 1480 material had approximately one half an order of magnitude improvement in stress rupture life over the SC MAR-M-246+Hf, and general superiority over the DS MAR-M-246+Hf between zero (no difference) and one half an order of magnitude.

The presence of water vapor (50% by weight) in the hydrogen atmosphere had no effect on the creep-rupture properties of PWA 1480 at 871°C (1600°F). However the creep-rupture behavior of SC MAR-M-246+Hf was degraded significantly, with a 70% reduction in stress rupture life due to the addition of water vapor to the environment when compared with hydrogen alone.

Creep strain vs time curves are plotted in figures 29 through 32 for all creep testing under this contract, and in figures 33 through 36 for the DS MAR-M-246+Hf tested under previous contract work (NAS8-30744, FR-7746).

As with the tensile and other testing under this contract, these conclusions are based on very limited testing (only a single H_2+H_2O test to examine environmental degradation) and the results could change with additional investigation using a statistically based test matrix. Other factors such as anisotropy, primary crystal axis orientation, and random data scatter may also have a large effect.

Results for the creep testing are listed in table 14.

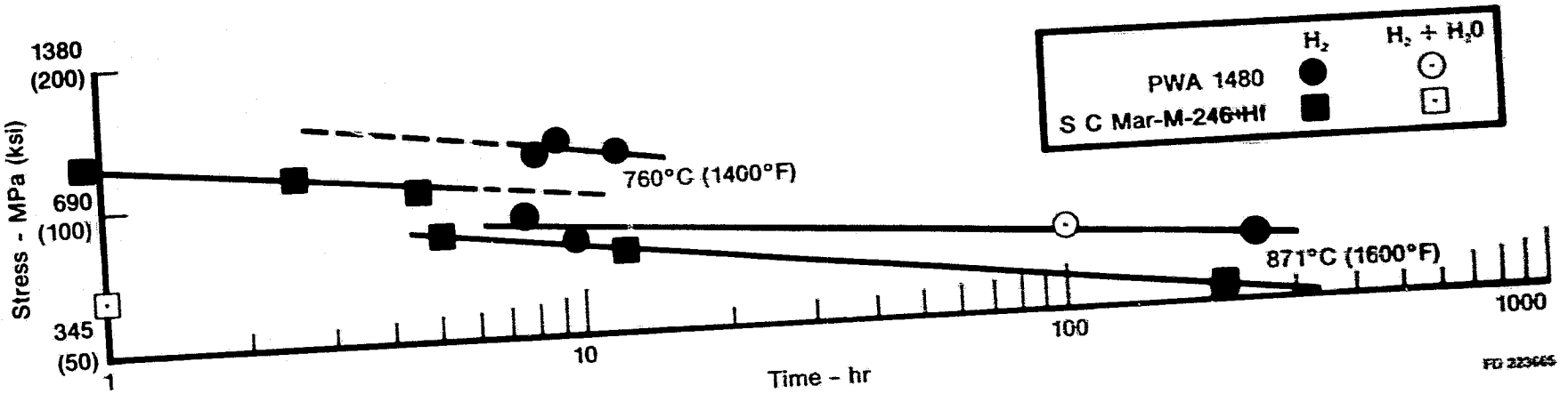

Figure 24. Creep Results of PWA 1480 and Single Crystal MAR-M-246 + Hf in 34.5 MPa (5000 psig) Gaseous Hydrogen Environments (Time to Creep 0.5%, Longitudinal Direction)

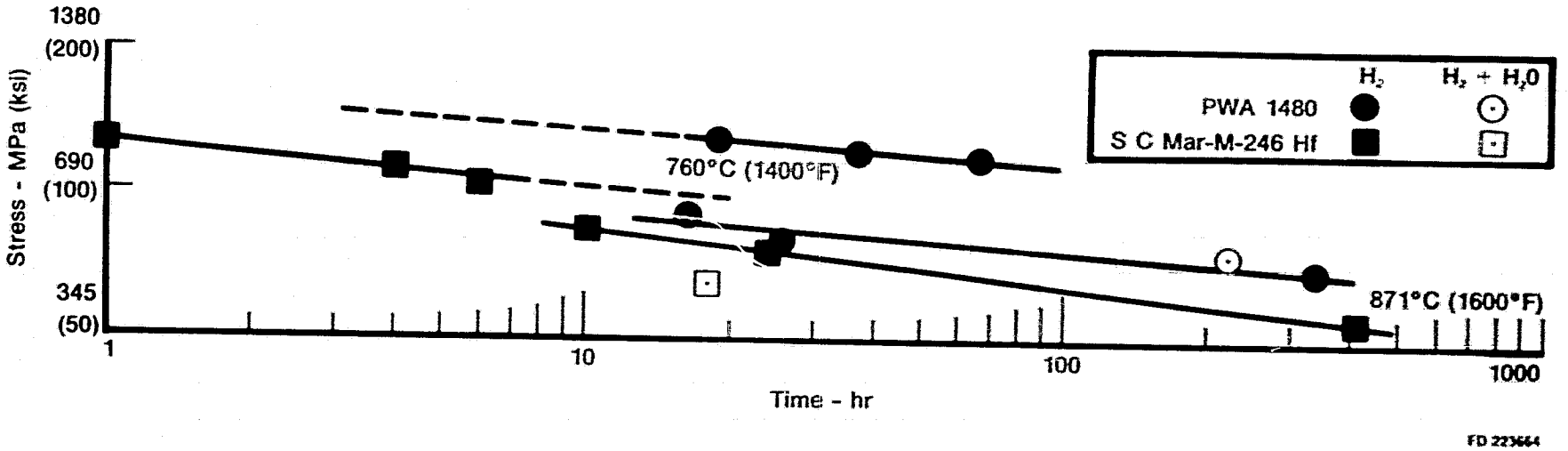

Figure 25. Creep Results of PWA 1480 and Single Crystal MAR-M-246 + Hf in 34.5 MPa (5000 psig) Gaseous Hydrogen Environments (Time to Creep 1.0%, Longitudinal Direction)

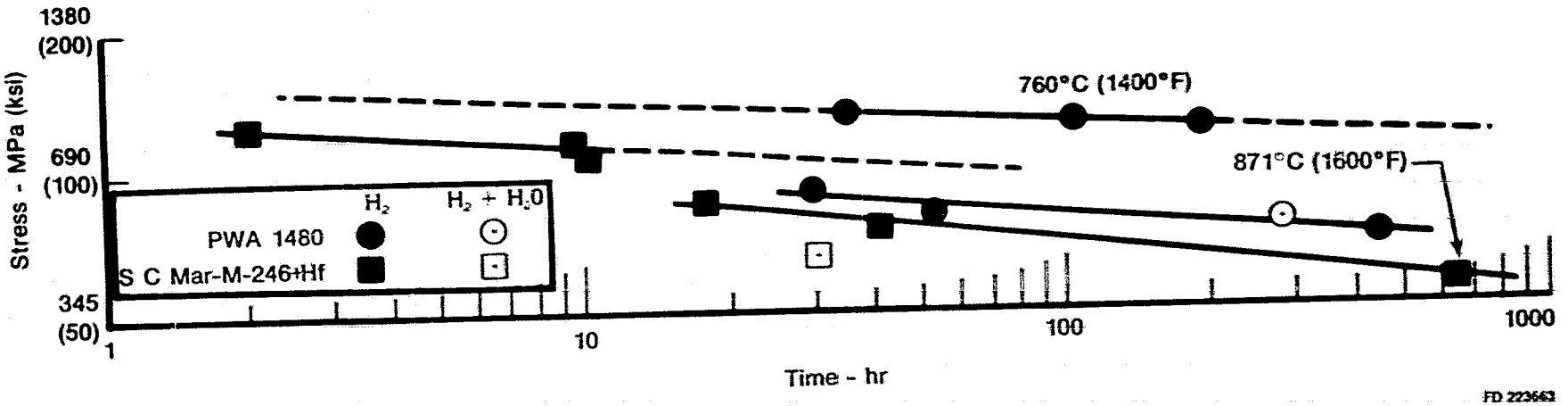

Figure 26. Creep Results of PWA 1480 and Single Crystal MAR-M-246 + Hf in 34.5 MPa (5000 psig) Gaseous Hydrogen Environments (Time to Creep 2.0%, Longitudinal Direction)

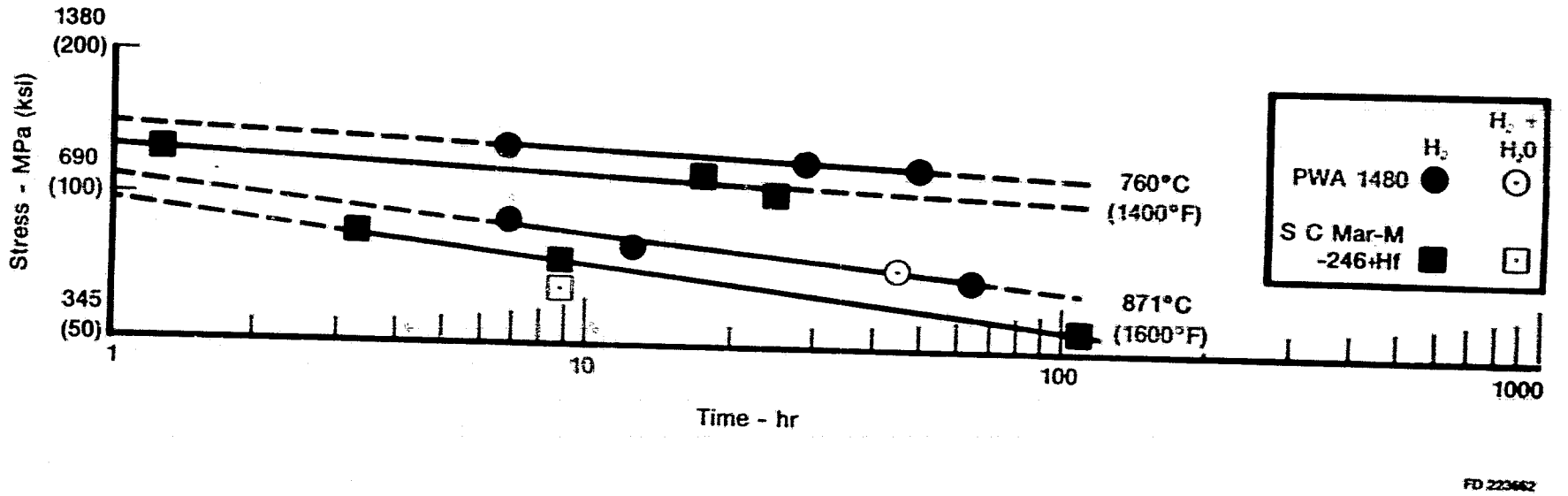

Figure 27. Stress-Rupture of PWA 1480 and Single Crystal MAR-M-246 + Hf in 34.5 MPa (5000 psig) Gaseous Hydrogen Environments (Time to Rupture Longitudinal Direction)

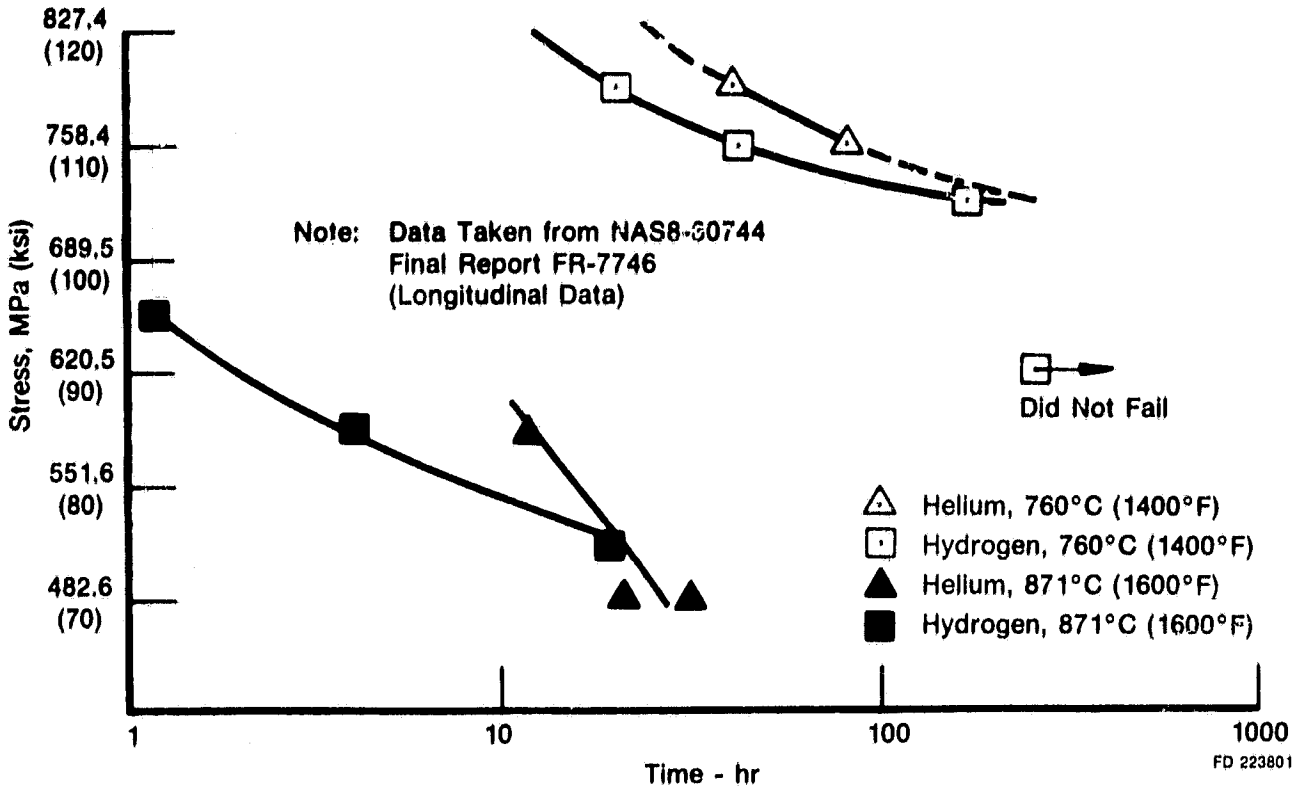

Figure 28. Stress-Rupture of Directionally Solidified (DS) MAR-M-246 + Hf in 34.5 MPa (5000 psig) Helium and Hydrogen (Longitudinal Direction)

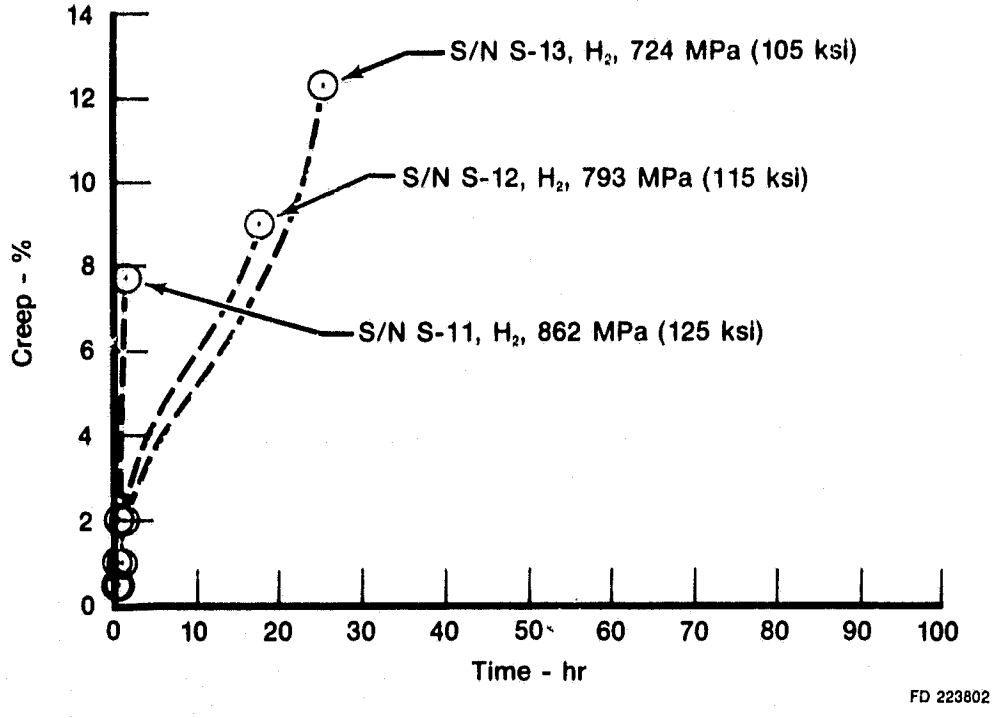

Figure 29. Creep Stress-Rupture for Single Crystal MAR-M-246 + Hf at 760°C (1400°F) in 34.5 MPa (5000 psig) Hydrogen Environment (Longitudinal Orientation)

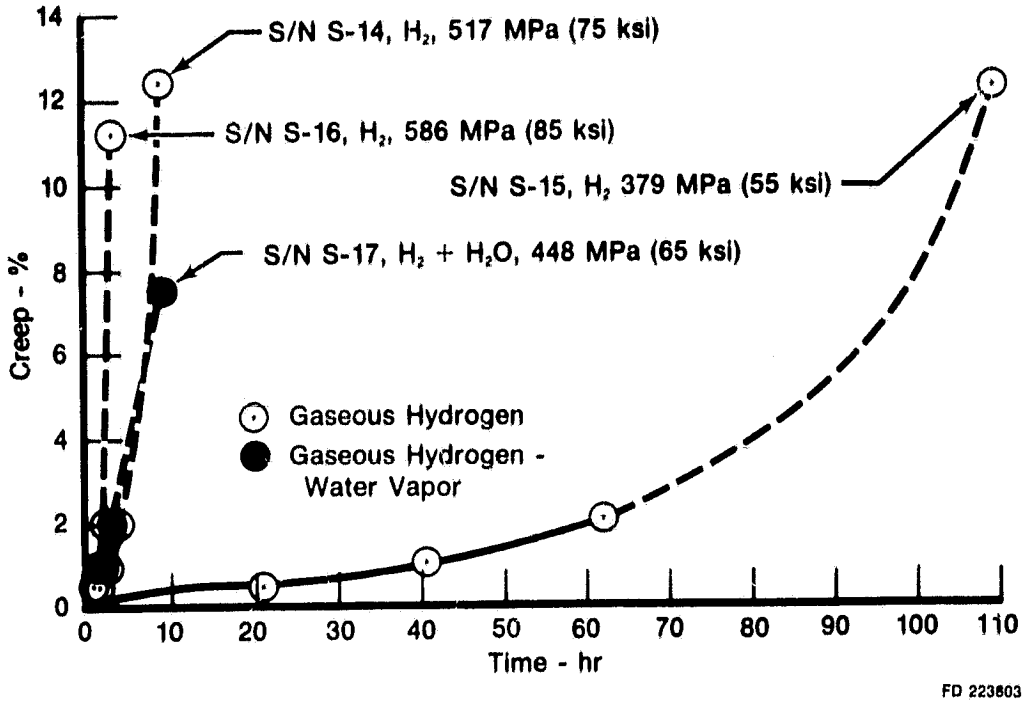

Figure 30. Creep Stress-Rupture for Single Crystal MAR-M-246 + Hf at 871°C (1600°F) in 34.5 MPa (5000 psig) Hydrogen Environment (Longitudinal Orientation)

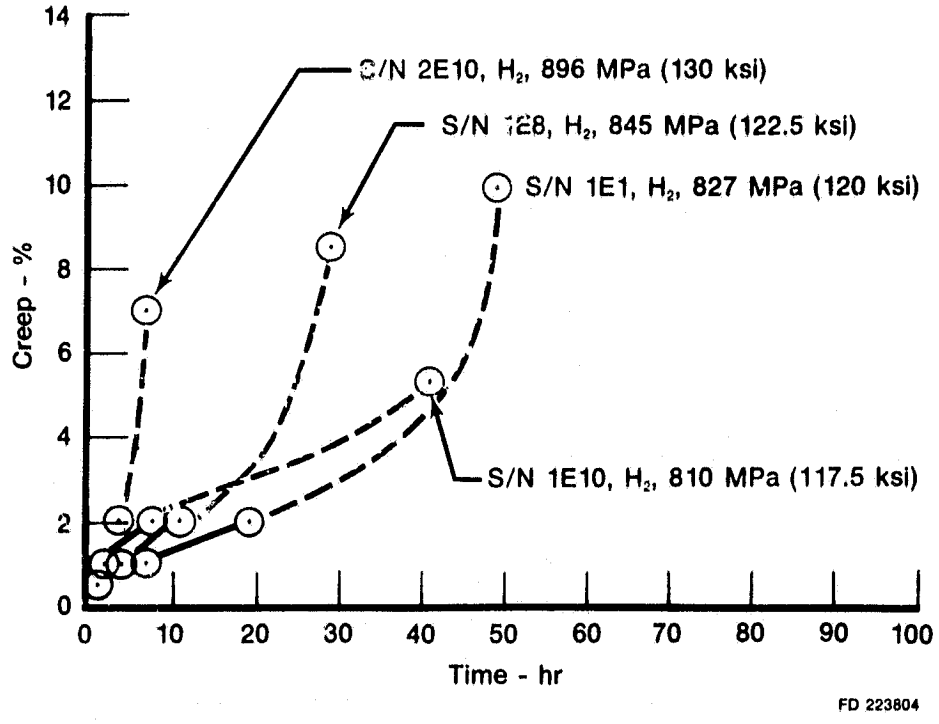

Figure 31. Creep Stress-Rupture for PWA 1480 at 760°C (1400°F) in 34.5 MPa (5000 psig) Hydrogen Environment (Longitudinal Orientation)

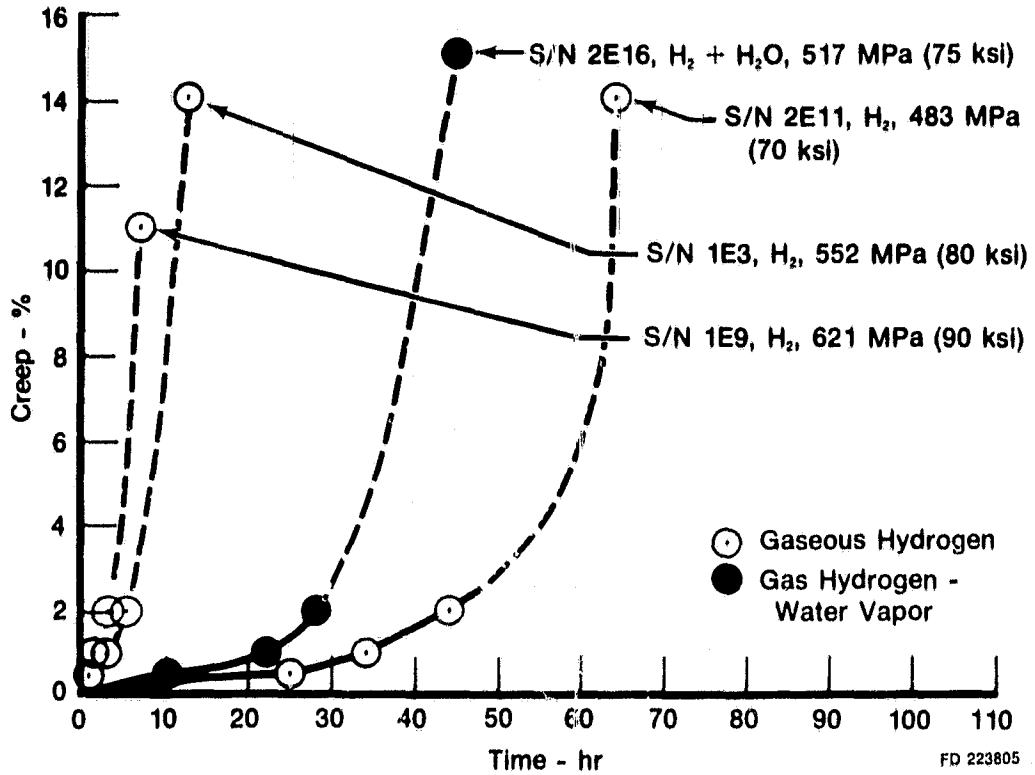

Figure 32. Creep Stress-Rupture for PWA 1480 at 871°C (1600°F) in 34.5 MPa (5000 psig) Hydrogen Environment (Longitudinal Orientation)

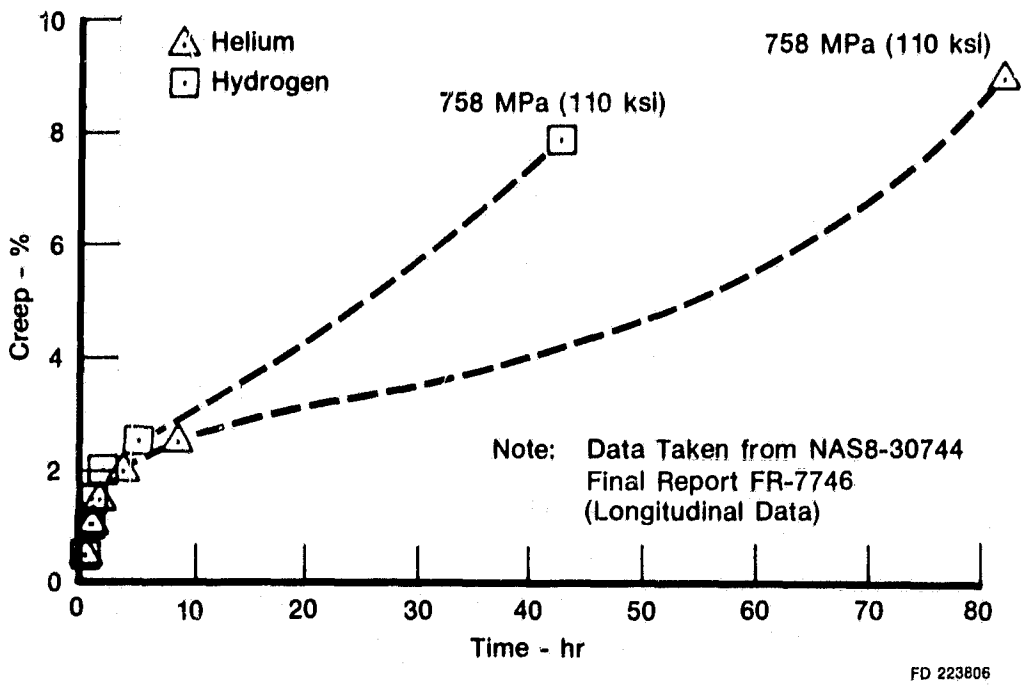

Figure 33. Creep Stress-Rupture of Directionally Solidified (DS) MAR-M-246 + Hf in 34.5 MPa (5000 psig) Gaseous Environments (Longitudinal Direction)

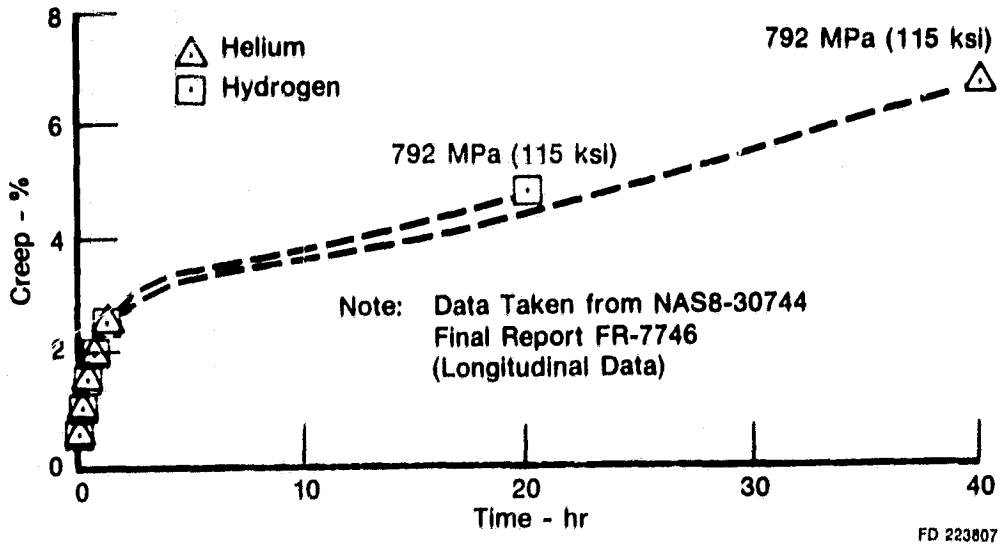

Figure 34. Creep Stress-Rupture of Directionally Solidified (DS) MAR-M-246 + Hf in 760°C (1400°F) 34.5 MPa (5000 psig) Gaseous Environments (Longitudinal Direction)

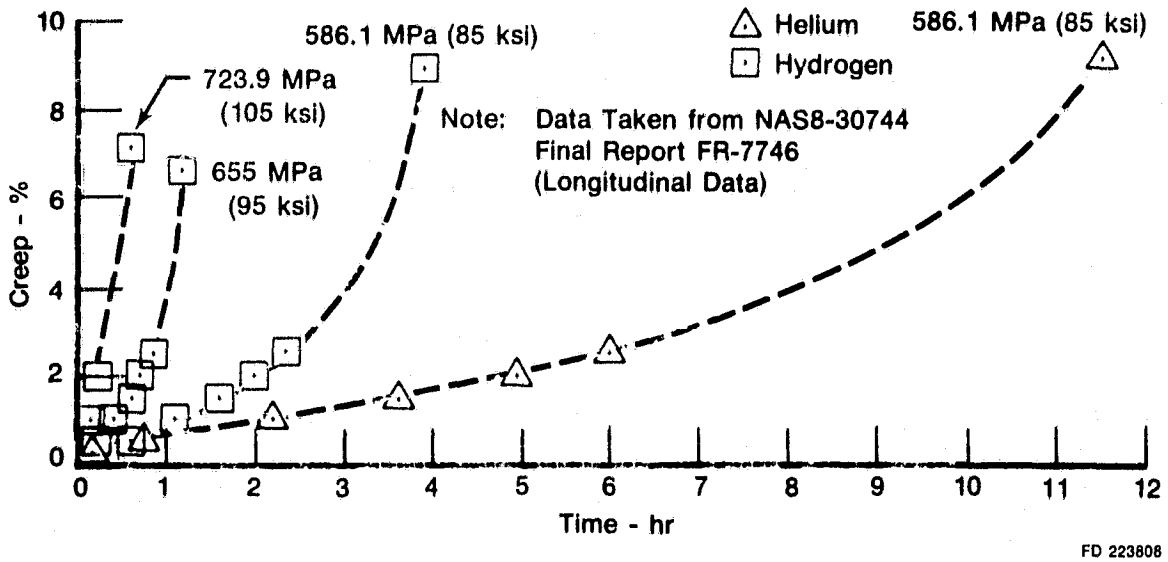

Figure 35. Creep Stress-Rupture of Directionally Solidified (DS) MAR-M-246 + Hf in 871°C (1600°F) 34.5 MPa (5000 psig) Gaseous Environments (Longitudinal Direction)

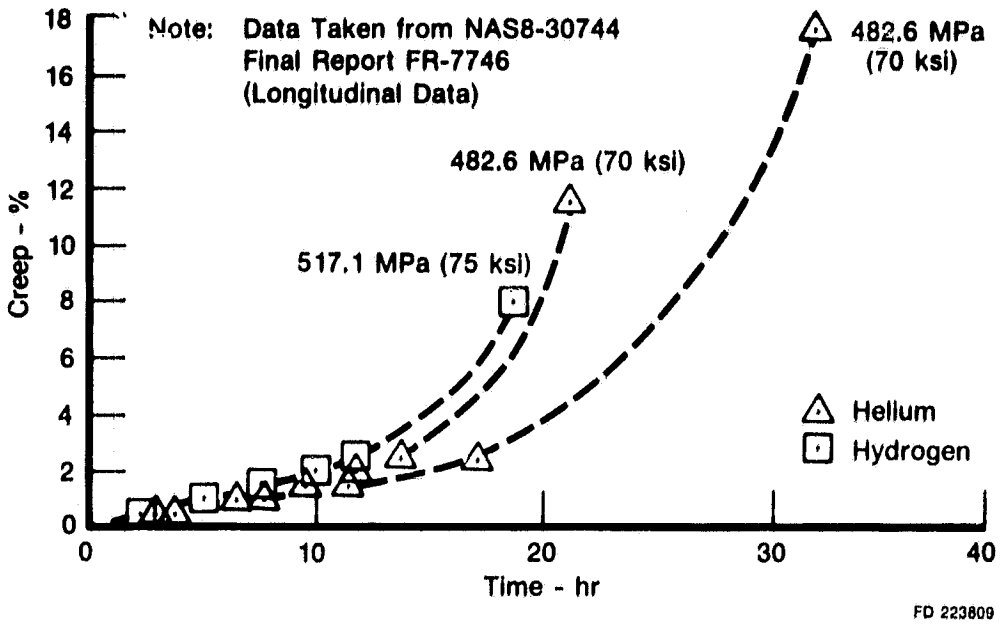

Figure 36. Creep Stress-Rupture of Directionally Solidified (DS) MAR-M-246 + Hf in 871°C (1600°F) 34.5 MPa (5000 psig) Gaseous Environments (Longitudinal Direction)

Table 14. Creep Rupture Results for Turbine Blade Alloys (34.5 MPa (5000 psig) Hydrogen Environments, Longitudinal Orientation)

Material	Environment	S/N	Stress		Time To Creep (hr)				Elongation (%)	Reduction Of Area (%)	Temperature	Angle From [001]
			Mpa	KSI	0.5% Creep	1% Creep	2% Creep	Rupture				
MAR-M-246+Hf SC	H_2	S-13	724	105	0.45	0.60	1.01	25.1	12.3	15.9	760°C (1400°F)	—
MAR-M-246+Hf SC	H_2	S-12	793	115	0.25	0.40	0.95	17.5	9.0	13.6	760°C (1400°F)	—
MAR-M-246+Hf SC	H_2	S-11	862	125	0.09	0.10	0.20	1.35	7.7	9.6	760°C (1400°F)	—
MAR-M-246+Hf SC	H_2	S-15	379	55	21.20	41.30	63.80	109.10	13.20	50.1	871°C (1600°F)	—
MAR-M-246+Hf SC	H_2	S-14	517	75	1.20	2.40	4.10	8.90	12.40	31.40	871°C (1600°F)	—
MAR-M-246+Hf SC	H_2	S-16	586	85	0.50	1.01	1.78	3.30	11.20	25.60	871°C (1600°F)	—
MAR-M-246+Hf SC	H_2+H_2O	S-17	448	65	0.10	1.80	3.00	8.90	7.50	15.60	871°C (1600°F)	—
PWA 1480	H_2	1E10	810.2	117.5	1.15	1.90	7.50	40.70	5.3	10.7	760°C (1400°F)	8.5°
PWA 1480	H_2	1E1	827.4	120.0	1.18	6.70	19.08	49.60	9.9	19.3	760°C (1400°F)	5.0°
PWA 1480	H_2	1E8	844.6	122.5	0.80	3.65	10.55	19.10	8.5	13.1	760°C (1400°F)	6.5°
PWA 1480	H_2	2E10	896.4	130.0	0.89	1.92	3.48	6.70	7.0	12.2	760°C (1400°F)	8.5°
PWA 1480	H_2	1E9	620.5	90.9	0.75	1.65	2.95	6.9	11.0	21.6	871°C (1600°F)	1.5°
PWA 1480	H_2	1E3	551.6	80.0	0.95	2.6	5.03	12.7	14.1	29.0	871°C (1600°F)	8.5°
PWA 1480	H_2	2E11	482.6	70.0	25.0	34.01	44.0	64.4	14.1	30.2	871°C (1600°F)	1.5°
PWA 1480	H_2+H_2O	2E16	517.1	75.0	10.0	22.2	28.0	45.1	15.1	30.8	871°C (1600°F)	9.0°

C. TEST PROCEDURE

Creep-rupture tests were conducted per ASTM E139-70, "Conducting Creep, Creep-Rupture, and Stress-Rupture Tests of Metallic Materials," where applicable, using round externally pressurized specimens. The test specimens used for the creep testing are described in Section III and detailed in figures 9 and 12.

All tests were conducted on a modified 53.4-kN (12,000-lb) capacity Arcweld Model JE creep-rupture machine. The test machine was explosion-proofed and located in a test cell open to the atmosphere (figure 37). Controls and data recording equipment were located in an adjacent blockhouse. A high-pressure test vessel (figures 37 and 38), similar in design and operation to the vessels used for the tensile and LCF tests, was suspended in the test machine and counterbalanced to maintain the load lever arm in a level position.

The design of the test specimen included pin holes for positive location and gripping of creep-measuring extensometer heads. Load rods and adapters incorporated pin joints, which, in effect, formed universal joints at the ends of the specimen to eliminate alignment errors and bending stresses on the specimen.

The extensometer system was a dual LVDT averaging-type and was located inside the high pressure vessel. The extensometer output was recorded in the adjacent blockhouse as elongation vs time for all creep-rupture tests. The extensometer system is shown in figure 39.

Elevated temperatures were obtained using a two-zone resistance-type furnace with individual zone temperature control and monitoring. The independent zone control provided even temperature over the specimen gage length. Temperature was monitored and controlled by three thermocouples looped around the specimen gage section. The furnace system was contained within the pressure vessel (figure 38C). The thermocouples and furnace leads can be seen extending to the base of the furnace in this figure.

The test and gas handling procedures used for the tensile tests were also used for the creep-rupture tests.

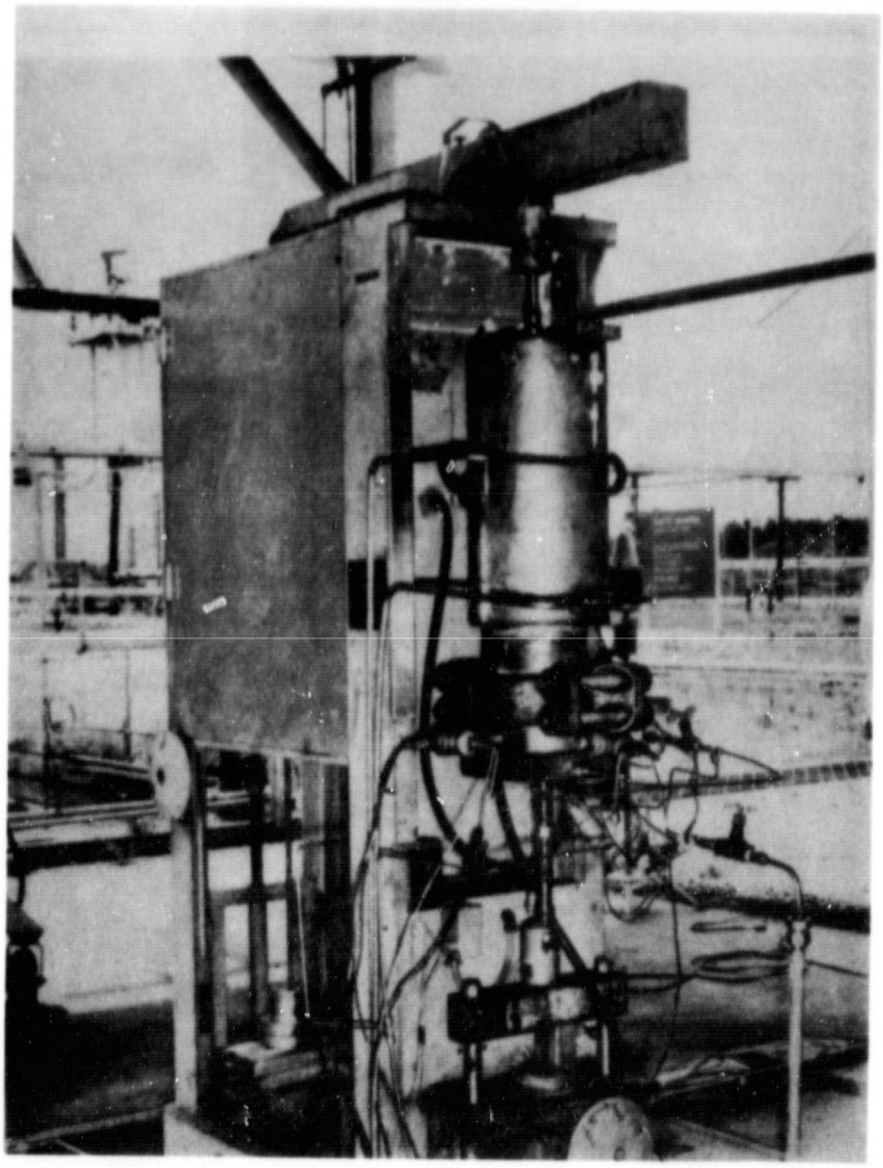

FC 42103
FD 92653

Figure 37. Creep Rupture Machine With Pressure Vessel Installed, Located in Test Cell

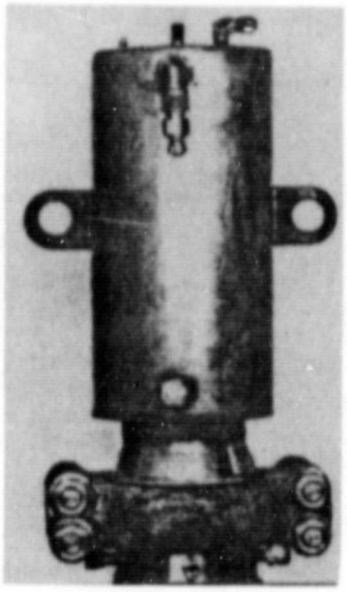

(a) Vessel Closed

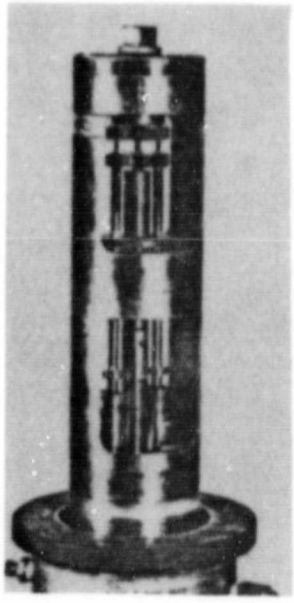

(b) Vessel Open Showing DS Material Specimen in Place

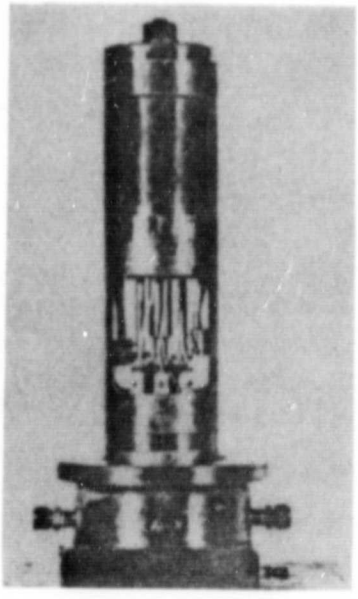

(c) Vessel Open With Furnace Installed

FD 101197A

Figure 38. Views of Creep-Rupture Pressure Vessel

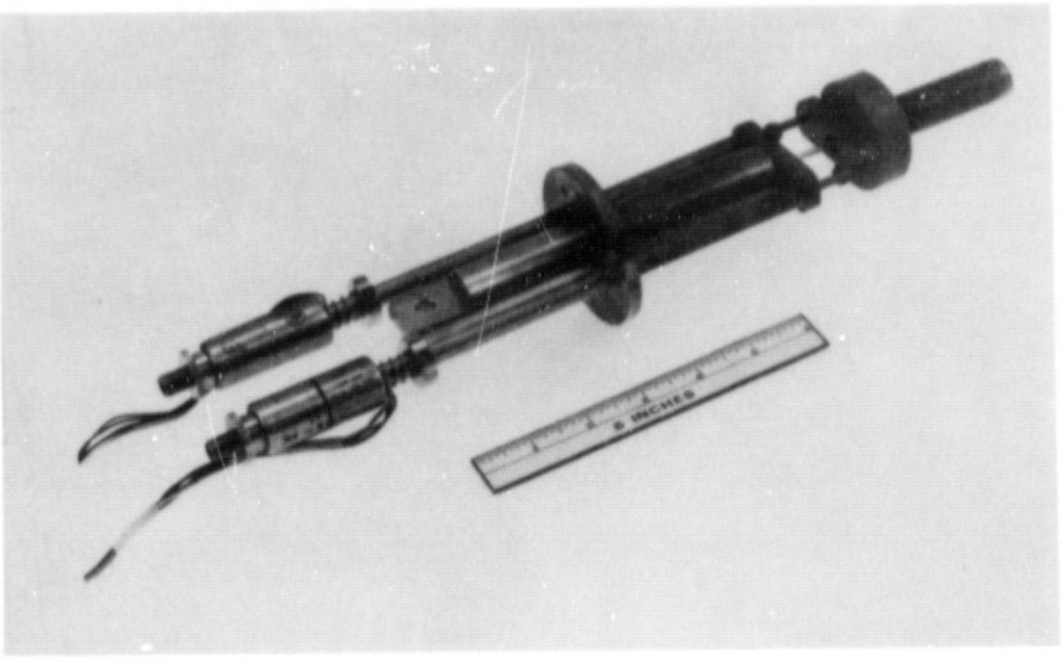

Figure 39. Creep Extensometer System

SECTION VI
LOW CYCLE FATIGUE

A. INTRODUCTION

Strain controlled low cycle fatigue (LCF) tests were conducted to establish cyclic life of single crystal and directionally solidfied MAR-M-246+Hf and PWA 1480 in gaseous hydrogen and steam enriched hydrogen environments. Specimens were oriented in both transverse and longitudinal directions relative to the casting solidification direction. Specimen orientations are shown in figures 6 and 12.

Smooth, round, solid specimens were used for the strain-controlled LCF tests conducted under this contract. The test specimen is depicted in figure 10. The specimen configuration incorporates integral machined extensometer collars. A calibration procedure has been established to relate the maximum strain-to-collar deflection during both the elastic and plastic portion of the strain cycle. The specimen design and calibration procedure were verified both experimentally and analytically.

Isothermal strain-controlled LCF characteristics were determined using a servo hydraulic, closed-loop on axial strain, LCF testing machine, designed and built at P&WA/GPD. The test machine is located in an isolated test cell with all controls and instrumentation located in an adjacent blockhouse.

Specimen axial strain was measured and controlled by means of a proximity probe extensometer. Split extensometer heads were attached to the specimen by mating the grooves in the heads with the integral collars on the specimen and bolting the assembly together. Collar deflection was measured and controlled via proximity probes attached to the open ends of the extensometer tubes so that the extensometer rod ends moved relative to the probes as the specimen collars deflected.

A typical cycle for a cyclic nondwell test with a fully reversed strain cycle ($\bar{\epsilon} = 0$) is illustrated in figure 40.

B. RESULTS AND CONCLUSIONS

Low cycle fatigue test results for all three alloys are presented in tables 15 through 19. Composite plots of all of the LCF hydrogen data produced in this contract plus DS and SC MAR M-246+Hf data generated under a previous contract (NAS8-33109, FR-11852) at 760°C (1400°F) appear in figures 41 and 42.

Some SC MAR-M-246+Hf data from the previous contract is classified as longitudinal since the crystal orientation was such that a primary axis was coincident with the loading axis of the specimen. This data was termed transverse in the previous report (FR-11852). From the composite plots in figures 41 and 42 it can be seen that at 760°C (1400°F) and $\Delta\epsilon_{total}$ above 1.5% the rank order of the fatigue capabilities is: PWA 1480 longitudinal, SC MAR-M-246+Hf transverse*, PWA 1480 transverse, SC MAR-M-246+Hf transverse and DS MAR-M-246+Hf transverse. At lower strain ranges (approximately 1.0%) the rank order is: SC MAR-M-246+Hf transverse*, PWA 1480 longitudinal, PWA 1480 transverse, SC MAR-M-246+Hf and DS MAR-M-246+Hf transverse.

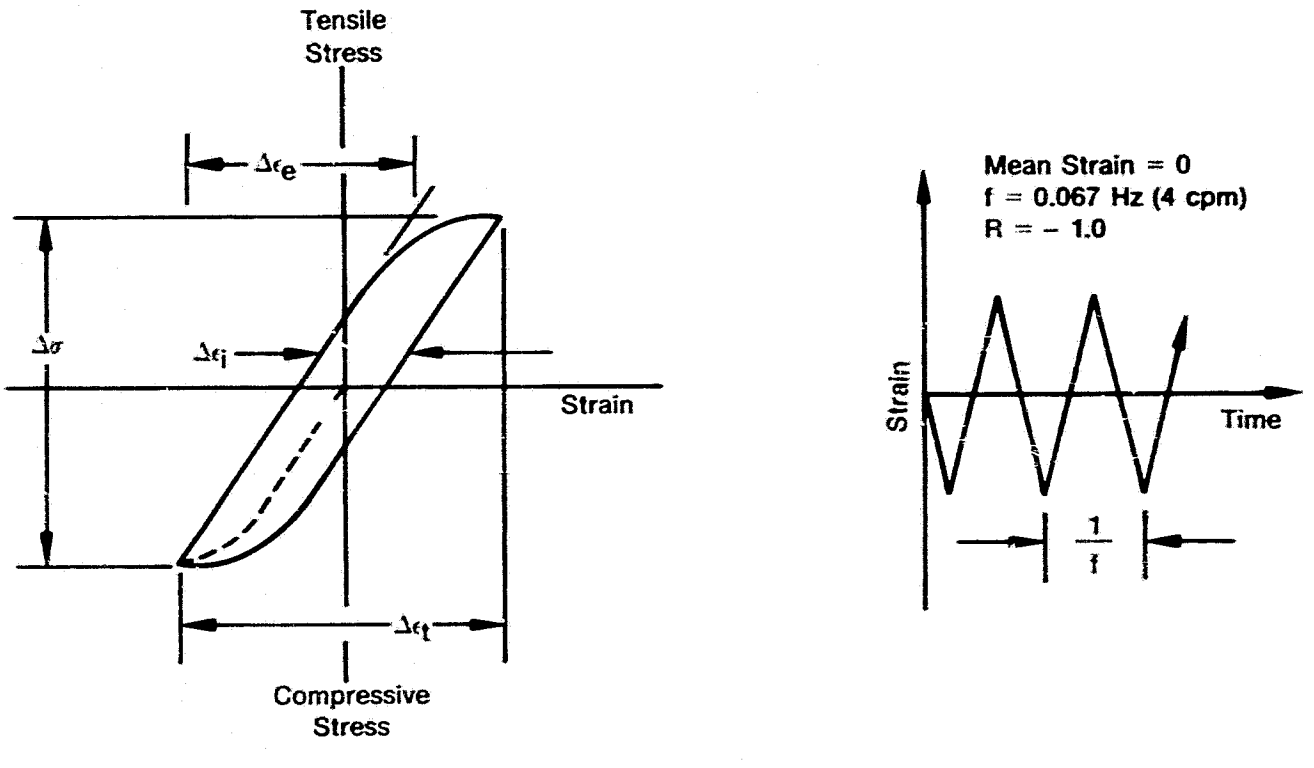

$\Delta\sigma$ = Total Stress Range
$\Delta\epsilon_t$ = Total Strain Range = $\Delta\epsilon_e + \Delta\epsilon_i$
$\Delta\epsilon_i$ = Inelastic Strain Range
$\Delta\epsilon_e$ = Elastic Strain Range = $\Delta\epsilon_t - \Delta\epsilon_i$
R = Minimum Strain/Maximum Strain
f = Cyclic Frequency

FD 223651

Figure 40. Typical Nondwell LCF Test With Mean Strain of Zero

Table 15. Strain Control LCF Results for PWA 1480 (Longitudinal Orientation) in Hydrogen Atmosphere at 34.5 MPa (5000 psig) Mean Strain = 0 Frequency = 0.067 Hz (4 cpm)

		Strain ϵ_t					
				Inelastic			
S/N	Temperature	Total	Elastic	Average	Min	Max	Cycles to Failure
AE-2	760°C (1400°F)	2.0	1.94	0.06	0.05	0.07	1,230
AR-2	760°C (1400°F)	1.5	1.49	0.015	<0.01	0.02	4,649
AZ-2	760°C (1400°F)	2.5	2.37	0.125	0.10	0.15	387
AS-2	760°C (1400°F)	1.2	1.19	<0.01	<0.01	0.01	8,914
BA-2	871°C (1600°F)	2.0	1.83	0.15	0.16	0.17	631
BB-2	871°C (1600°F)	1.5	1.43	0.07	0.06	0.08	1,047
F-1	871°C (1600°F)	2.5	2.17	0.325	0.30	0.35	123
K-2	871°C (1600°F)	1.0	0.96	0.035	<0.03	0.04	5,544

Table 16. Strain Control LCF Results for PWA 1480 (Transverse Orientation) in Hydrogen Atmosphere at 34.5 MPa (5000 psig) Mean Strain = 0 Frequency = 0.067 Hz (4 cpm)

		Strain ϵ_t					
				Inelastic			
S/N	Temperature	Total	Elastic	Average	Min	Max	Cycles to Failure
4L	760°C (1400°F)	1.5	1.43	0.07	0.08	0.09	442
5L	760°C (1400°F)	1.0	0.98	<0.015	0.01	<0.02	6,275
6L-2	760°C (1400°F)	2.0	1.51	0.49	0.43	0.55	33
7L	871°C (1600°F)	1.5	1.14	0.36	0.34	0.38	126
8L	871°C (1600°F)	1.0	0.87	0.13	0.12	0.14	474
9L	871°C (1600°F)	0.75	0.69	0.055	0.04	0.07	2,425

Table 17. Strain Control LCF Results for Directionally Solidified MAR-M-246+Hf (Transverse Orientation) in Hydrogen Atmosphere at 34.5 MPa (5000 psig) Mean Strain = 0 Frequency = 0.067 Hz (4 cpm)

		Strain ϵ_t					
				Inelastic			
S/N	Temperature	Total	Elastic	Average	Min	Max	Cycles to Failure
D-14	871°C (1600°F)	0.9	0.86	0.04	0.02	0.06	826
D-15	871°C (1600°F)	1.2	1.09	0.11	0.08	0.14	230
D-16	871°C (1600°F)	0.7	0.69	<0.01	<0.01	0.01	1,276
D-17	871°C (1600°F)	0.5	0.49	<0.01	<0.01	<0.01	8,435

Table 18. Strain Control LCF Results for Single Crystal MAR-M-246+Hf (Transverse Orientation) in Hydrogen Atmosphere at 34.5 MPa (5000 psig) Mean Strain = 0 Frequency = 0.067 Hz (4 cpm)

		Strain, %					
				Inelastic			
S/N	Temperature	Total	Elastic	Average	Min	Max	Cycles to Failure
TS 11	871°C (1600°F)	1.00	0.89	0.11	0.08	0.13	885
TS 13	871°C (1600°F)	1.50	1.21	0.29	0.26	0.32	65
TS 15	871°C (1600°F)	0.70	0.66	0.04	0.03	0.05	26,959
TS 16	871°C (1600°F)	0.80	0.75	0.05	0.03	0.07	66,349
TS 18	871°C (1600°F)	1.0	0.90	0.095	0.08	0.11	6,579*

*Did not fail
(Termination caused by instrument malfunction)

Table 19. Strain Control LCF Results of Turbine Blade Alloys in Gaseous H$_2$+H$_2$O (50% Water Vapor by Weight) at 34.5 MPa (5000 psig) Mean Strain = 0 Frequency = 0.067 Hz (4 cpm)

				Strain, %					
						Inelastic			
Alloy	Orientation	S/N	Temperature	Total	Elastic	Average	Min	Max	Cycles to Failure
PWA 1480	Transverse	13-L	871°C (1600°F)	1.0	0.855	0.145	0.14	0.15	552
PWA 1480	Longitudinal	L-2	871°C (1600°F)	1.5	1.37	0.13	0.09	0.17	878
DS MAR-M-246+Hf	Transverse	D-18	871°C (1600°F)	0.9	0.83	0.07	0.06	0.08	340
SC MAR-M-246+Hf	Transverse	TS-17	871°C (1600°F)	1.0	0.94	0.06	0.05	0.07	5,791

At 871°C (1600°F) and $\Delta\epsilon_{total}$ above 1.3% the rank order of the fatigue capabilities is: PWA 1480 longitudinal, PWA 1480 transverse, DS MAR-M-246+Hf transverse, SC MAR-M-246+Hf transverse. Here the PWA 1480 longitudinal material had a fatigue capability approximately one order of magnitude greater than the other alloys, and there was little difference between PWA 1480, DS MAR-M-246+Hf and SC MAR-M-246+Hf in the transverse direction. At the lower strain ranges the rank order is: SC MAR-M-246+Hf transverse, PWA 1480 longitudinal, PWA 1480 transverse, and DS MAR-M-246+Hf transverse. At these conditions there was little difference between the SC MAR-M-246+Hf transverse and PWA 1480 longitudinal. Fatigue lives were also similar between PWA 1480 transverse and DS MAR-M-246+Hf transverse. There was a significant difference between the pairs with the SC MAR-M-246+Hf transverse and PWA 1480 longitudinal pair having a fatigue life approximately one order of magnitude greater than the PWA 1480 transverse and DS MAR-M-246+Hf transverse pair.

*This material more closely exhibited longitudinal behavior due to the transverse orientation of the cast bar supplying the specimens actually being aligned with a principal crystal axis. This data was from earlier testing (NAS8-33109, FR-11852).

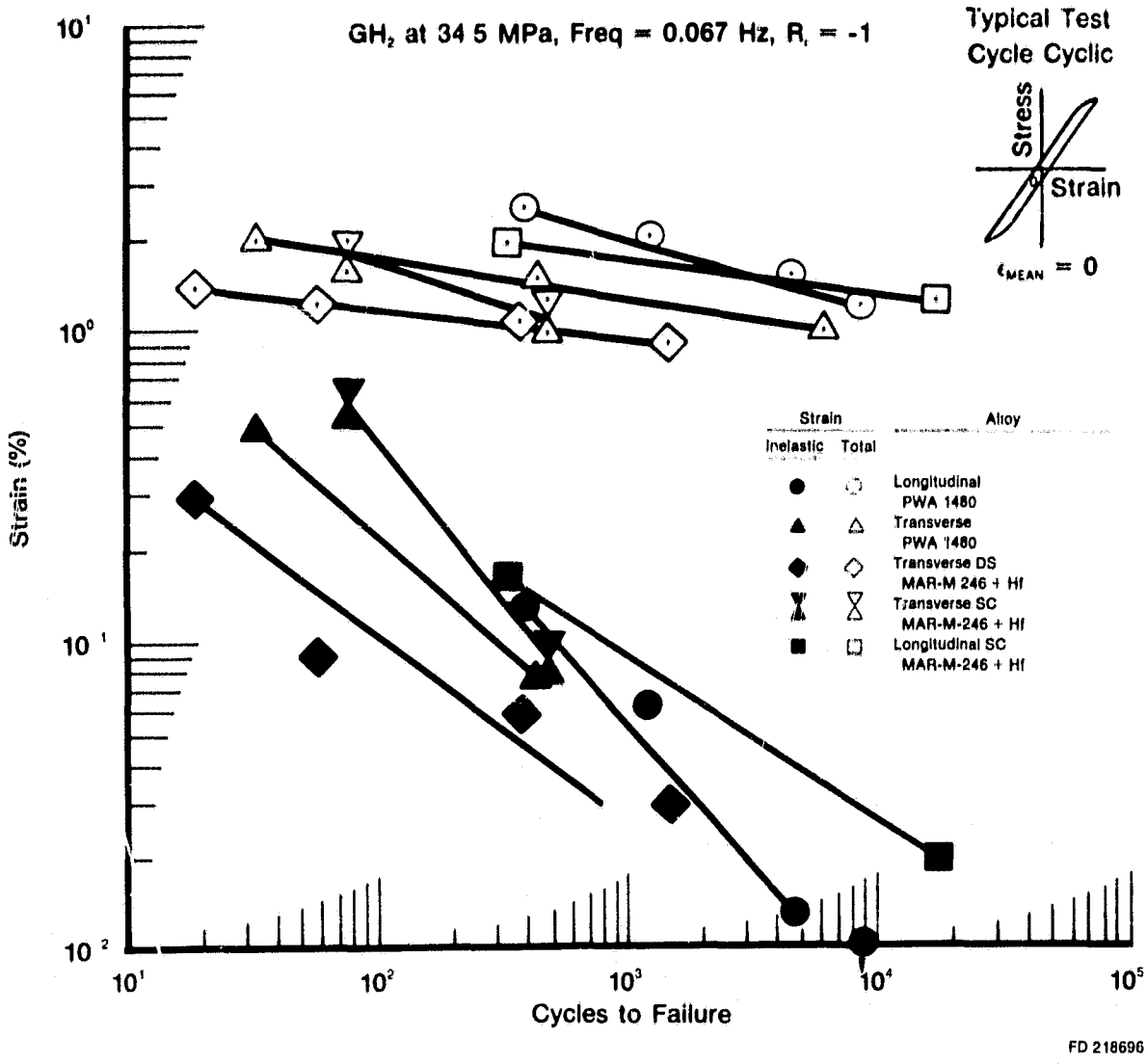

Figure 41. Comparison of PWA 1480 (Longitudinal and Transverse) Transverse SC and DS, MAR-M-246 + Hf and Longitudinal SC, MAR-M-246 + Hf in GH_2 at 34.5 MPa, Frequency = 0.067 Hz, R = −1, Temperature = 760°C (1400°F)

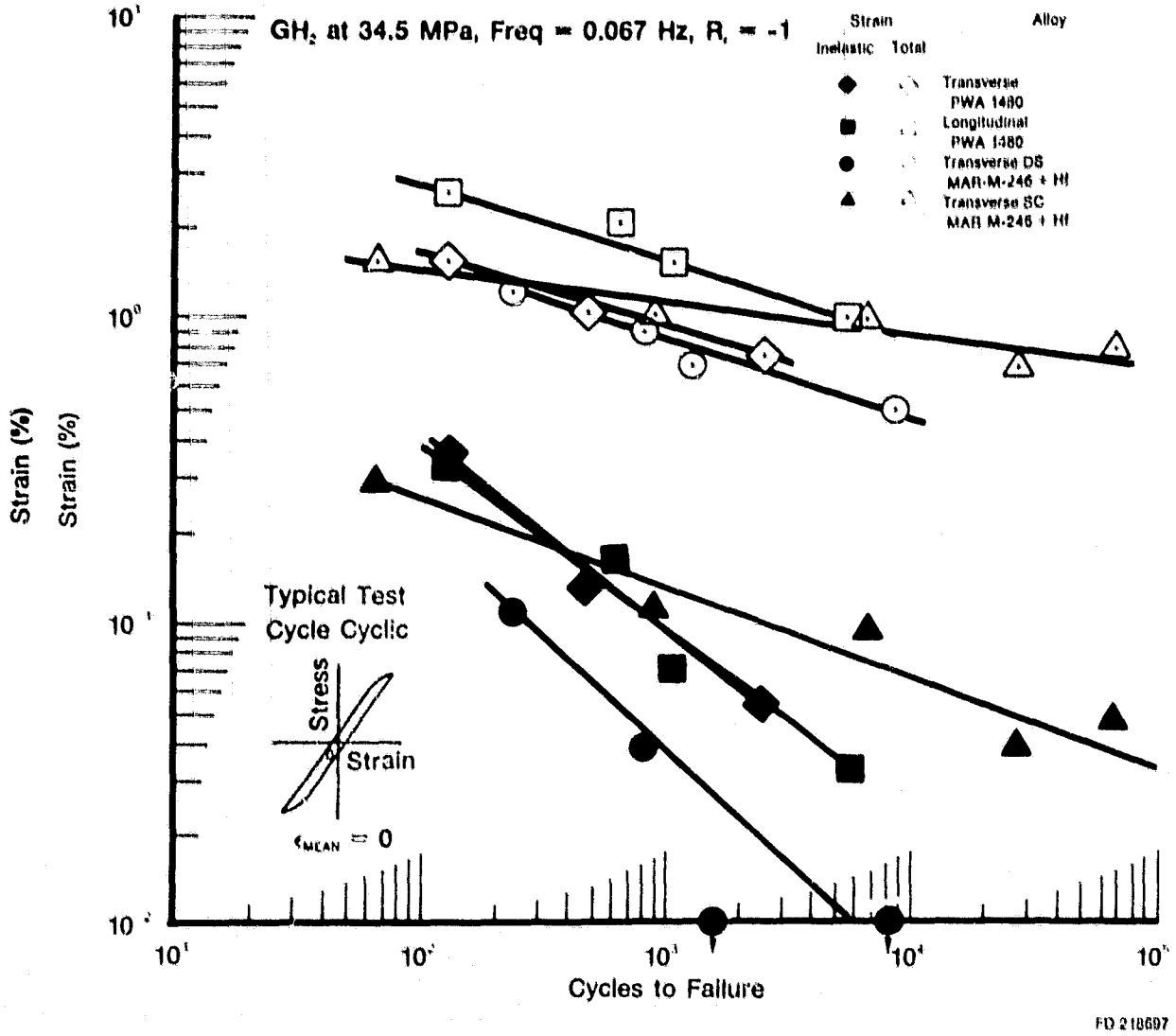

Figure 42. Comparison of PWA 1480 (Longitudinal and Transverse), Transverse SC and DS, and MAR-M-246 + Hf in GH_2 at 34.5 MPa, Frequency = 0.067 Hz, R = -1, Temperature = 871°C (1600°F)

The addition of steam had little effect on PWA 1480 or SC MAR-M-246+Hf but degraded DS MAR-M-246+Hf by 60 percent.

MAR-M-246+Hf data from this contract is plotted in figures 43 and 44. PWA 1480 longitudinal/transverse comparison plots appear in figures 45 and 46, and PWA 1480 871°C (1600°F) hydrogen/hydrogen plus steam comparisons for longitudinal and transverse orientations appear in figures 47 and 48. In both cases, 760°C (1400°F) and 871°C (1600°F), longitudinal PWA 1480 was superior to transverse by approximately one order of magnitude.

These conclusions are based on very limited testing and extrapolation of the data curves. Further testing could change the results presented here.

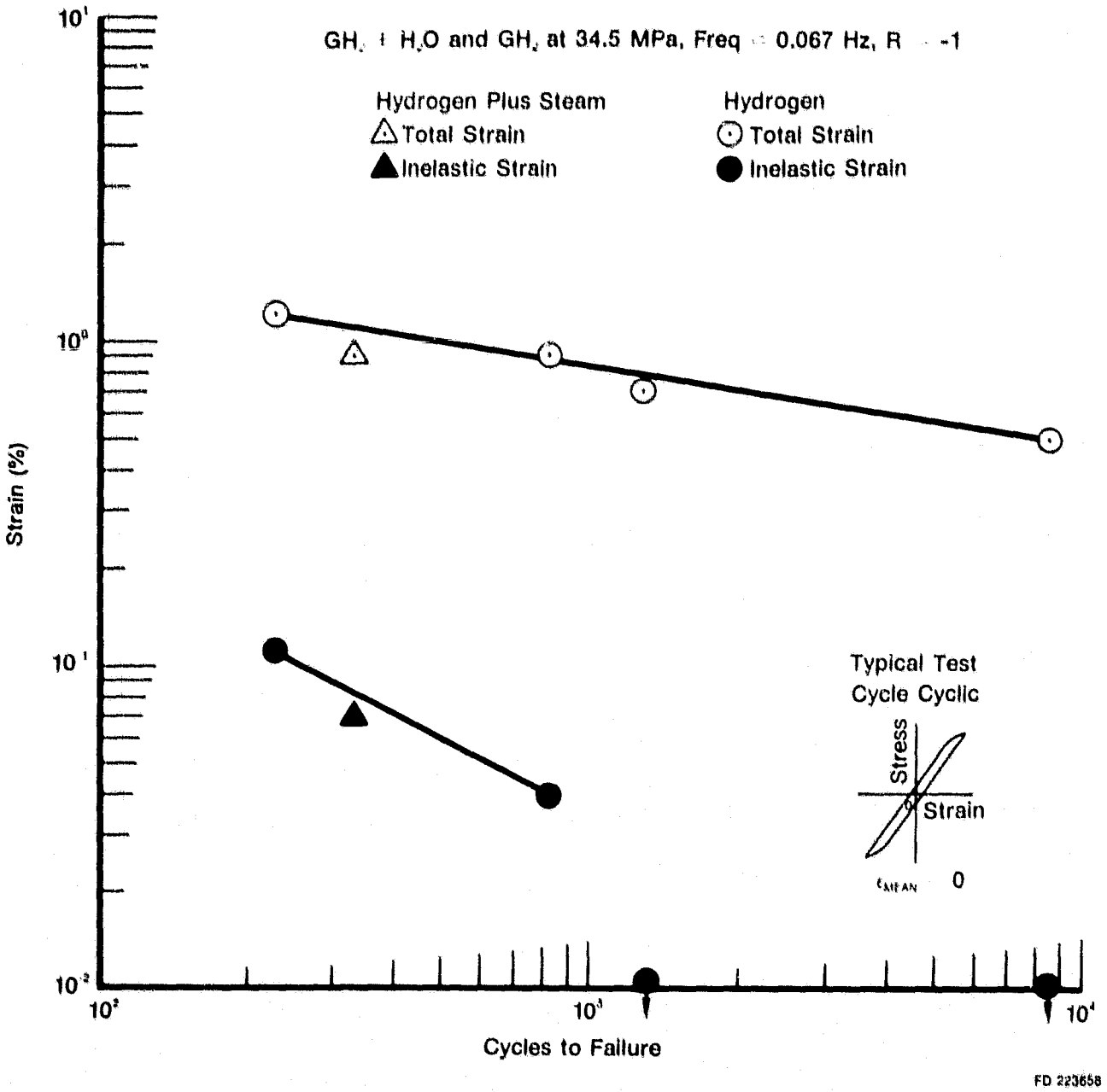

Figure 43. Strain Control LCF Results of Transverse Directionally Solidified MAR-M-246 + Hf at 871°C (1600°F)

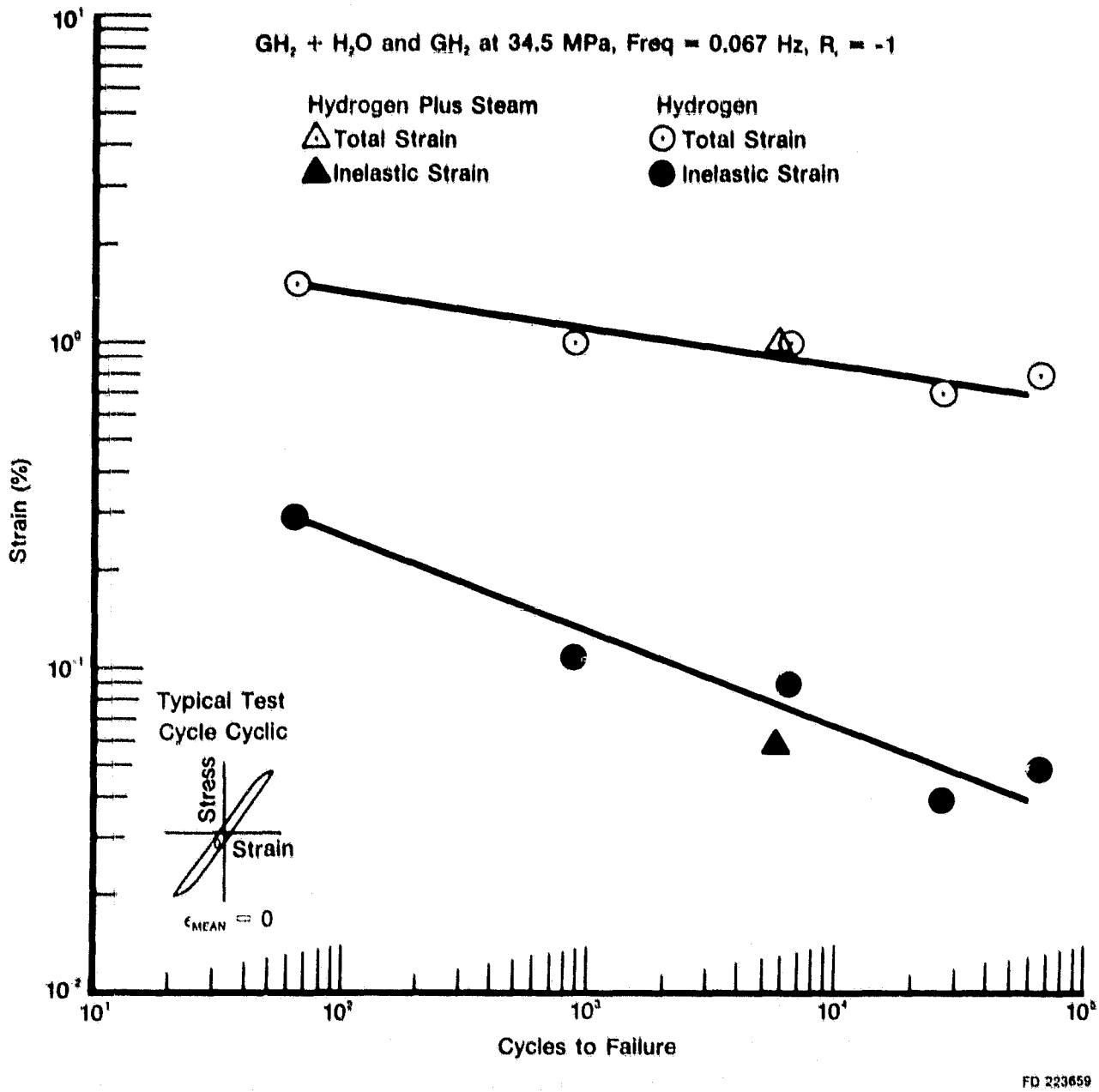

Figure 44. Strain Control LCF Results of Transverse Single Crystal MAR-M-246 + Hf at 871°C (1600°F)

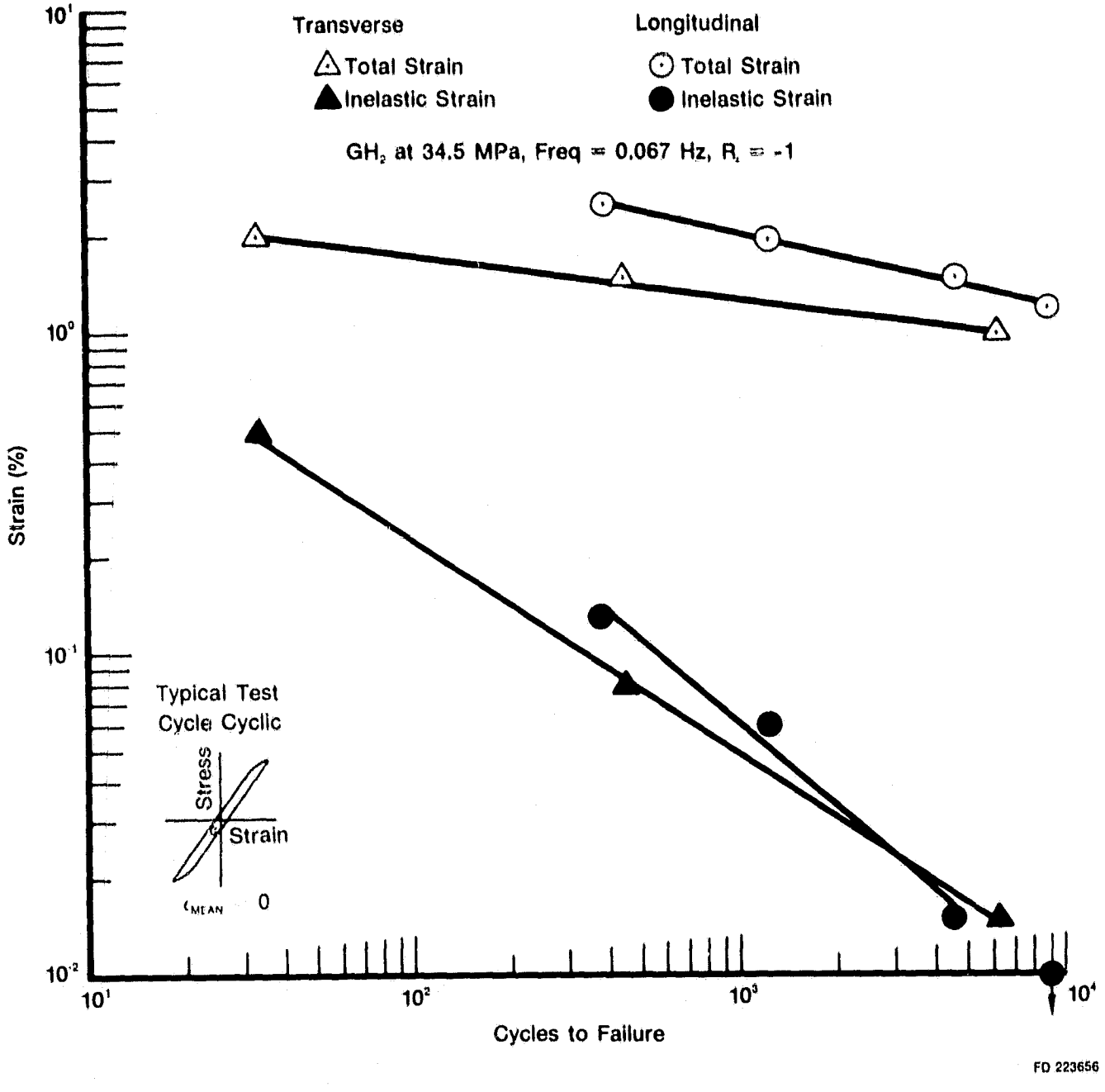

Figure 45. Strain Control LCF Results Transverse and Longitudinal PWA 1480 at 760°C (1400°F)

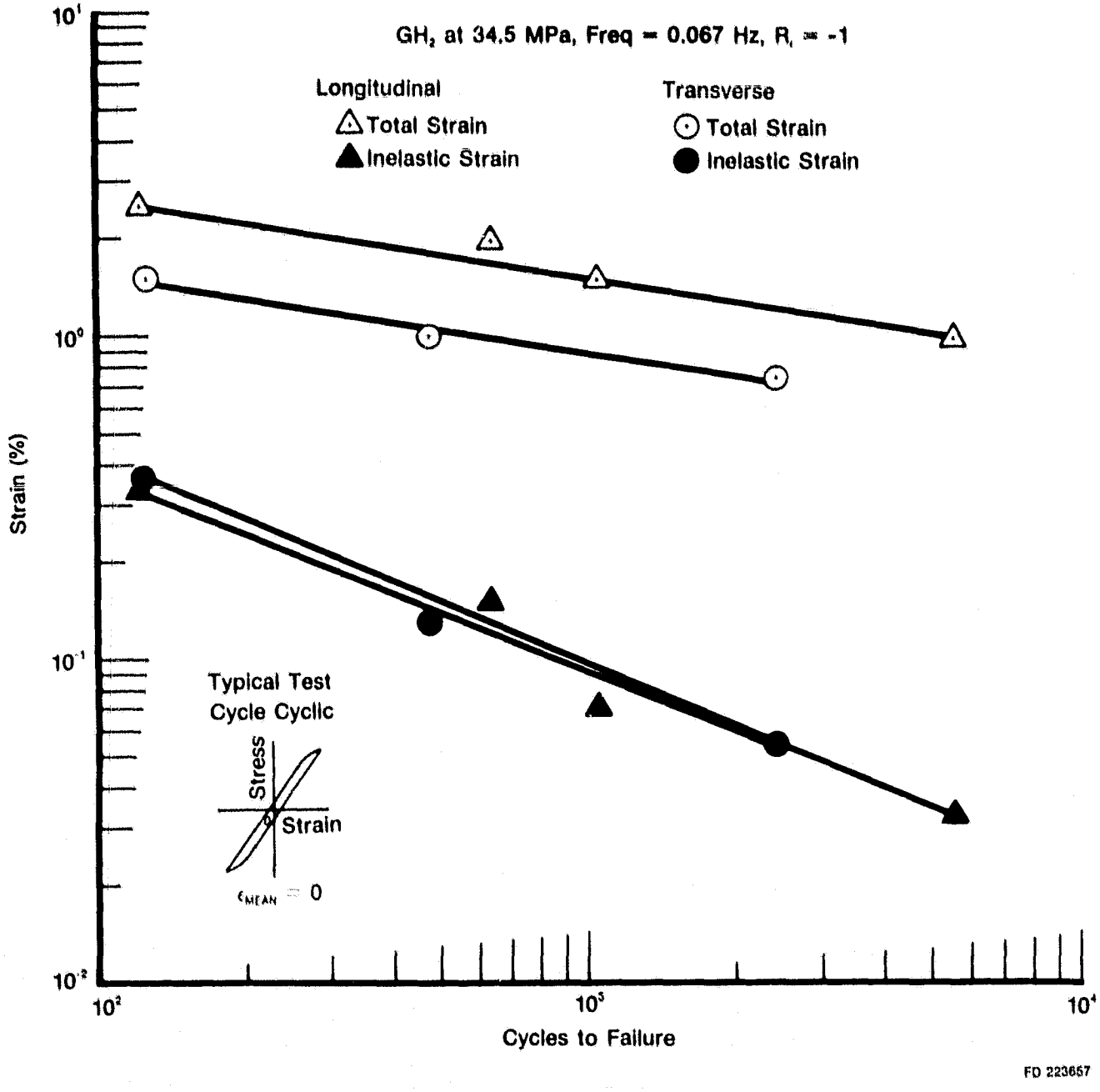

Figure 46. Strain Control LCF Results of Transverse and Longitudinal PWA 1480 at 871°C (1600°F)

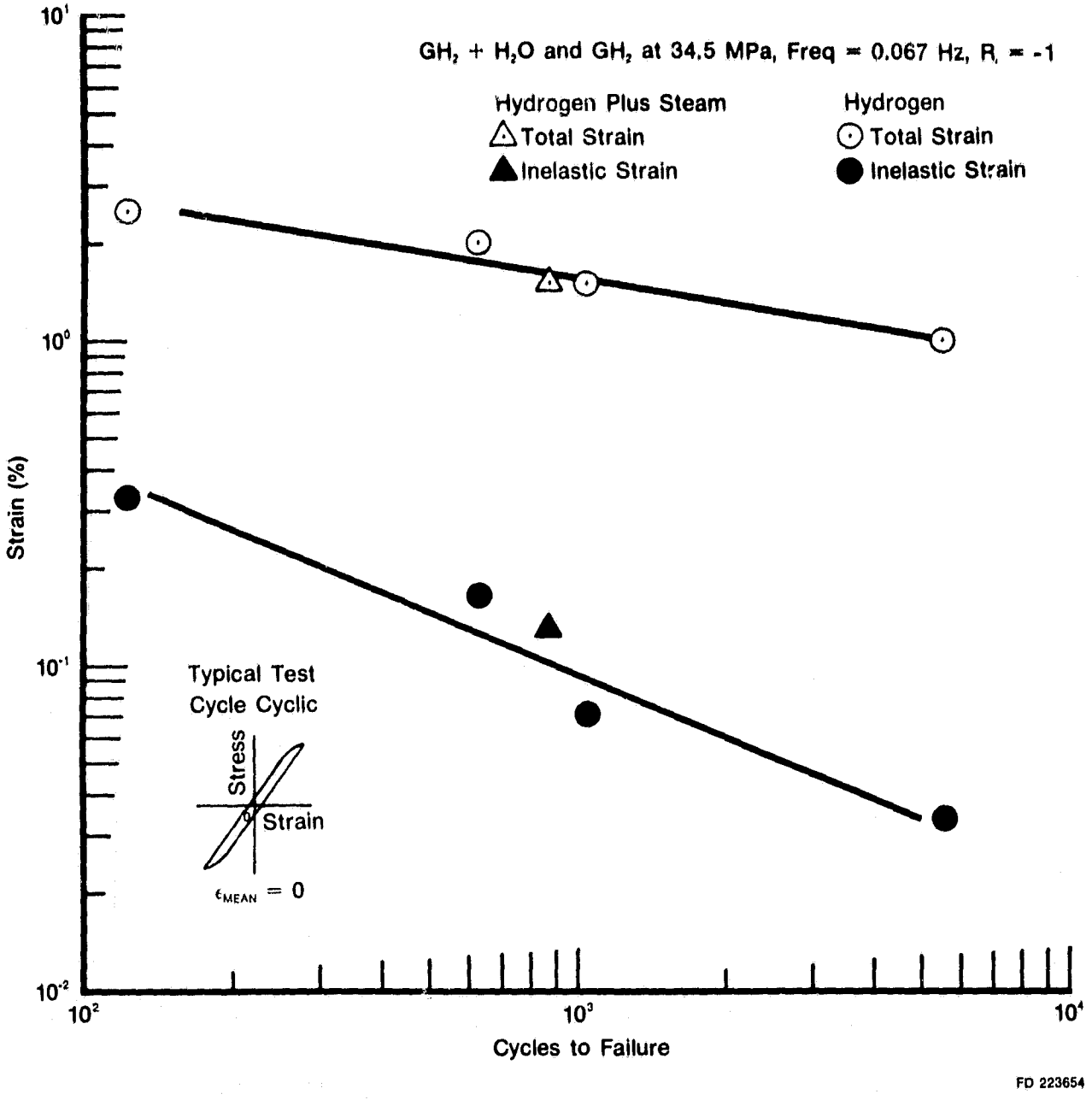

Figure 47. Strain Control LCF Results of Longitudinal PWA 1480 at 871°C (1600°F)

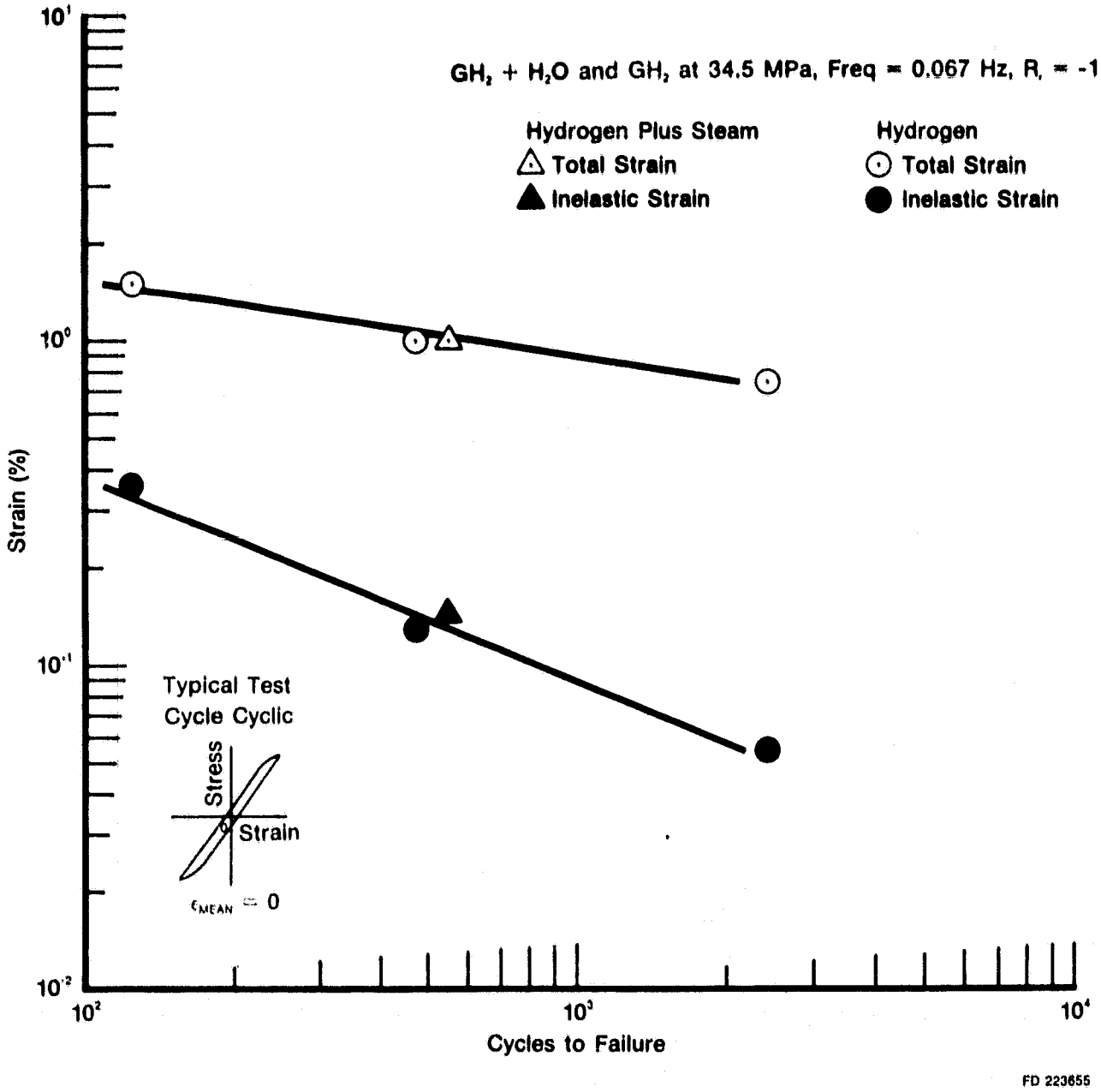

Figure 48. Strain Control LCF Results of Transverse PWA 1480 at 871°C (1600°F)

C. TEST PROCEDURE

Smooth, round, solid specimens were used for the strain-controlled LCF tests conducted under this contract. The test specimens used are described in Section III and detailed in figures 10 and 12. The specimen configuration incorporates integral machined extensometer collars. A calibration procedure has been established to relate the strain to the collar deflection during both the elastic and inelastic portion of the strain cycle. The specimen design and calibration procedure were verified both experimentally and analytically.

High-pressure environmental tests were conducted on a closed-loop-type, hydraulically actuated test machine. The test machine is located in an isolated test cell with all controls and instrumentation located in an adjacent blockhouse (figure 49). A P&WA designed pressure vessel was mounted on the upper platen of the test machine. The vessel incorporates a Grayloc type high-pressure flange for sealing and ease of assembly. The test machine compensates through the servosystem for the load in the specimen due to pressure acting over differential specimen/adapter areas. A pressure transducer is use to provide a feedback signal, proportional to chamber pressure, to the servocontroller. This signal was used in controlling a mean load applied to the linkage so zero strain was maintained in the specimen gage when the vessel assembly was pressurized. This same load was then superimposed on the cyclic load during testing.

Both internal (to the pressure vessel) and external load cells were used to obtain cyclic load; thus, the effect of friction at the load rod seals was known and accounted for. Electrical connections to the load cell, extensometer system, furnace (for elevated temperature tests), and thermocouples were made through the vessel wall via high-pressure bulkhead connectors. Setups of the pressure vessel showing the extensometer system and furnace arrangement are shown in figure 50.

For elevated temperature testing, a two-zone resistance furnace with separate control systems for each zone was used. The furnace surrounds the specimen and fits within the frame of the pressure vessel (figure 50C). Thermocouples attached to the specimen gage section were used to monitor and control temperature during test.

The hydrogen and water vapor environment was obtained utilizing triple-distilled water in a pure hydrogen-containing retort system so the water was vaporized by furnace heat. The retort system, containing the test specimen and water, fits within the furnace and consists of a piston/tube type arrangement (figures 51 and 52). The piston, attached to the lower pull rod, incorporates an O-ring which provides a seal against the inner surface of a tube (cylinder), which is attached to the upper pull rod. During testing, the tube remains basically stationary relative to the piston. The base of the piston incorporates O-ring holes for passage of the extensometer tubes, and check valves which allow hydrogen to enter the retort and prevent water from escaping. Pressure inside the retort and vessel are equalized; therefore, the retort could contain the hydrogen and water vapor environment and not be subjected to any stresses due to differential (internal to external) pressure. Thermocouples also exit the retort via connectors installed in the base of the piston. They monitor and control specimen and water vapor temperature. By controlling the lower zone of the furnace, water was vaporized at a temperature which assured 500,000-ppm water vapor (50% by weight).

Strain, as sensed by the extensometer system, was recorded on the X axis of an X-Y recorder, and load (sensed by the external load cell) was recorded on the Y axis, thus providing hysteresis loops, as desired, during the cyclic life of all tests.

Prior to test, specimens were rinsed with trichlorethylene, wiped dry, rinsed with acetone, wiped dry, and inserted into the test fixture. All handling of specimens was done with clean gloves.

The test and gas handling procedures used for the tensile tests were also used for the LCF testing.

FC 42237

Figure 49. High-Pressure Environment Low-Cycle Fatigue Testing Machine, Environmental Controls, and Data Acquisition Equipment

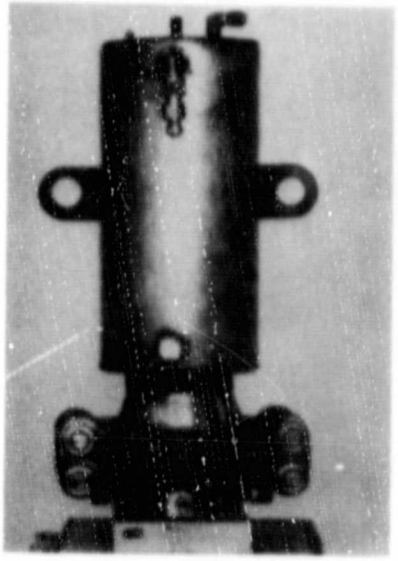

FAE 146129

a) Test Vessel Closed

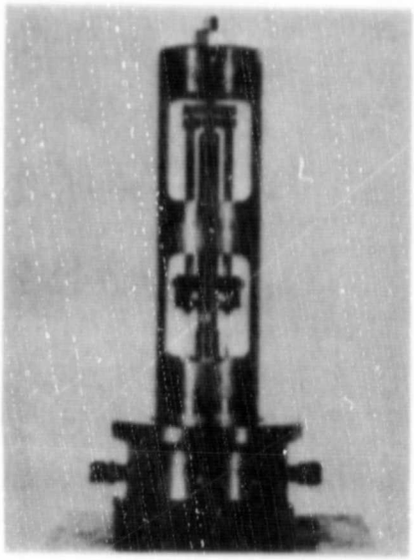

FAE 146121

b) Test Vessel Open Showing Extensometer System

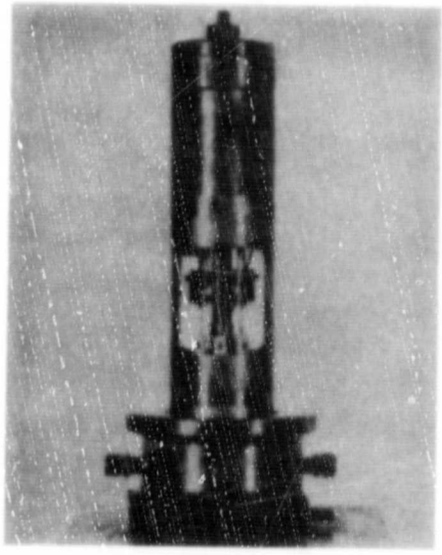

FAE 146122

c) Test Vessel Open Showing Furnace In Place

FD 92640

Figure 50. Low-Cycle Fatigue High-Pressure Environmental Test Vessel

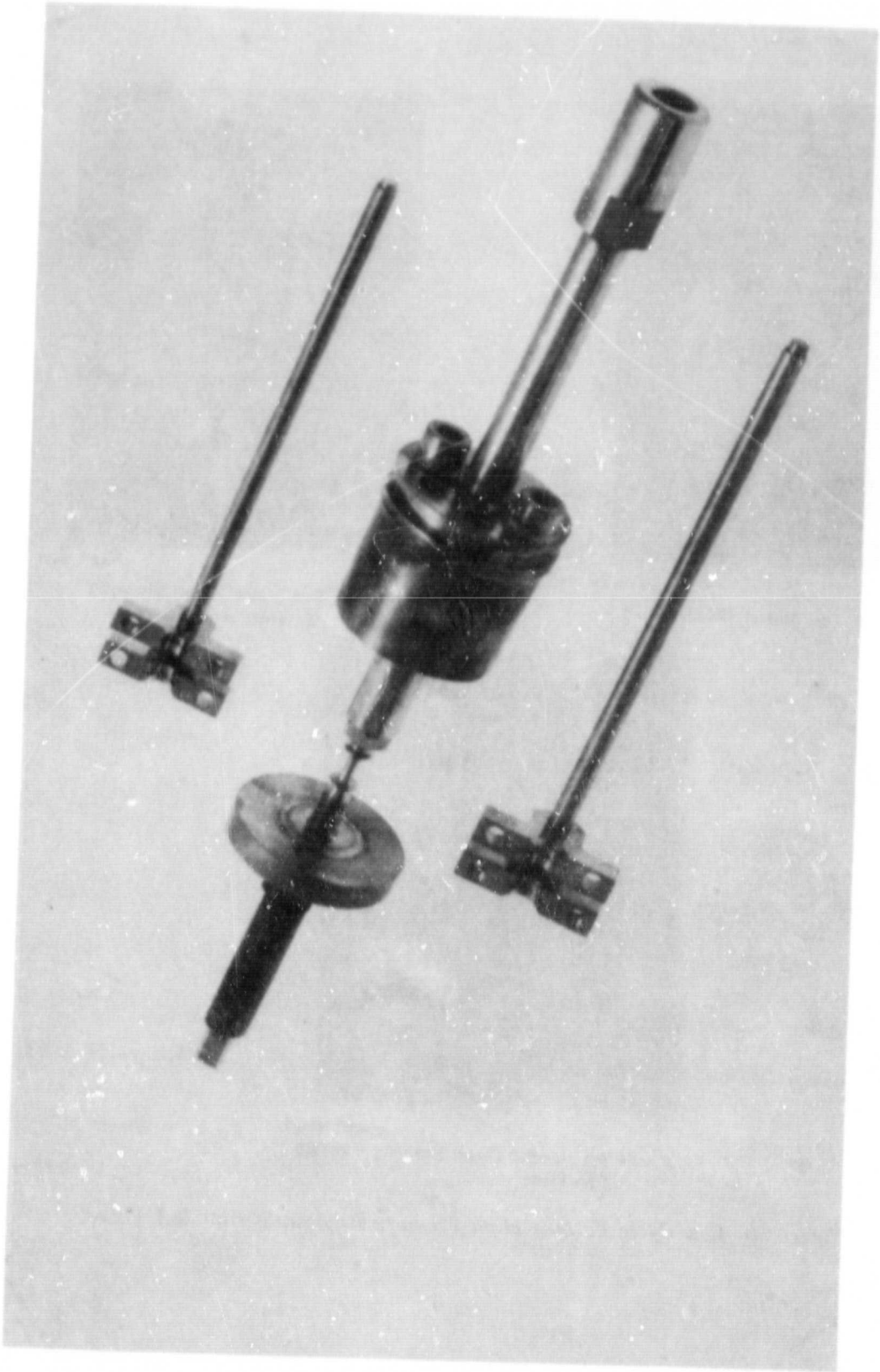

Figure 51. Open Extensometer Head Assembly, Low-Cycle Fatigue Specimen, and Retort Pistons

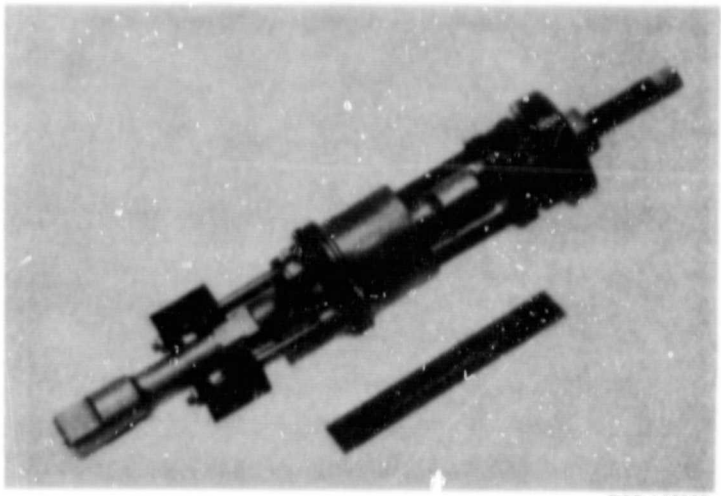

FAE 146128

a) Retort With Cylinder Removed Showing Piston, Extensometer System and Thermocouple Leads

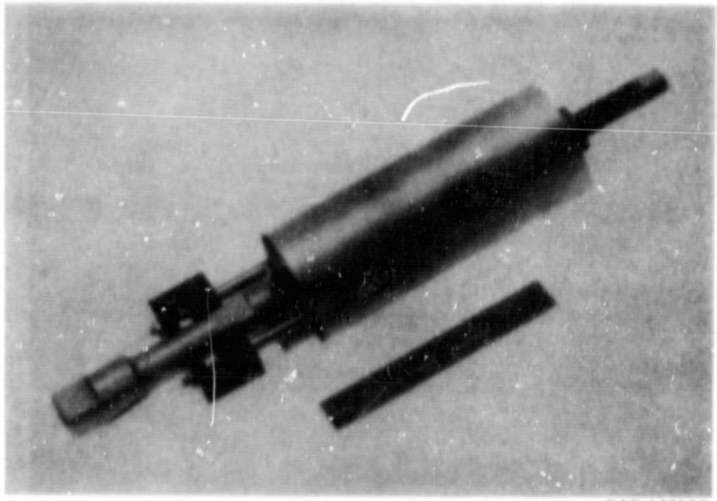

FAE 146132

b) Retort System With Cylinder In Place

FD 92641

Figure 52. Low-Cycle Fatigue Test Retort System

SECTION VII
CRACK GROWTH

A. INTRODUCTION

Crack growth rate tests were conducted on PWA 1480 and MAR-M-246+Hf at 760°C (1400°F) and 871°C (1600°F) in 34.5 MPa (5000 psig) gaseous hydrogen or hydrogen plus water vapor (50% by weight) environments.

The test program was designed to generate crack growth rate (da/dn) versus cyclic stress intensity (ΔK) curves to determine the effects of temperature and environment on the crack growth properties of these materials.

The PWA 1480 material was supplied in the form of cast blocks. MAR-M-246+Hf was supplied in two forms, single crystal (SC), and directionally solidified (DS). The test specimen used for all testing was the lw compact specimen shown in figure 11 incorporating a chevron-type crack-starter notch and integral knife edges per ASTM E399-74. All specimens were oriented such that crack propagation would be perpendicular to the solidification direction (figure 7).

Crack growth tests were conducted in the load controlled mode. The test consisted of cyclic loading of the specimen between the minimum load and the maximum load until complete fracture occurred. The loading cycle was all tensile with a 480-second hold time at the maximum load. All specimens were tested at an R ratio (minimum load/maximum load) of 0.1. The test loading cycle is shown in figure 53.

Crack growth data for this program was analyzed using the hyberbolic sine based "SINH" model, an interpolative model developed for the analysis of elevated temperature fatigue crack propagation data.* The model has been successfully used to describe the parametric effects of three fundamental influences on crack propagation: frequency (ν), stress ratio (R), and temperature (T).

This interpolative model is based on the hyperbolic sine equation,

$$\log (da/dn) = C_1 \sinh (C_2(\log (\Delta K)+C_3)) + C_4$$

where the coefficients are simple empirical functions of test frequency, stress ratio, and temperature:

C_1 = material constant
$C_2 = f_2 (R, \nu, T)$
$C_3 = f_3 (C_4, \nu, R)$
$C_4 = f_4 (\nu, R, T)$

This model presents a flexible alternative to the familiar Paris equation and has gained acceptance in the aerospace industry. In several cases for this data a Paris fit would have worked as well, but in most cases SINH was used because it is the standard model for P&WA GPD.

*Annis, C.G., R.M. Wallace, and D.L. Sims, "An Interpolative Model for Elevated Temperature Fatigue Crack Propagation," Final Report No. AFML-TR-76-176, November 1976.

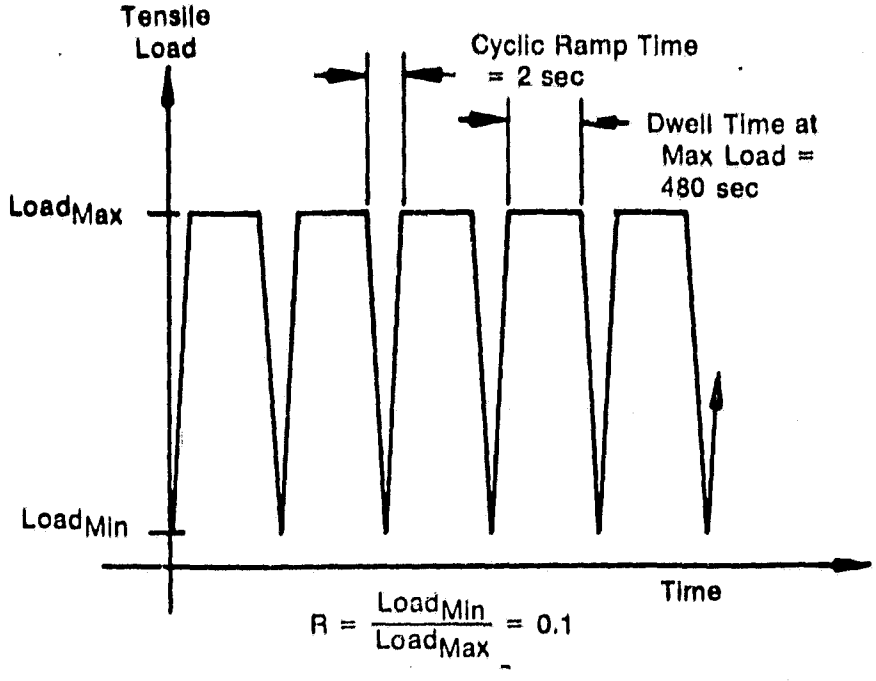

Figure 53. Typical Crack Growth Load-Controlled Test Cycle

B. RESULTS AND CONCLUSIONS

Crack growth rate curves (da/dn vs ΔK) were generated for PWA 1480 at 760°C (1400°F) and 871°C (1600°F) in 34.5 MPa (5000 psig) hydrogen (figures 54 through 56). Testing was also conducted at 871°C (1600°F) in 34.5 MPa (5000 psig) hydrogen and water vapor (figure 56) to define environmental degradation. A composite plot of all three temperature-environment conditions (figures 57 and 58) revealed that there was no significant increase in the crack growth rate with the increase in test temperature, or due to the hydrogen-water vapor environment.

Crack growth rate curves for MAR-M-246+Hf in the single crystal (SC) form are presented in figures 59 through 63. Testing was performed at 760°C (1400°F) and 871°C (1600°F) in 34.5 MPa (5000 psig) hydrogen, and at 871°C (1600°F) in 34.5 MPa (5000 psig) hydrogen and water vapor (50% by weight). The MAR-M-246+Hf SC material exhibited an increase in crack growth rate with increasing temperature. The effect of the hydrogen-water vapor environment was negligible when compared with the hydrogen environment.

The MAR-M-246+Hf material in the directionally solidified (DS) form was tested at 871°C (1600°F). The test results are plotted in figures 64 through 66. The addition of water to the hydrogen environment caused no significant increases in the crack growth rate. Crack growth data parallel to the solidification direction obtained in a previous contract (NAS8-30744) appears in figures 67 through 70.

Complete crack growth test conditions and results are listed in table 20.

The above conclusions are drawn on the basis of limited test data. Variations in specimen transverse orientation with respect to crystal planes and data scatter negate the ability to make exact comparisons. Crack length vs. cycles was plotted for each test to augment the da/dn curves. They appear in figures 71 through 86.

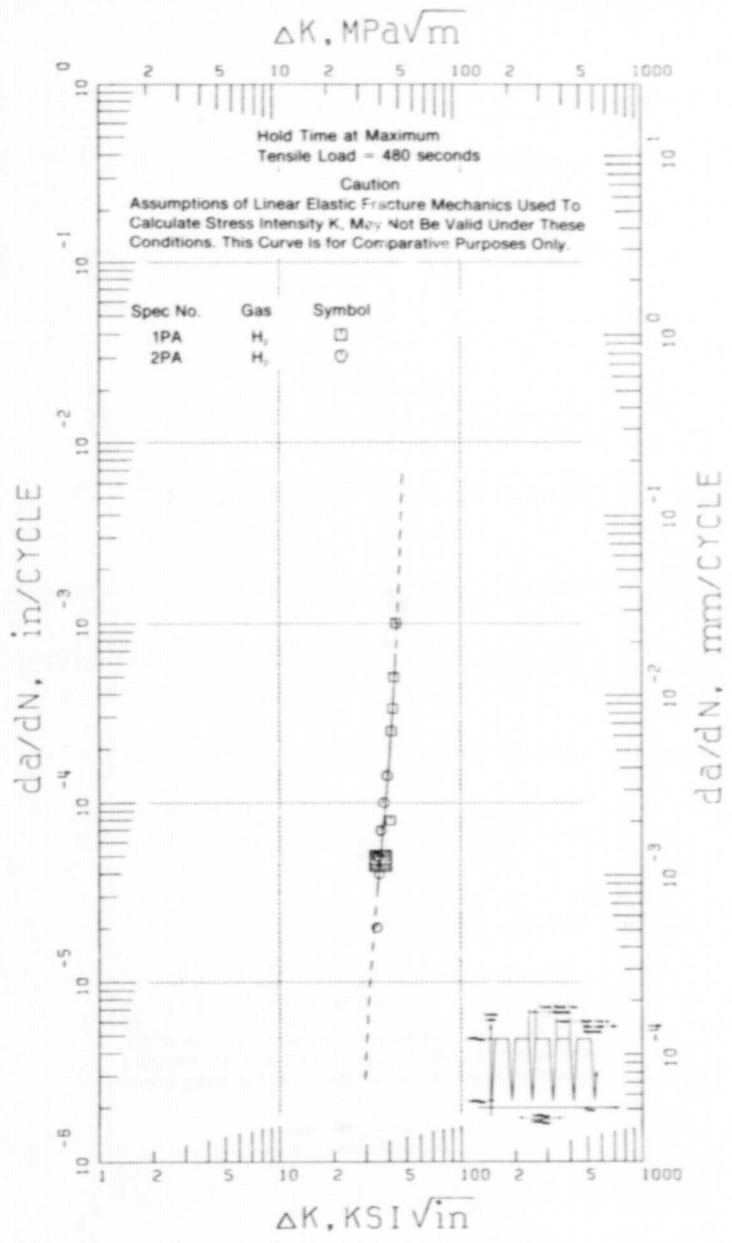

METRIC CONVERSIONS

C1 METRIC = C1 ENGLISH C2 METRIC = C2 ENGLISH
C3 METRIC = C3 ENGLISH - 0.040935 C4 METRIC = C4 ENGLISH + 1.40483

CURVE	SYMBOL	SPEC NO	MATERIAL	TEMP	ATM	FREQ	R	TYPE	THIK	REMARKS	P/R
1		1PA	PWA 1480	1400F	H 2	8MDWL	R=.10	MCT	.4974		5.766
1		2PA	PWA 1480	1400F	H 2	8MDWL	R=.10	MCT	.4990		1.161

FD 223724

Figure 54. Crack Growth Rate vs Stress Intensity for PWA 1480 in 34.5 MPa (5000 psig) Hydrogen at 760°C (1400°F) Perpendicular to the Solidification Direction

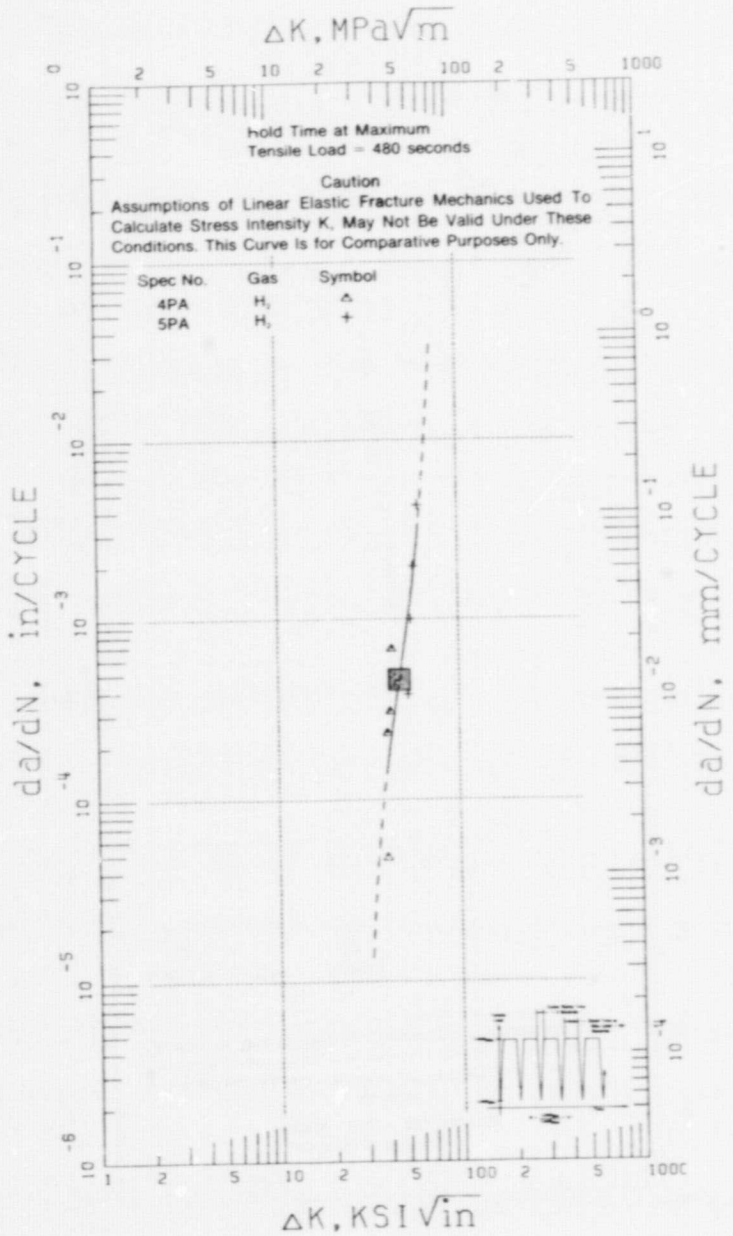

HYPERBOLIC SINE MODEL COEFFICIENTS

T= C1 * SINH(C2 * (X + C3)) + C4

WHERE T= LOG(da/dN) AND X=LOG(ΔK)

CURVE	SYMBOL	C1	C2	C3	C4	Δ K RANGE	NPTS	R^2	SEE
2	Δ +	0.7000	9.1499	-1.6688	-3.3362	39.23, 60.441	8	0.7485	0.3571

METRIC CONVERSIONS

C1 METRIC = C1 ENGLISH — C2 METRIC = C2 ENGLISH

C3 METRIC = C3 ENGLISH - 0.040935 — C4 METRIC = C4 ENGLISH + 1.40483

CURVE	SYMBOL	SPEC NO	MATERIAL	TEMP	ATM	FREQ	R	TYPE	THIK	REMARKS	P/A
2	Δ	4PA	PWA 1480	1600F	H 2	SHOWL	R=.10	MCT	.4991		1.202
2	+	5PA	PWA 1480	1600F	H 2	SHOWL	R=.10	MCT	.4985		0.680

FD 223723

Figure 55. Crack Growth Rate vs Stress Intensity for PWA 1480 in 34.5 MPa (5000 psig) Hydrogen at 871°C (1600°F) Perpendicular to the Solidification Direction

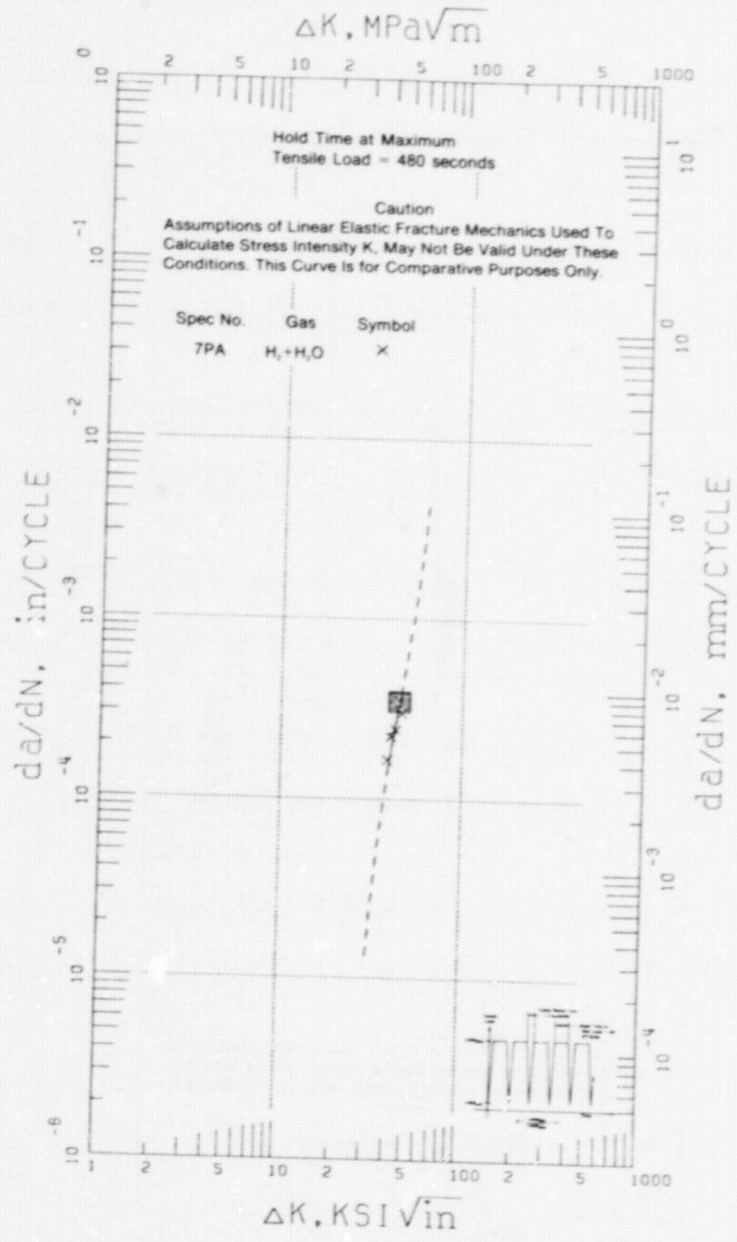

HYPERBOLIC SINE MODEL COEFFICIENTS

T= C1 * SINH[C2 * (X + C3)] + C4

WHERE T= LOG(da/dN) AND X=LOG(ΔK)

CURVE	SYMBOL	C1	C2	C3	C4	Δ K RANGE	NPTS	R^2	SEE
3	×	0.7000	8.8631	-1.0574	-3.4623	[38.90, 46.35]	4	0.9353	0.1910

METRIC CONVERSIONS

C1 METRIC = C1 ENGLISH C2 METRIC = C2 ENGLISH

C3 METRIC = C3 ENGLISH - 0.040935 C4 METRIC = C4 ENGLISH + 1.40483

CURVE	SYMBOL	SPEC NO	MATERIAL	TEMP	ATM	FREQ	R	TYPE	THIK	REMARKS	P/A
3	×	7PA	PWA 1480	1600F	H20	8MDWL	R=.10	MCT	.4989		0.995

FD 223721

Figure 56. Crack Growth Rate vs Stress Intensity for PWA 1480 in 34.5 MPa (5000 psig) Steam Enriched Hydrogen (50% Water Vapor by Weight) at 871°C (1600°F) Perpendicular to the Solidification Direction

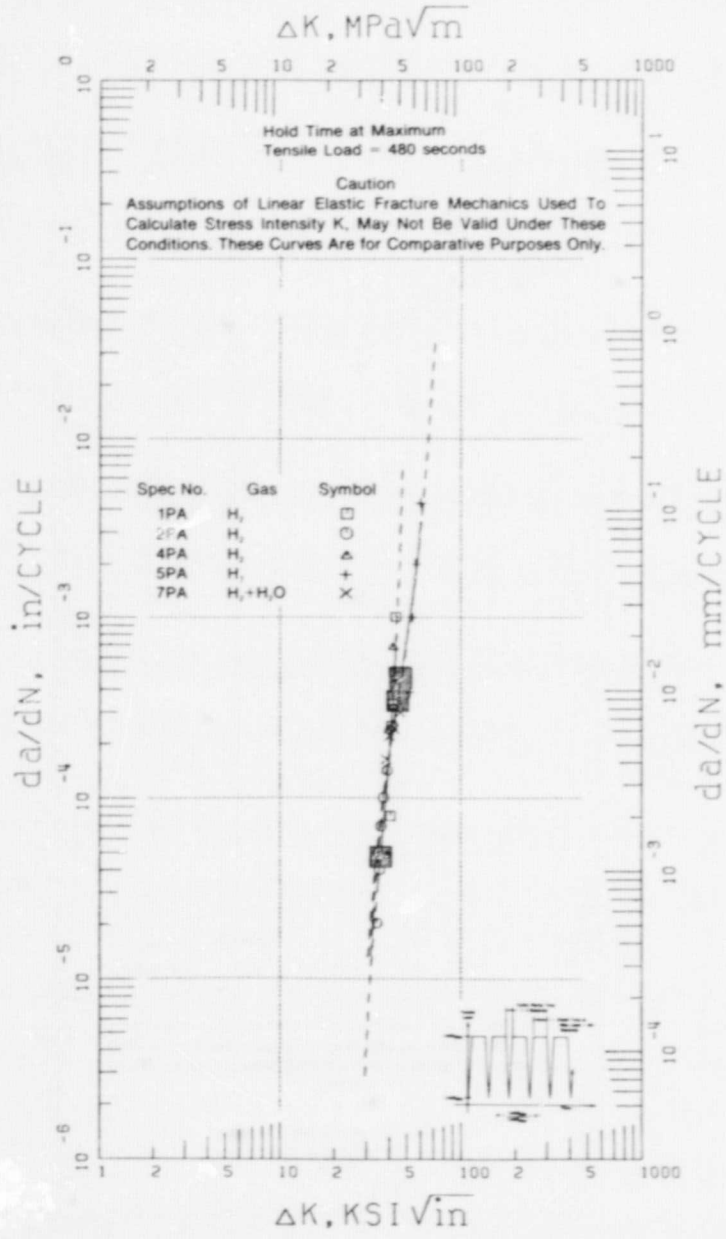

HYPERBOLIC SINE MODEL COEFFICIENTS

Y= C1 * SINH(C2 * (X + C3)) + C4

WHERE Y= LOG(da/dN) AND X=LOG(ΔK)

CURVE	SYMBOL	C1	C2	C3	C4	ΔK RANGE	NPTS	R^2	SEE
1	□ ○	0.7000	15.0500	-1.5568	-4.3260	(34.53, 43.71)	11	0.8787	0.1984
2	△ +	0.7000	9.1499	-1.6688	-3.3352	(39.23, 60.44)	8	0.7485	0.3571
3	×	0.7000	8.8631	-1.6524	-3.4623	(38.90, 46.35)	4	0.9353	0.1910

METRIC CONVERSIONS

C1 METRIC = C1 ENGLISH C2 METRIC = C2 ENGLISH

C3 METRIC = C3 ENGLISH - 0.040935 C4 METRIC = C4 ENGLISH + 1.40483

CURVE	SYMBOL	SPEC NO	MATERIAL	TEMP	ATM	FREQ	R	TYPE	THIK	REMARKS	P/A
1	□	1PA	PWA 1480	1400F	H 2	8HZWL	R=.10	MCT	.4974		0.766
1	○	2PA	PWA 1480	1400F	H 2	8HZWL	R=.10	MCT	.4990		1.16
2	△	4PA	PWA 1480	1600F	H 2	8HZWL	R=.10	MCT	.4981		1.20e
2	+	5PA	PWA 1480	1600F	H 2	8HZWL	R=.10	MCT	.4985		0.680
3	×	7PA	PWA 1480	1600F	H20	8HZWL	R=.10	MCT	.4989		0.995

FD 2&3722

Figure 57. Crack Growth Rate vs Stress Intensity for PWA 1480 in 34.5 MPa (5000 psig) Environments Perpendicular to the Solidification Direction

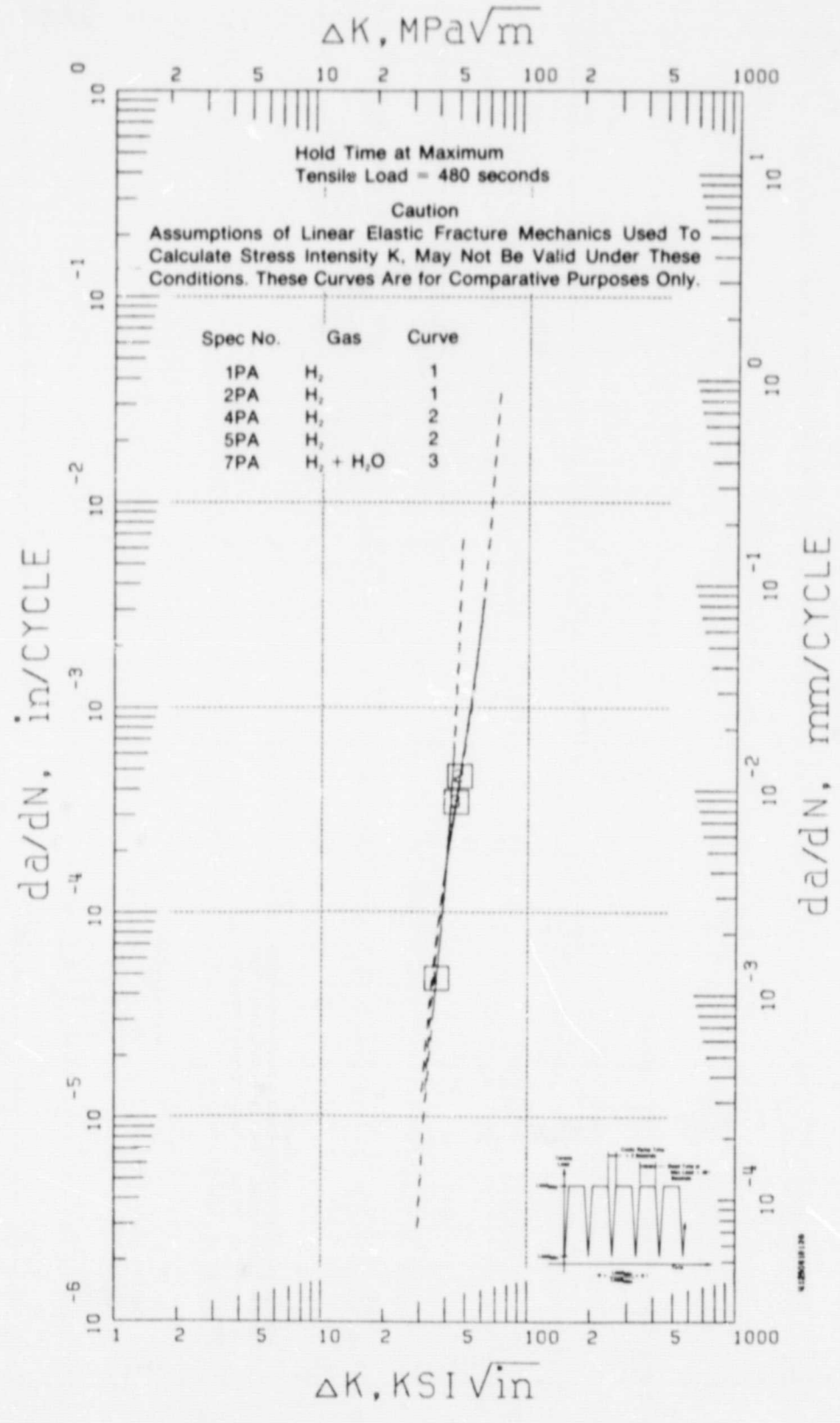

Figure 58. Crack Growth Rate vs Stress Intensity for PWA 1480 in 34.5 MPa (5000 psig) Environments Perpendicular to the Solidification Direction 1. 760°C (1400°F) H_2 2. 871°C (1600°F) H_2 3. 871°C (1600°F) $H_2 + H_2O$

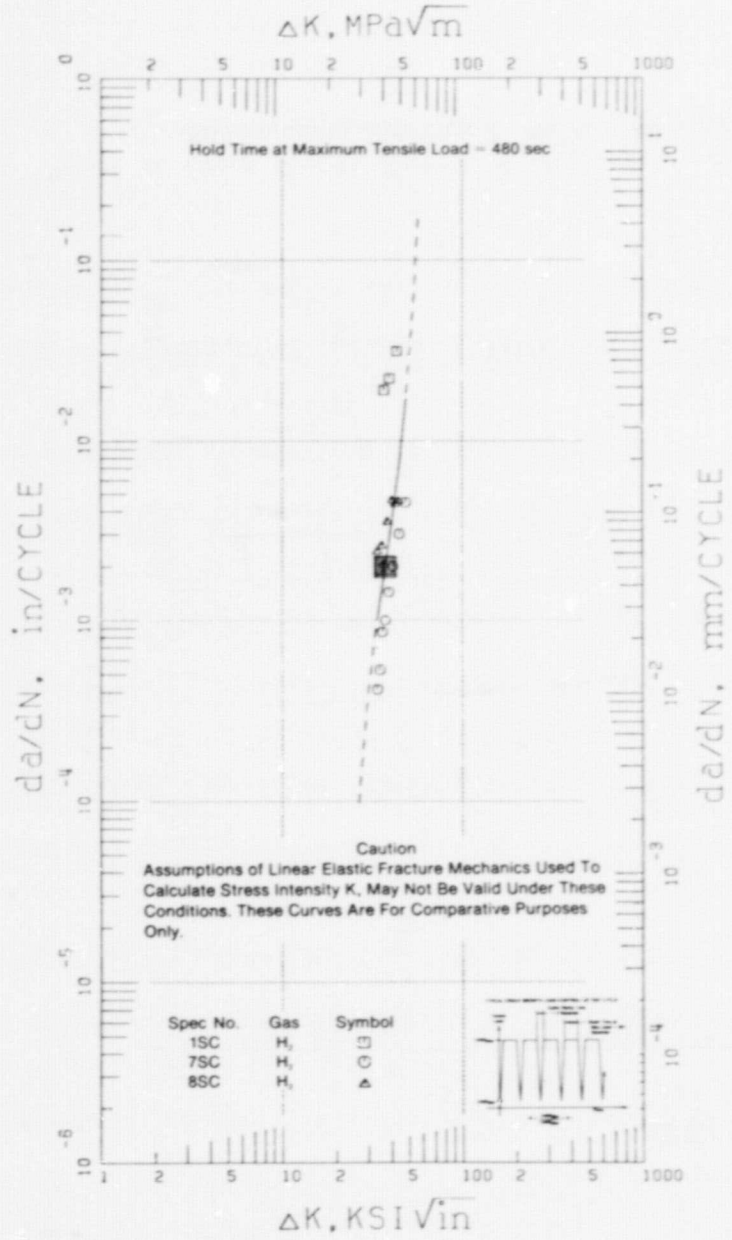

HYPERBOLIC SINE MODEL COEFFICIENTS

T= C1 * SINH(C2 * (X + C3)) + C4

WHERE T= LOG(da/dN) AND X=LOG(ΔK)

CURVE	SYMBOL	C1	C2	C3	C4	Δ K RANGE	NPTS	R^2	SEE
1	□○△	0.7000	9.5712	-1.5707	-2.7000	(33.67, 48.24)	17	0.2163	0.5129

METRIC CONVERSIONS

C1 METRIC = C1 ENGLISH — C2 METRIC = C2 ENGLISH

C3 METRIC = C3 ENGLISH - 0.040935 — C4 METRIC = C4 ENGLISH + 1.40487

CURVE	SYMBOL	SPEC NO	MATERIAL	TEMP	ATM	FREQ	R	TYPE	THIK	REMARKS	P/R
1	□	1SC	SCMGRMHF	1400F	H 2	8HZWL	R=.10	MCT	.4975		7.667
1	○	7SC	SCMGRMHF	1400F	H 2	8HZWL	R=.10	MCT	.5020		0.457
1	△	8SC	SCMGRMHF	1400F	H 2	8HZWL	R=.10	MCT	.5005		1.583

FD 223727

Figure 59. Crack Growth Rate vs Stress Intensity for Single Crystal MAR-M-246 + Hf in 34.5 MPa (5000 psig) Hydrogen at 760°C (1400°F) Perpendicular to the Solidification Direction

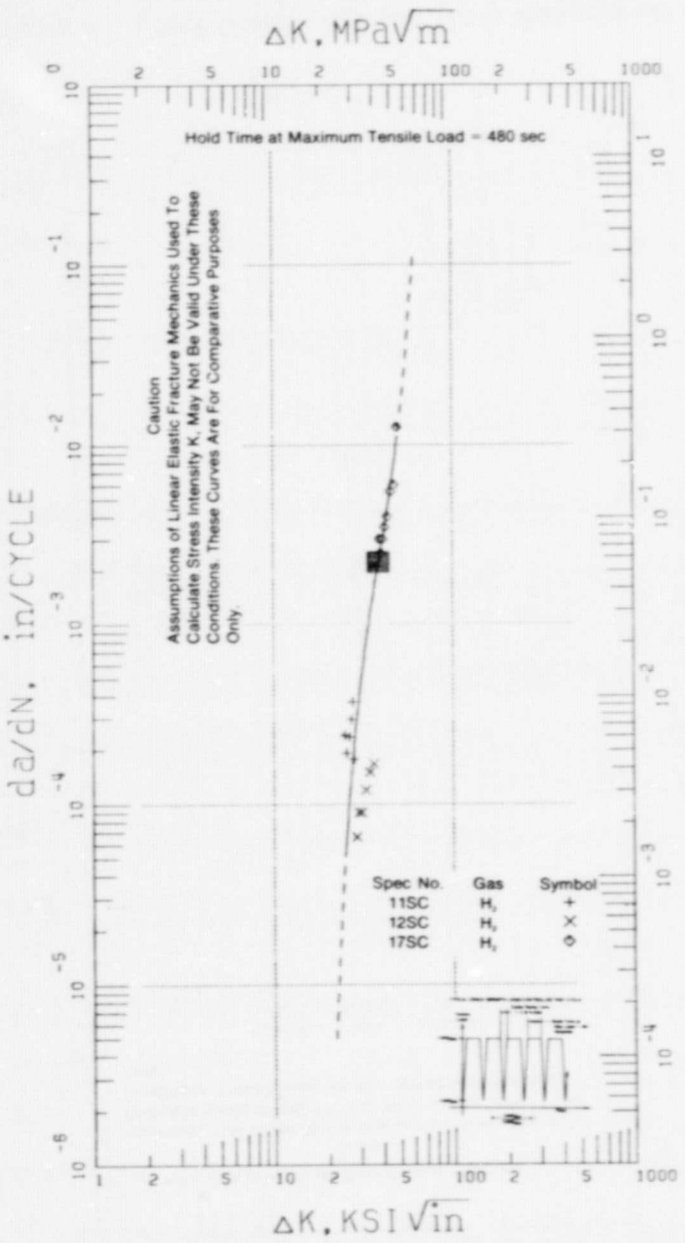

HYPERBOLIC SINE MODEL COEFFICIENTS

Y= C1 * SINH(C2 * (X + C3)) + C4

WHERE Y= LOG(da/dN) AND X=LOG(ΔK)

CURVE	SYMBOL	C1	C2	C3	C4	Δ K RANGE	NPTS	R^2	SEE
2	+ × ◇	5.7000	8.2406	-1.5861	-2.6553	24.75, 49.081	20	0.6297	0.5197

METRIC CONVERSIONS

C1 METRIC = C1 ENGLISH C2 METRIC = C2 ENGLISH

C3 METRIC = C3 ENGLISH - 0.040935 C4 METRIC = C4 ENGLISH + 1.40443

CURVE	SYMBOL	SPEC NO	MATERIAL	TEMP	ATM	FREQ	R	TYPE	THIK	REMARKS	P/A
2	+	11SC	SCMARMHF	1600F	H 2	8HZWL	R=.10	MCT	.4995		2.439
2	×	12SC	SCMARMHF	1600F	H 2	8HZWL	R=.10	MCT	.4997		0.183
2	◇	17SC	SCMARMHF	1600F	H 2	8HZWL	R=.10	MCT	.4985		0.923

FD 223729

Figure 60. Crack Growth Rate vs Stress Intensity for Single Crystal MAR-M-246 + Hf in 34.5 MPa (5000 psig) Hydrogen at 871°C (1500°F) Perpendicular to the Solidification Direction

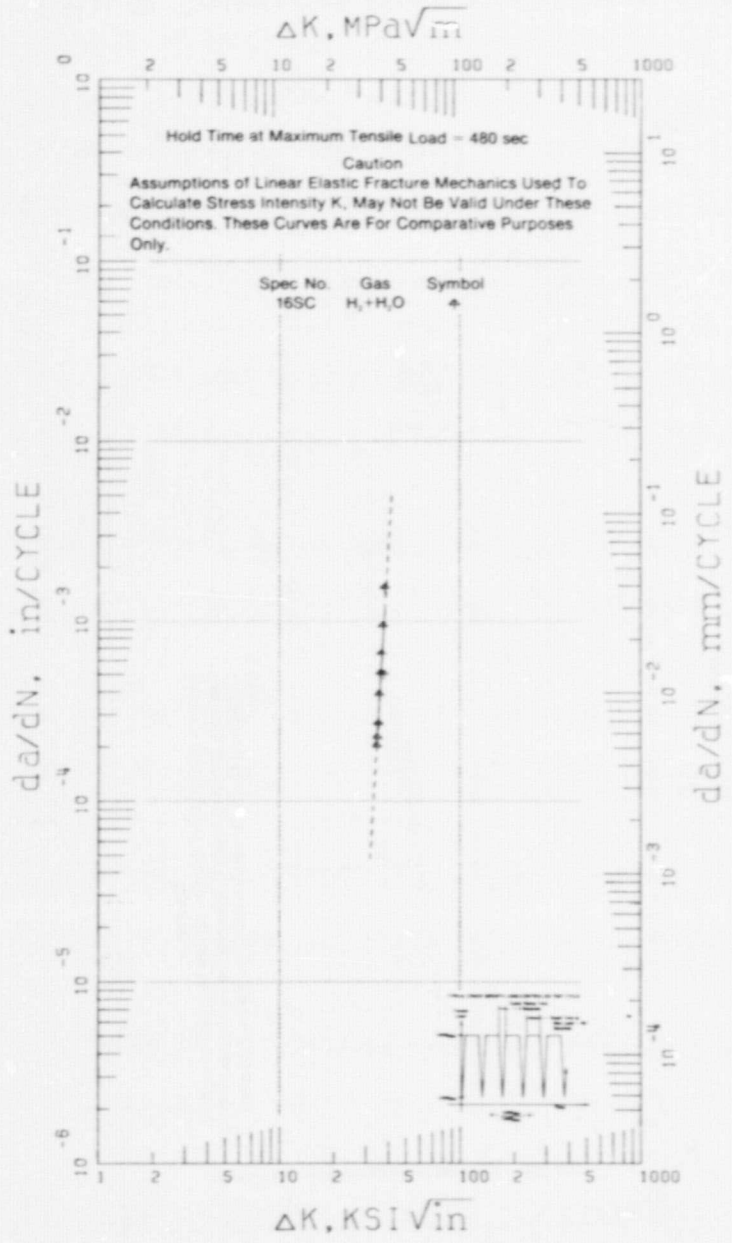

TABLE I

HYPERBOLIC SINE MODEL COEFFICIENTS

Y= C1 * SINH(C2 * (X + C3)) + C4

WHERE Y= LOG(da/dN) AND X=LOG(ΔK)

CURVE	SYMBOL	C1	C2	C3	C4	Δ K RANGE	NPTS	R^2	SEE
3	+	16.6529	-29.4084	(SEE NOTE)		34.73, 38.54	9	0.8686	0.1134

NOTE PARIS FIT USED: LOG(DA/DN) = C1 * (LOG(ΔK)) + C2

METRIC CONVERSIONS

C1 METRIC = C1 ENGLISH — C2 METRIC = C2 ENGLISH

C3 METRIC = C3 ENGLISH - 0.040935 — C4 METRIC = C4 ENGLISH + 1.40483

TABLE II

CURVE	SYMBOL	SPEC NO	MATERIAL	TEMP	ATM	FREQ	R	TYPE	THIK	REMARKS	P/A
3	+	16SC	SCMAR246F	1600F	H2O	8HZWL	R=.10	MCT	.4984		1.029

FD 223726

Figure 61. Crack Growth Rate vs Stress Intensity for Single Crystal MAR-M-246 + Hf in 34.5 MPa (5000 psig) Steam Enriched Hydrogen (50% Water Vapor by Weight) Perpendicular to the Solidification Direction at 871°C (1600°F)

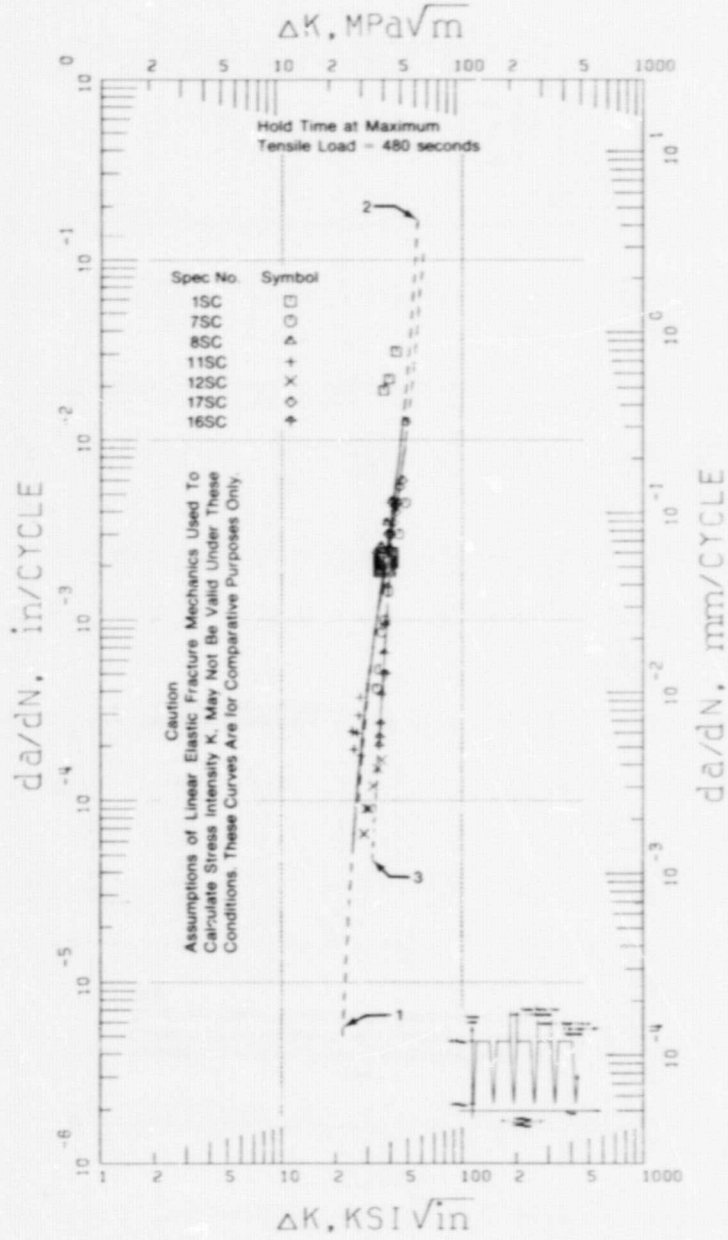

HYPERBOLIC SINE MODEL COEFFICIENTS

T= C1 * SINH(C2 * (X + C3)) + C4

WHERE T= LOG(da/dN) AND X=LOG(ΔK)

CURVE	SYMBOL	C1	C2	C3	C4	Δ K RANGE	NPTS	R^2	SEE
1	□ ○ △	0.7000	9.5712	-1.5707	-2.7000	33.67, 98.24	17	0.2163	0.5129
2	+ X ◇	0.7000	8.2408	-1.5861	-2.4553	24.75, 99.08	20	0.6297	0.5197
3	✦	16.6529	-29.4084	(SEE NOTE)		34.73, 38.54	9	0.8686	0.1134

*Note: Paris Fit Used: Log DA/DN = C_1 (Log(ΔK) + C_2

METRIC CONVERSIONS

C1 METRIC = C1 ENGLISH C2 METRIC = C2 ENGLISH

C3 METRIC = C3 ENGLISH - 0.060335 C4 METRIC = C4 ENGLISH + 1.40483

CURVE	SYMBOL	SPEC NO	MATERIAL	TEMP	ATM	FREQ	R	TYPE	THIK	REMARKS	P/m
1	□	1SC	SC MAR-M-246+Hf	1400F	H 2	0.20HZ	R=.10	MCT	.4975		7.667
1	○	7SC	SC MAR-M-246+Hf	1400F	H 2	0.20HZ	R=.10	MCT	.5020		0.457
1	△	8SC	SC MAR-M-246+Hf	1400F	H 2	0.20HZ	R=.10	MCT	.5005		1.583
2	+	11SC	SC MAR-M-246+Hf	1600F	H 2	0.20HZ	R=.10	MCT	.4959		2.478
2	X	12SC	SC MAR-M-246+Hf	1600F	H 2	0.20HZ	R=.10	MCT	.4997		0.183
2	◇	17SC	SC MAR-M-246+Hf	1600F	H 2	0.20HZ	R=.10	MCT	.4985		0.923
3	✦	16SC	SC MAR-M-246+Hf	1600F	H20	0.20HZ	R=.10	MCT	.4984		1.029

FD 223725

Figure 62. Crack Growth Rate vs Stress Intensity for Single Crystal MAR-M-246 + Hf in 34.5 MPa (5000 psig) Gaseous Environments Perpendicular to the Solidification Direction 1. 760°C (1400°F) H_2 2. 871°C (1600°F) H_2 3. 871°C (1600°F) H_2 + H_2O

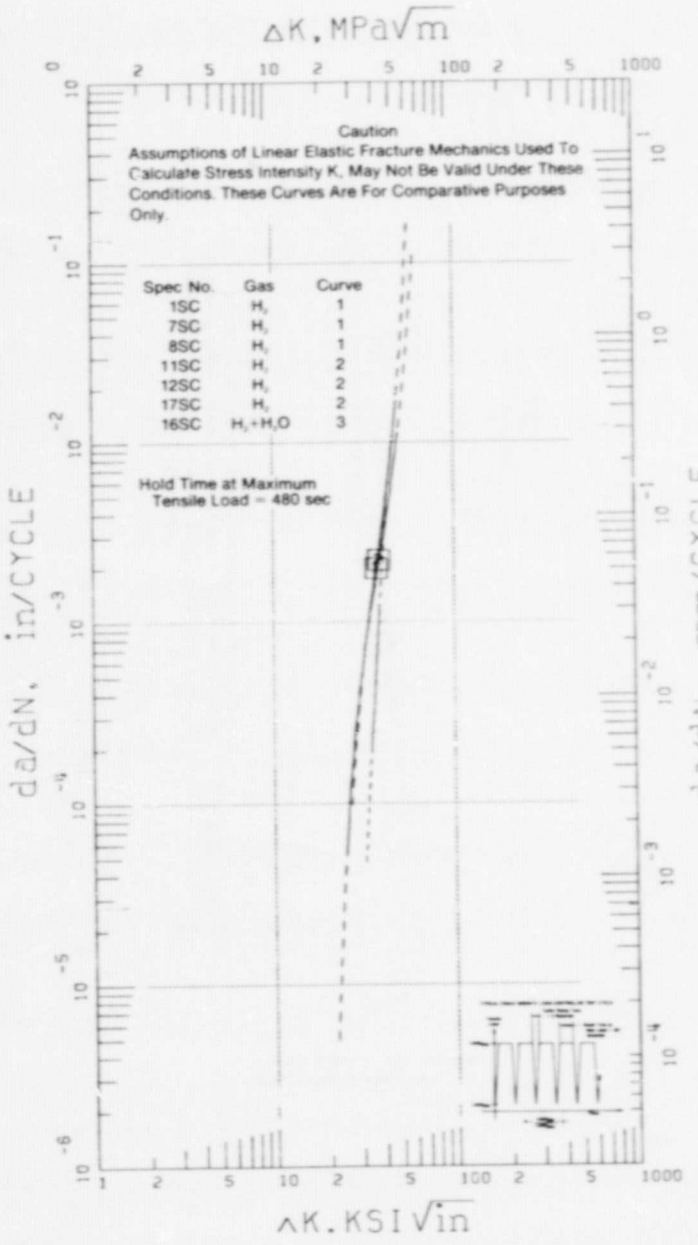

HYPERBOLIC SINE MODEL COEFFICIENTS

Y= C1 * SINH(C2 * X + C3) + C4

WHERE Y= LOG(da/dN) AND X=LOG(ΔK)

CURVE	SYMBOL	C1	C2	C3	C4	ΔK RANGE	NPTS	R^2	SEE
1		0.7000	5.5712	-1.5707	-2.7000	(33.67, 48.24)	17	0.2163	0.5125
2		0.7000	8.2408	-1.5861	-2.6553	(24.75, 49.08)	20	0.6297	0.5197
3		16.6929	-29.4084	(SEE NOTE)		(34.73, 38.54)	9	0.8686	0.1134

Note: Paris Fit Used: Log DA/DN = C_1 (Log(ΔK))+C_2

METRIC CONVERSIONS

C1 METRIC = C1 ENGLISH C2 METRIC = C2 ENGLISH

C3 METRIC = C3 ENGLISH - 0.040935 C4 METRIC = C4 ENGLISH + 1.40483

CURVE	SYMBOL	SPEC NO	MATERIAL	TEMP	ATM	FREQ	R	TYPE	THIK	REMARKS	P/R
1		1SC	SCMAR#HF	1400F	H 2	8HZWL	R=.10	MCT	.4975		7.557
1		7SC	SCMAR#HF	1400F	H 2	8HZWL	R=.10	MCT	.5320		0.457
1		8SC	SCMAR#HF	1400F	H 2	8HZWL	R=.10	MCT	.5005		1.583
2		11SC	SCMAR#HF	1600F	H 2	8HZWL	R=.10	MCT	.4999		2.438
2		12SC	SCMAR#HF	1600F	H 2	8HZWL	R=.10	MCT	.4997		0.183
2		17SC	SCMAR#HF	1600F	H 2	8HZWL	R=.10	MCT	.4985		0.923
3		16SC	SCMAR#HF	1600F	H20	8HZWL	R=.10	MCT	.4984		1.029

FD 223728

Figure 63. Crack Growth Rate vs Stress Intensity for Single Crystal MAR-M-246 + Hf in 34.5 MPa (5000 psig) Gaseous Environments Perpendicular to the Solidification Direction

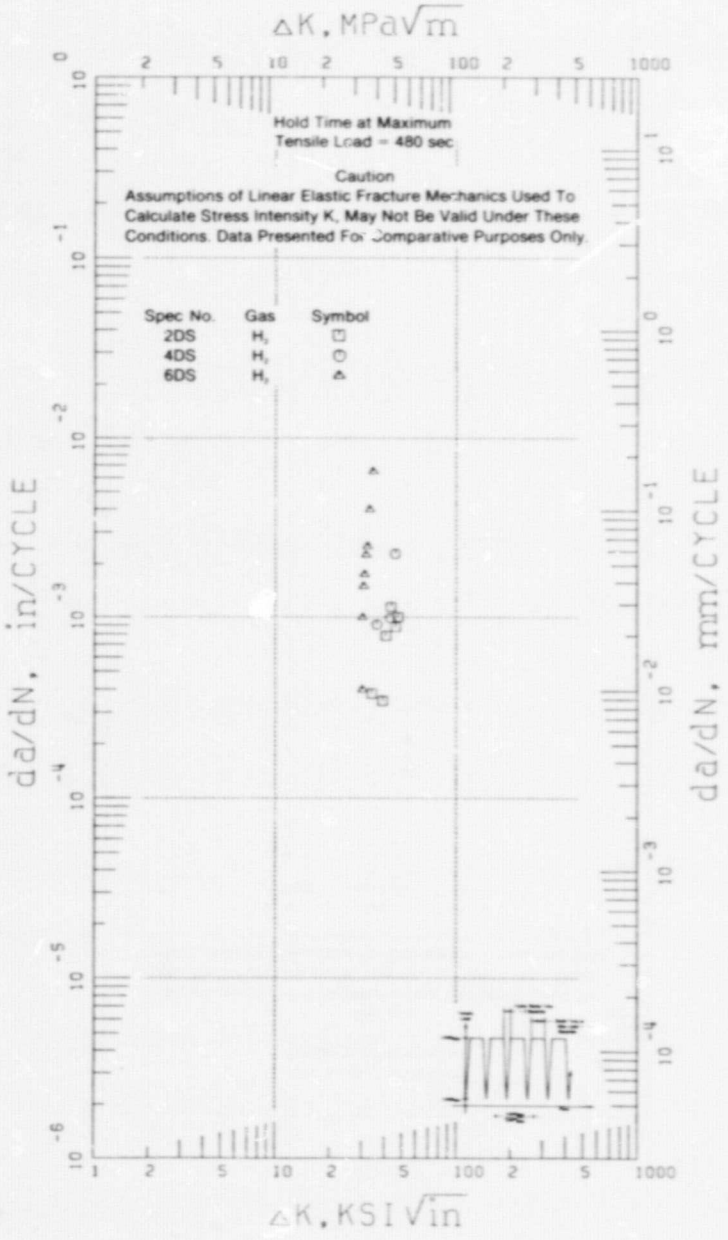

CURVE	SYMBOL	SPEC NO	MATERIAL	TEMP	ATM	FREQ	R	TYPE	THIK	REMARKS	P/R
□		2DS	DSMARMHF	1600F	H 2	8HZWL	R=.10	MCT	.5010		
○		4DS	DSMARMHF	1600F	H 2	8HZWL	R=.10	MCT	.4985		
△		6DS	DSMARMHF	1600F	H 2	8HZWL	R=.10	MCT	.4985		

FD 223731

Figure 64. Crack Growth Rate vs Stress Intensity for Directionally Solidified MAR-M-246 + Hf in 34.5 MPa (5000 psig) Hydrogen at 871°C (1600°F) Perpendicular to the Solidification Direction

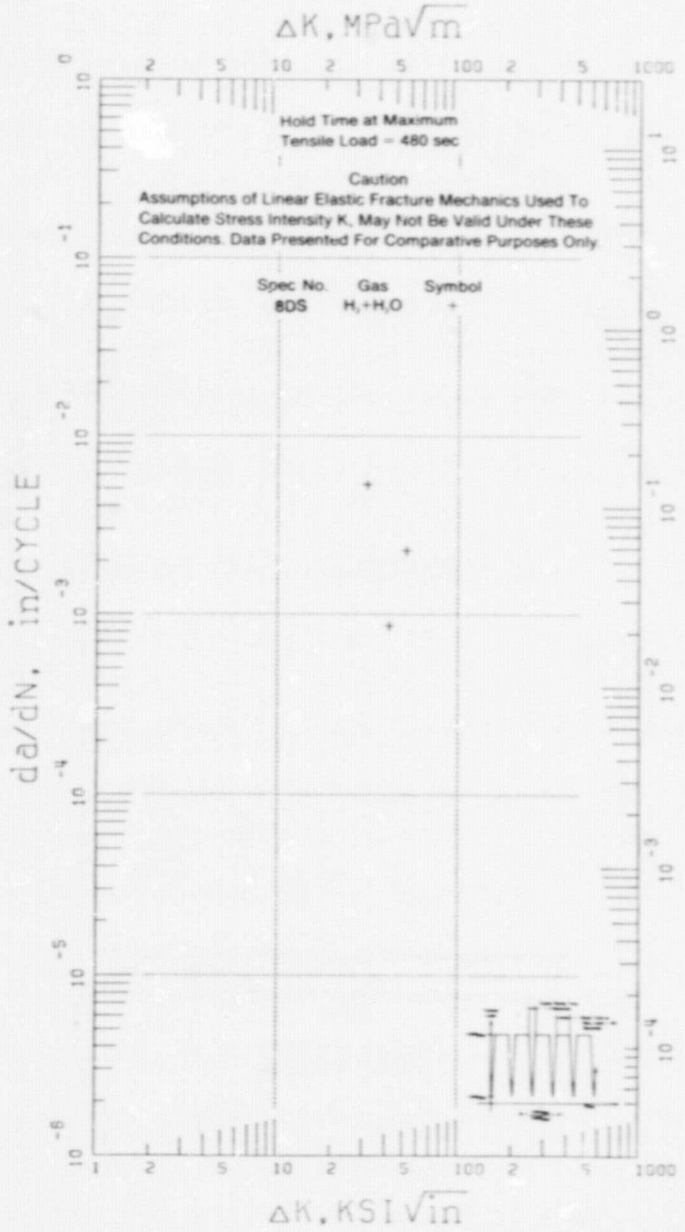

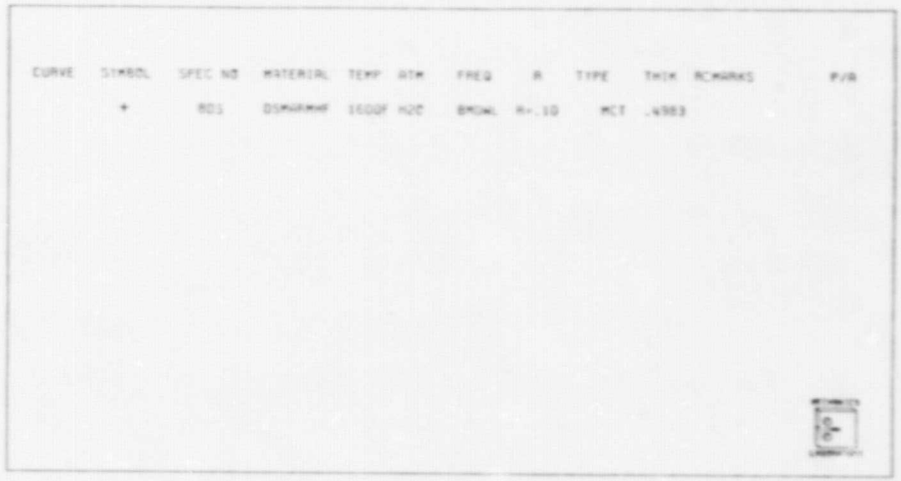

FD 223730

Figure 65. Crack Growth Rate vs Stress Intensity for Directionally Solidified MAR-M-246 + Hf in 34.5 MPa (5000 psig) Steam Enriched Hydrogen (50% Water Vapor by Weight) at 871°C (1600°F) Perpendicular to the Solidification Direction

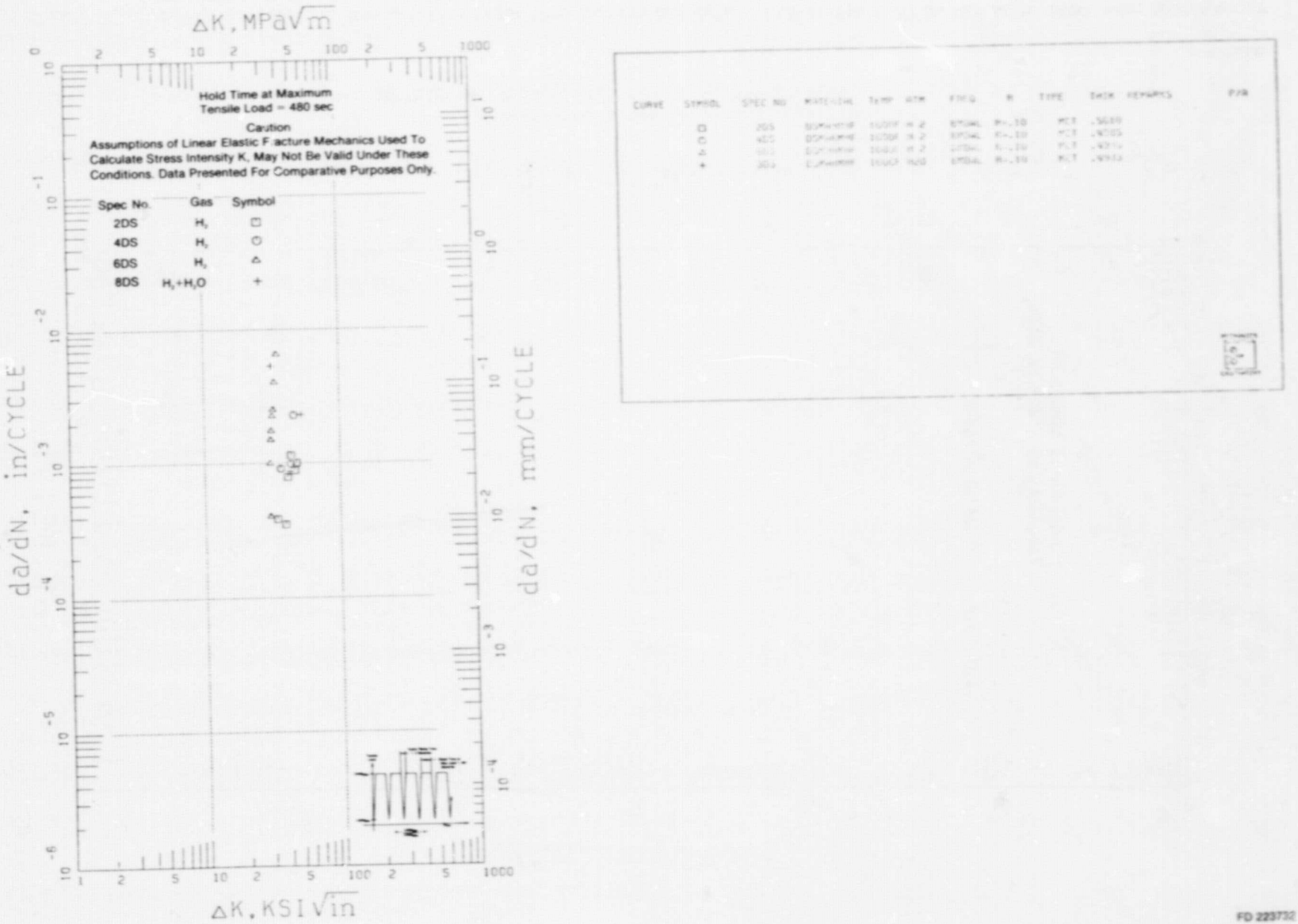

FD 223732

Figure 66. Crack Growth Rate vs Stress Intensity for Directionally Solidified MAR-M-246 + Hf in 34.5 MPa (5000 psig) Hydrogen vs Steam Enriched Hydrogen (50% Water Vapor by Weight) at 871°C (1600°F) Perpendicular to the Solidification Direction

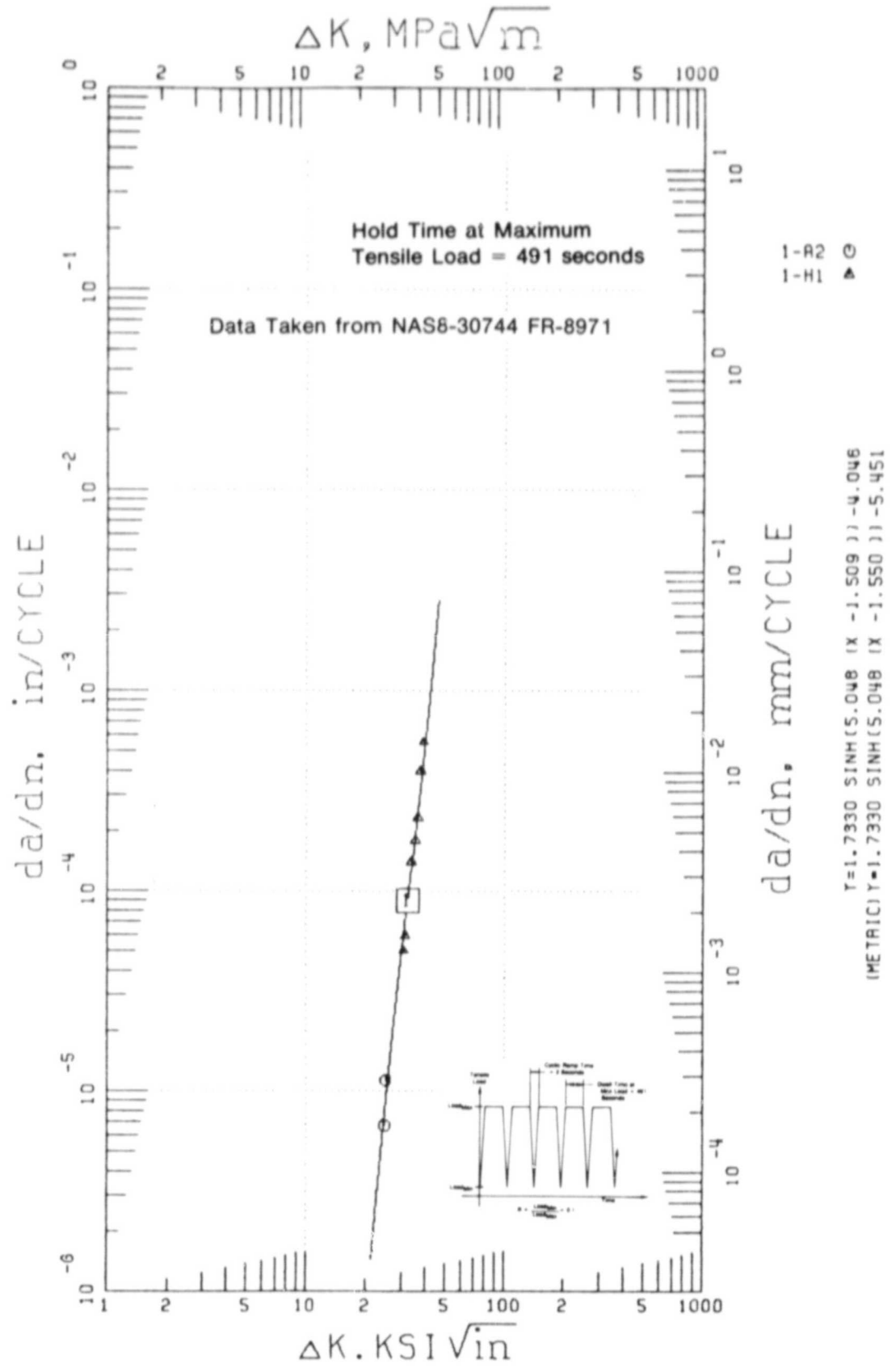

Figure 67. Crack Growth Rate vs Stress Intensity for Directionally Solidified MAR-M-246 + Hf in 34.5 MPa (5000 psig) Hydrogen at 538°C (1000°F) Parallel to the Solidification Direction

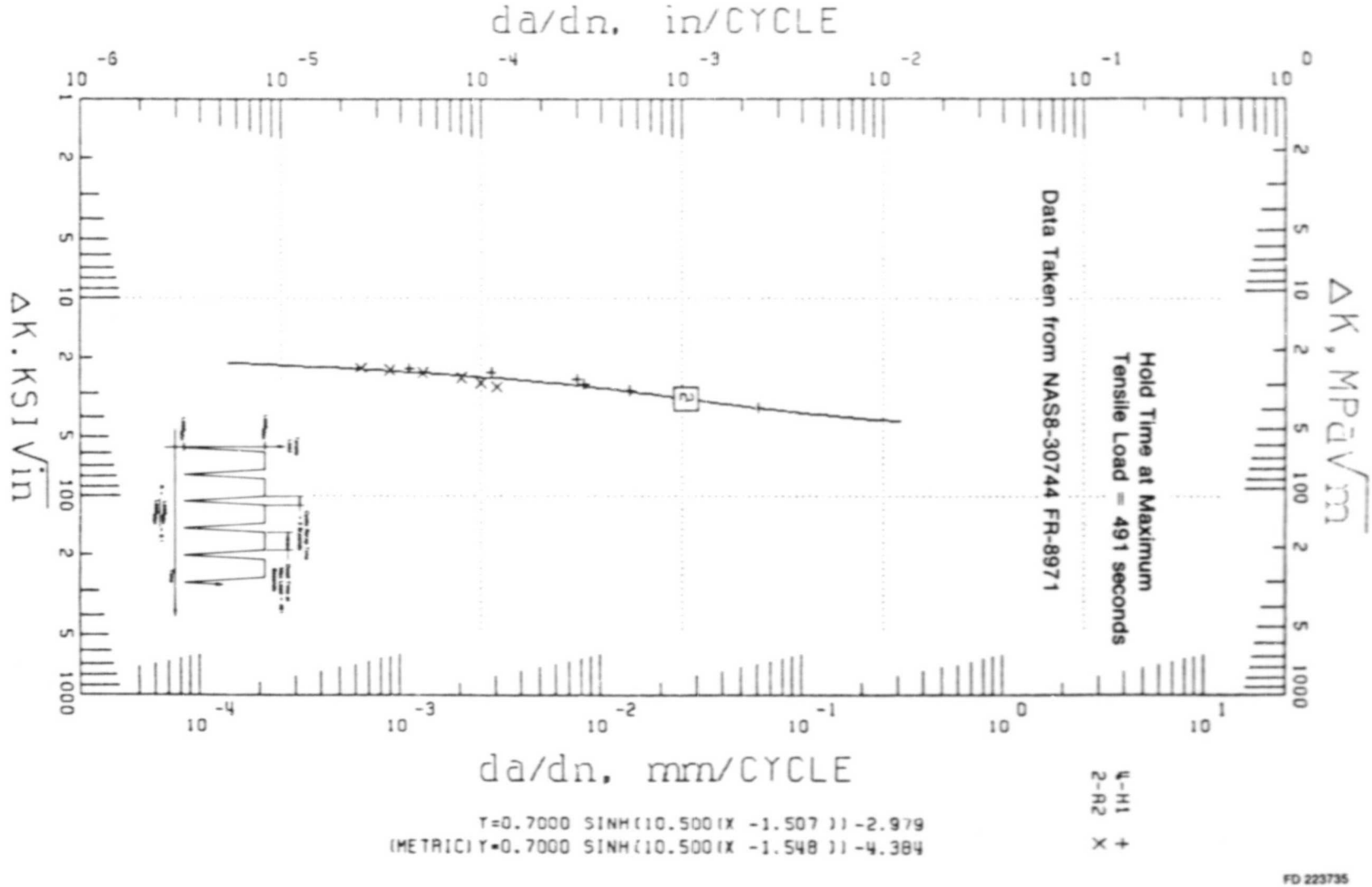

Figure 68. Crack Growth Rate vs Stress Intensity for Directionally Solidified MAR-M-246 + Hf in 34.5 MPa (5000 psig) Hydrogen at 871°C (1600°F) Parallel to the Solidification Direction

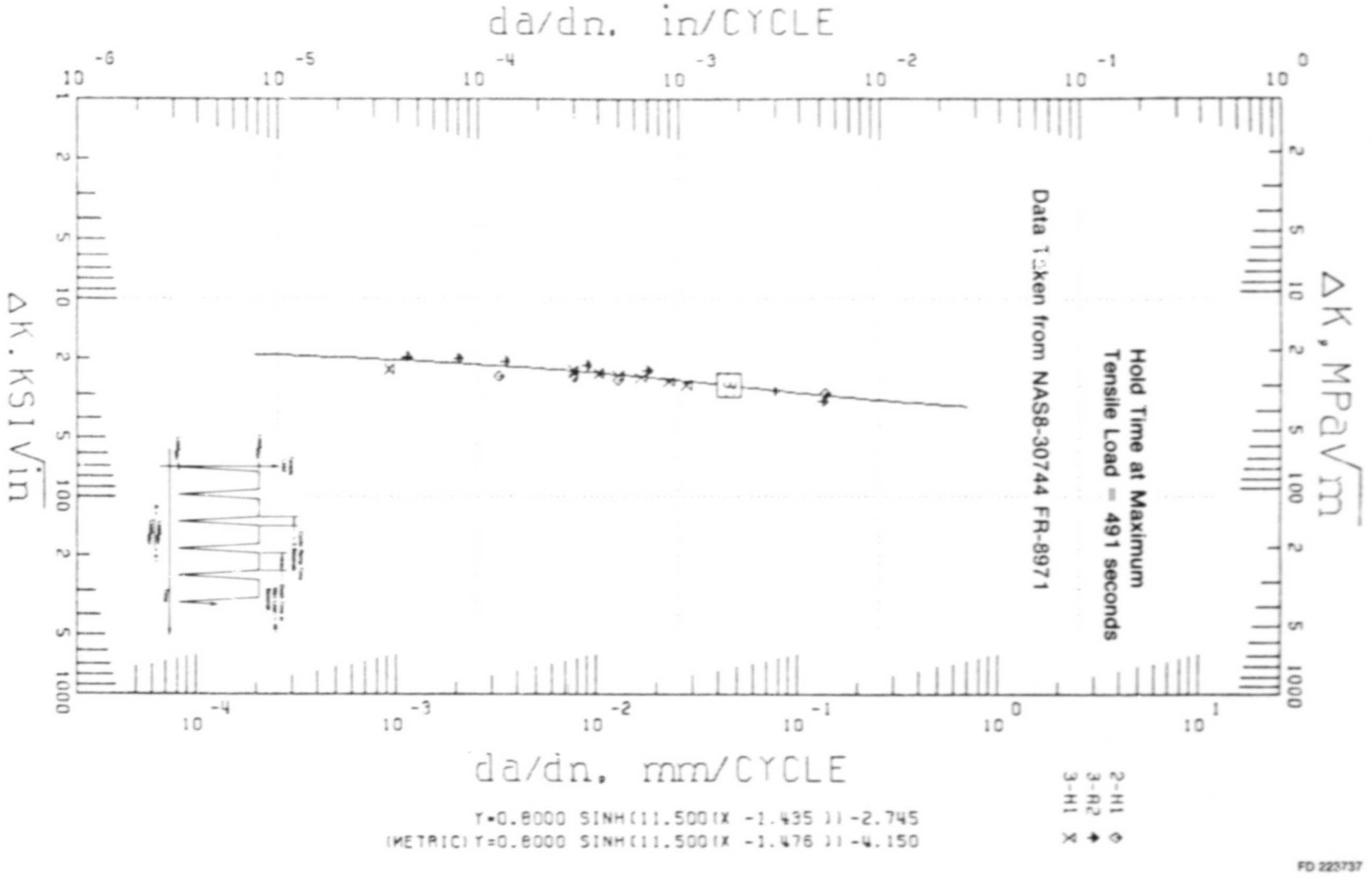

Figure 69. Crack Growth Rate vs Stress Intensity for Directionally Solidified MAR-M-246 + Hf in 34.5 MPa (5000 psig) Hydrogen and Water Vapor at 871°C (1600°F) Parallel to the Solidification Direction

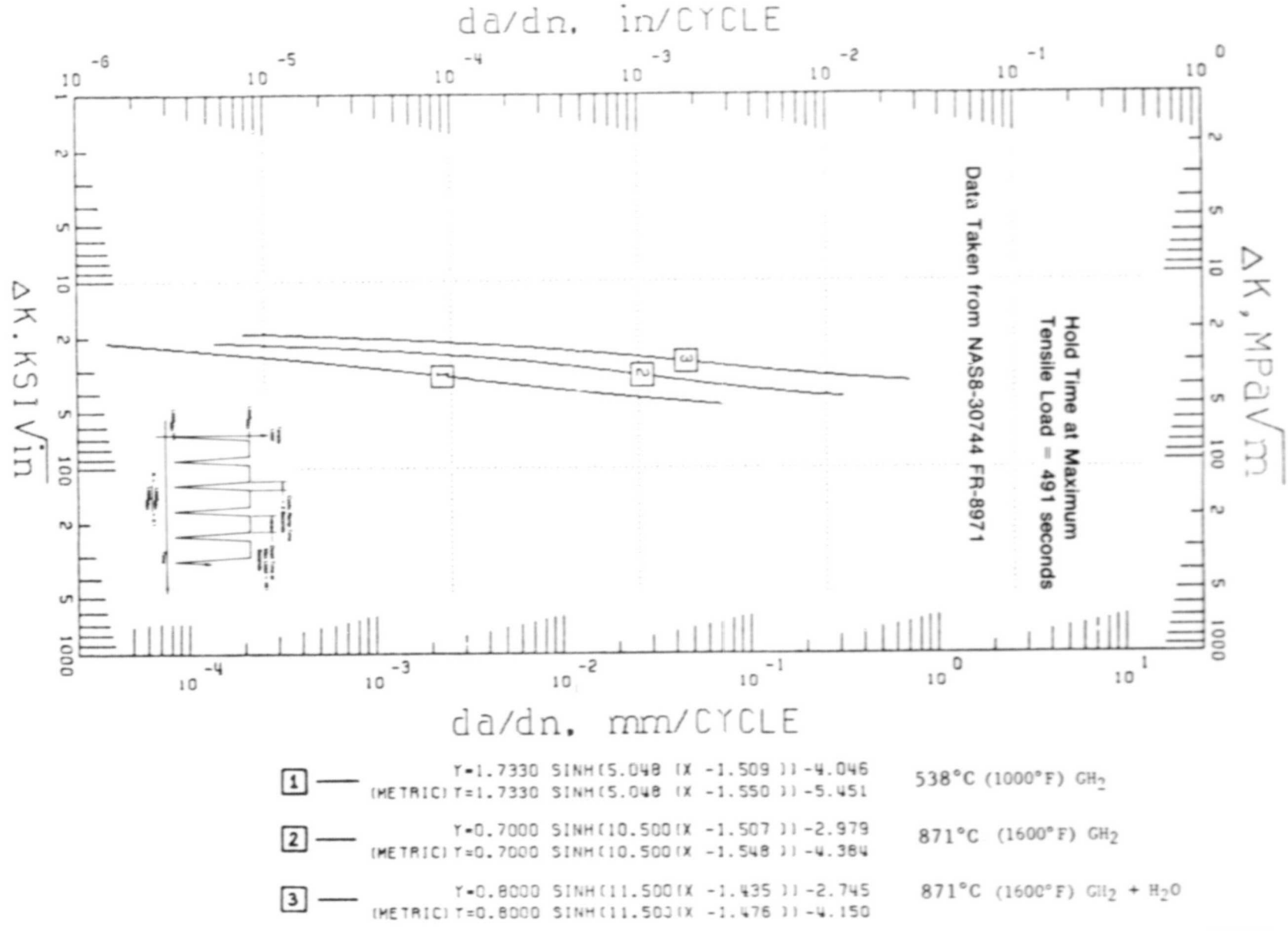

Figure 70. Crack Growth Rate vs Stress Intensity for Directionally Solidified MAR-M-246 + Hf in 34.5 MPa (5000 psig) Gaseous Environments at 538°C (1000°F) and 871°C (1600°F)

Table 20. Crack Growth Rate Testing of PWA 1480 and MAR-M-246+Hf in 34.5 MPa (5000 psig) Gaseous Environments

Material	Form	Test Specimen S/N	Temperature °C	Temperature °F	Test Conditions: Environment	Initial Stress Intensity MPa/√m	Initial Stress Intensity Ksi/in.	Max Load N	Max Load lb	Dwell Time[2] (Seconds)	Test Results: Cycles to Failure
MAR-M-246+Hf	Directionally Solidified	DS 2	871	1600	GH_2	35.2	32.0	5315	1195	480	206
MAR-M-246+Hf	Directionally Solidified	DS 4	871	1600	GH_2	37.4	34.0	5560	1250	480	87
MAR-M-246+Hf	Directionally Solidified	DS 6	871	1600	GH_2	34.8	31.6	5177	1164	480	16
MAR-M-246+Hf	Directionally Solidified	DS 8	871	1600	GH_2+H_2O	33.3	30.3	4448	1000	480	82
MAR-M-246+Hf	Single Crystal	SC 1	760	1400	GH_2	40.8	37.1	8407	1890	480	6
MAR-M-246+Hf	Single Crystal	SC 7	760	1400	GH_2	37.9	34.5	8229	1850	480	106
MAR-M-246+Hf	Single Crystal	SC 8	760	1400	GH_2	38.5	35.0	6761	1520	480	30
MAR-M-246+Hf	Single Crystal	SC 11	871	1600	GH_2	30.2	27.5	4893	1100	480	143
MAR-M-246+Hf	Single Crystal	SC 12	871	1600	GH_2	42.9	39.1	5049	1135	480	553
MAR-M-246+Hf	Single Crystal	SC 17	871	1600	GH_2	35.9	32.7	6450	1450	480	15
MAR-M-246+Hf	Single Crystal	SC 16	871	1600	GH_2+H_2O	39.2	35.6	6672	1500	480	103
PWA 1480	Single Crystal	P1	760	1400	GH_2	38.1	34.7	6227	1400	480	252
PWA 1480	Single Crystal	P2	760	1400	GH_2	38.9	35.4	6672	1500	480	599
PWA 1480	Single Crystal	P3	Failed Due to Power Failure								
PWA 1480	Single Crystal	P4	871	1600	GH_2	43.7	39.8	6338	1425	480	95
PWA 1480	Single Crystal	P5	871	1600	GH_2	38.5	35.0	3990	897	480	55
PWA 1480	Single Crystal	P6	Failed During Precracking								
PWA 1480	Single Crystal	P7	871	1600	GH_2+H_2O	41.9	38.2	5738	1290	480	267

[1]Environment:

GH_2 — Gaseous hydrogen (with oxygen content less than 1 part per million)
GH_2+H_2O — 50 gaseous hydrogen + 50 water vapor by weight

[2]Dwell Time is the period of time the specimen is held at the maximum tensile load
[3]Electrical Power Failure caused overstress and premature failure
[4]Max Load is as tabulated: Min load = 10 of Max load. R = $Load_{min}/Load_{max}$ = 0.1.

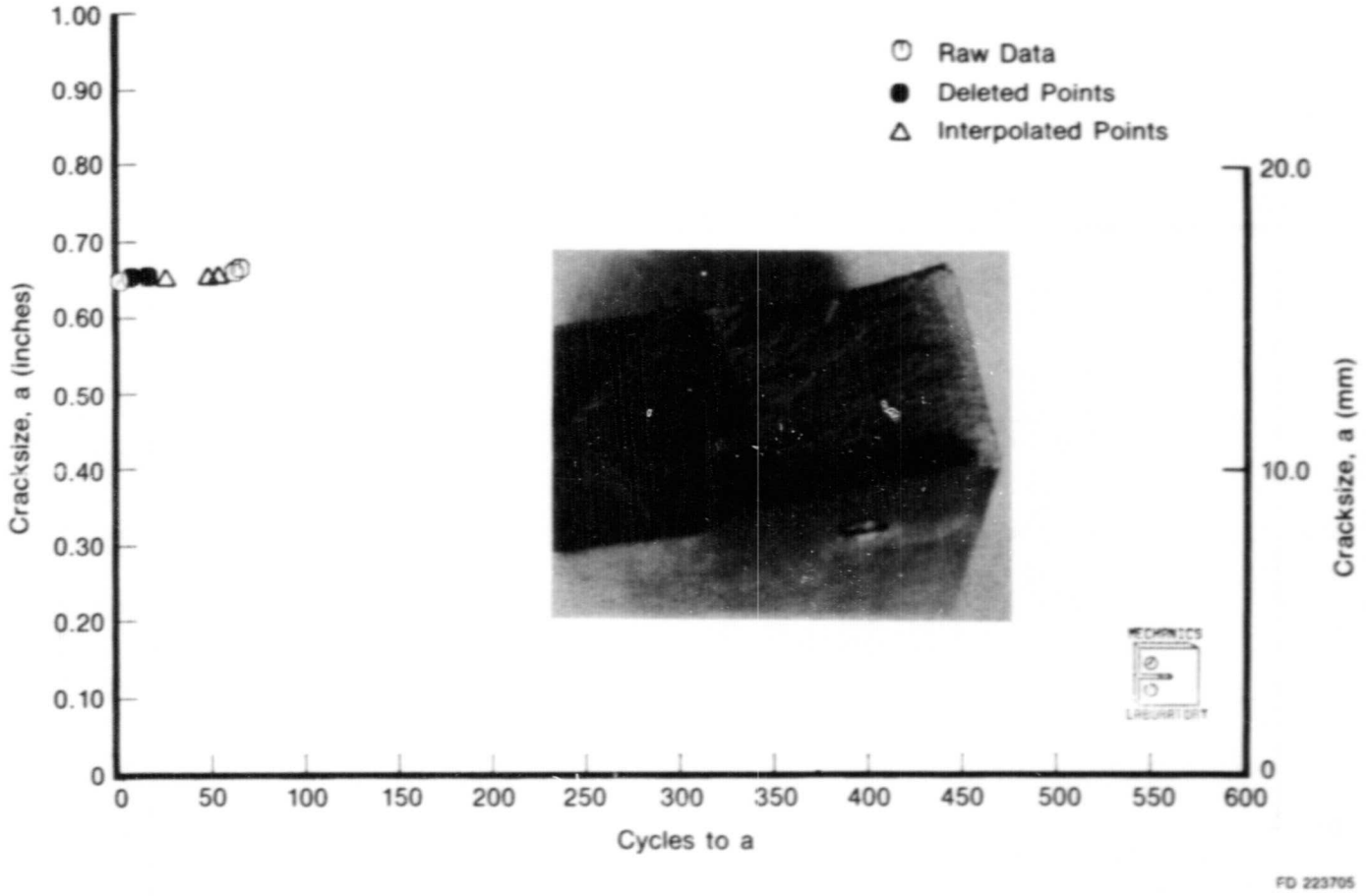

Figure 71. Crack Size vs Life for PWA 1480 S/N 1 760°C (1400°F)

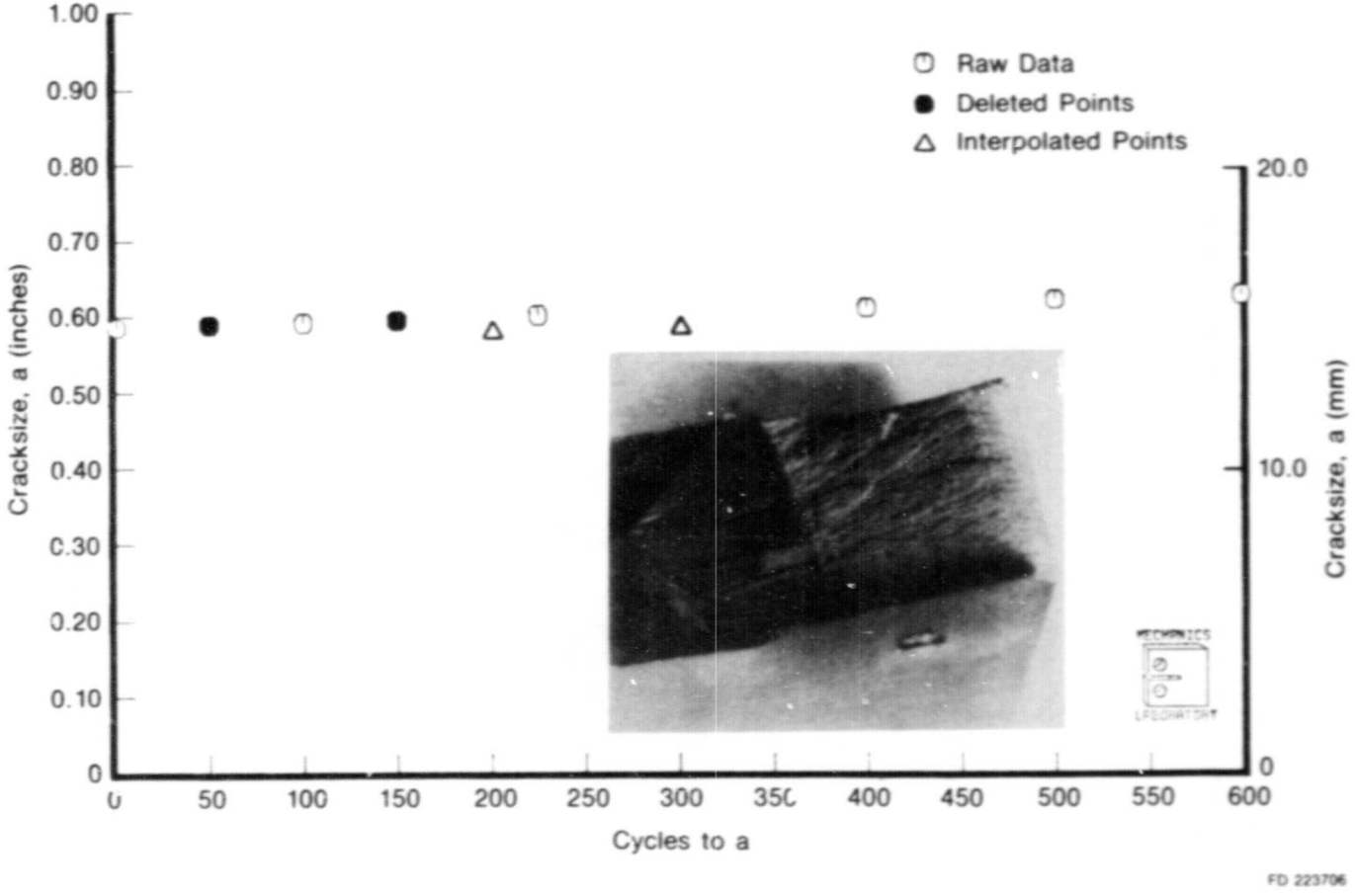

Figure 72. Crack Size vs Life for PWA 1480 S/N 2 760°C (1400°F)

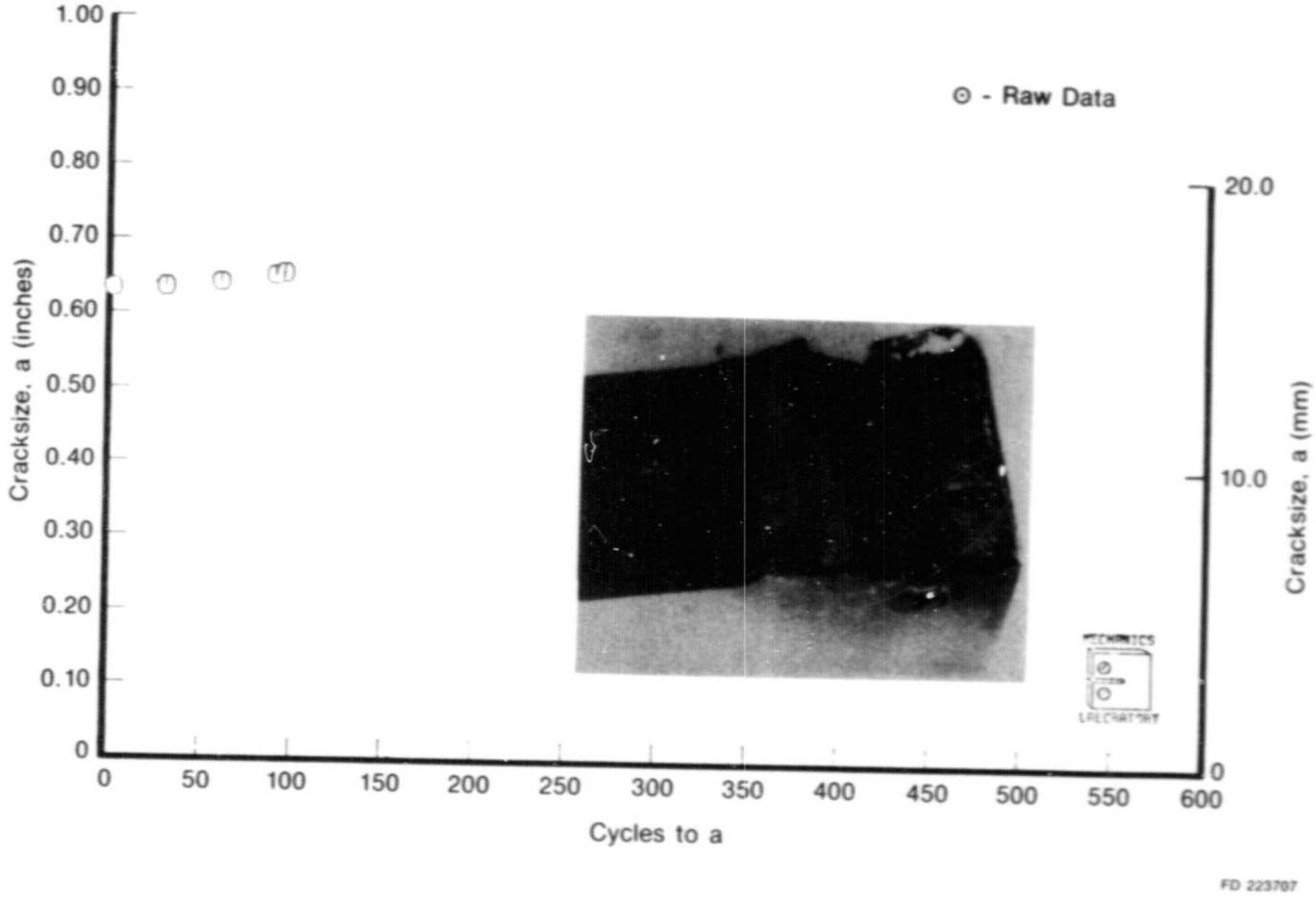

Figure 73. Crack Size vs Life for PWA 1480 S/N 4 871°C (1600°F)

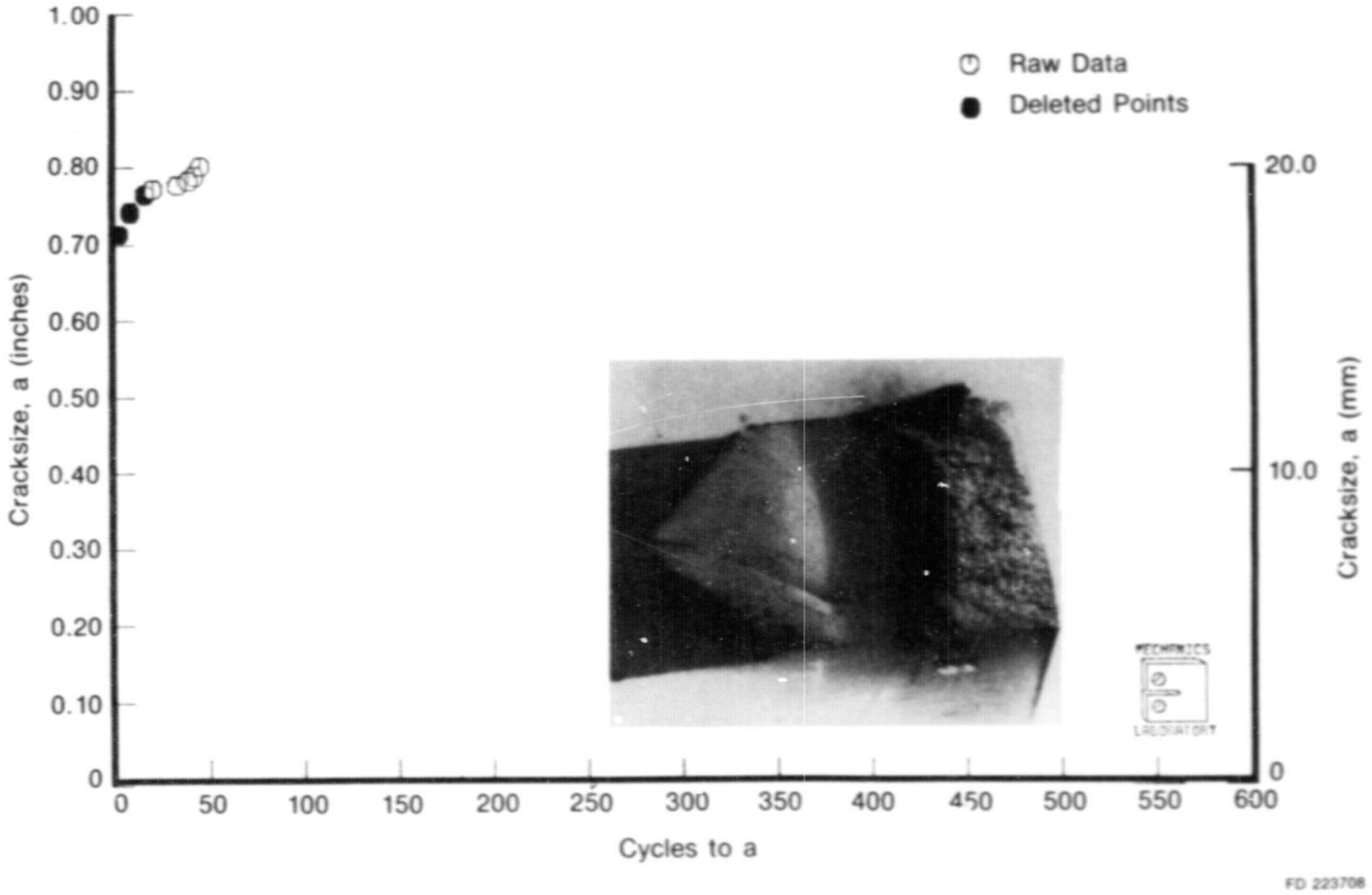

Figure 74. Crack Size vs Life for PWA 1480 S/N 5 871°C (1600°F)

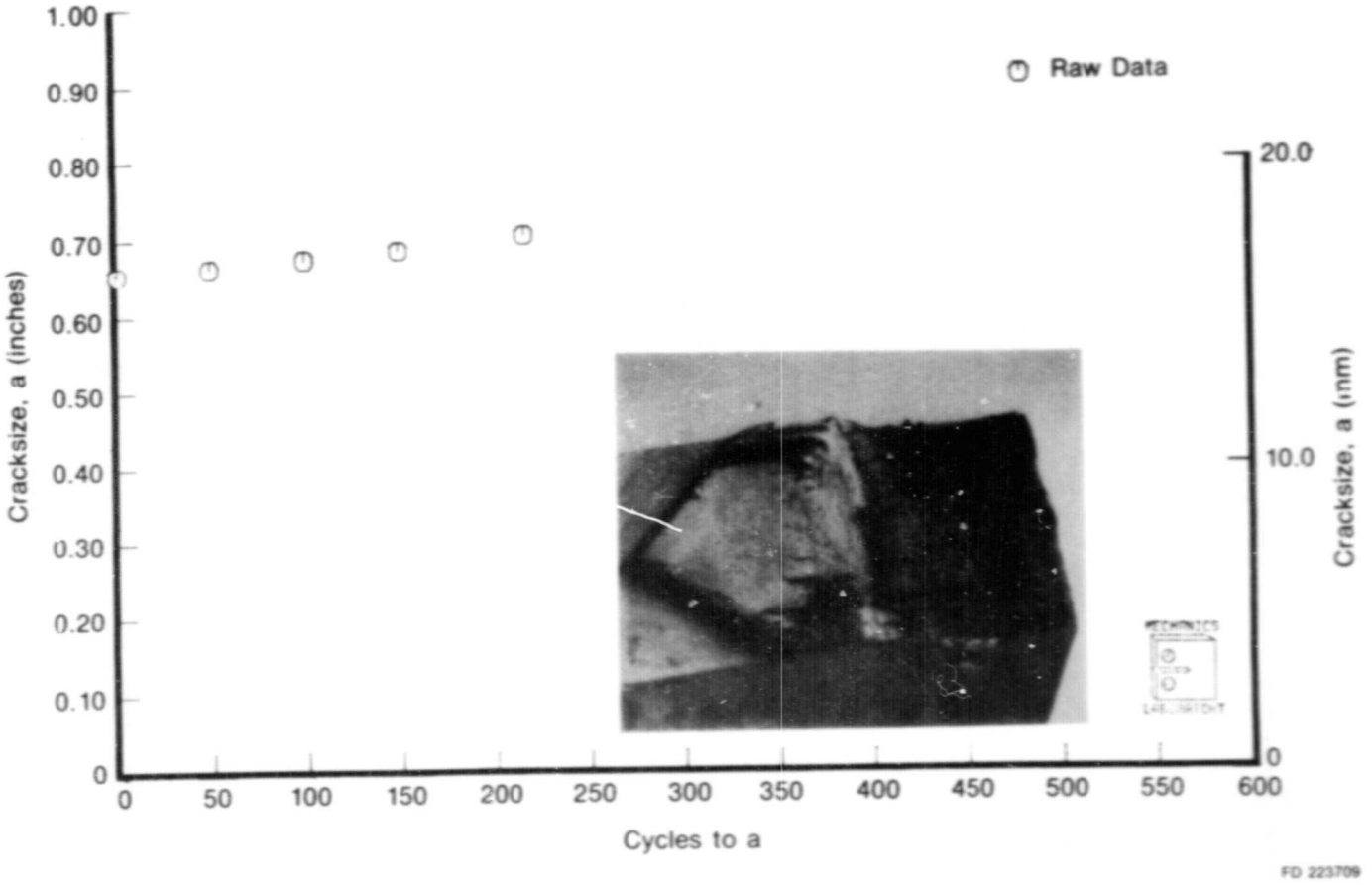

Figure 75. Crack Size vs Life for PWA 1480 S/N 7 871°C (1600°F)

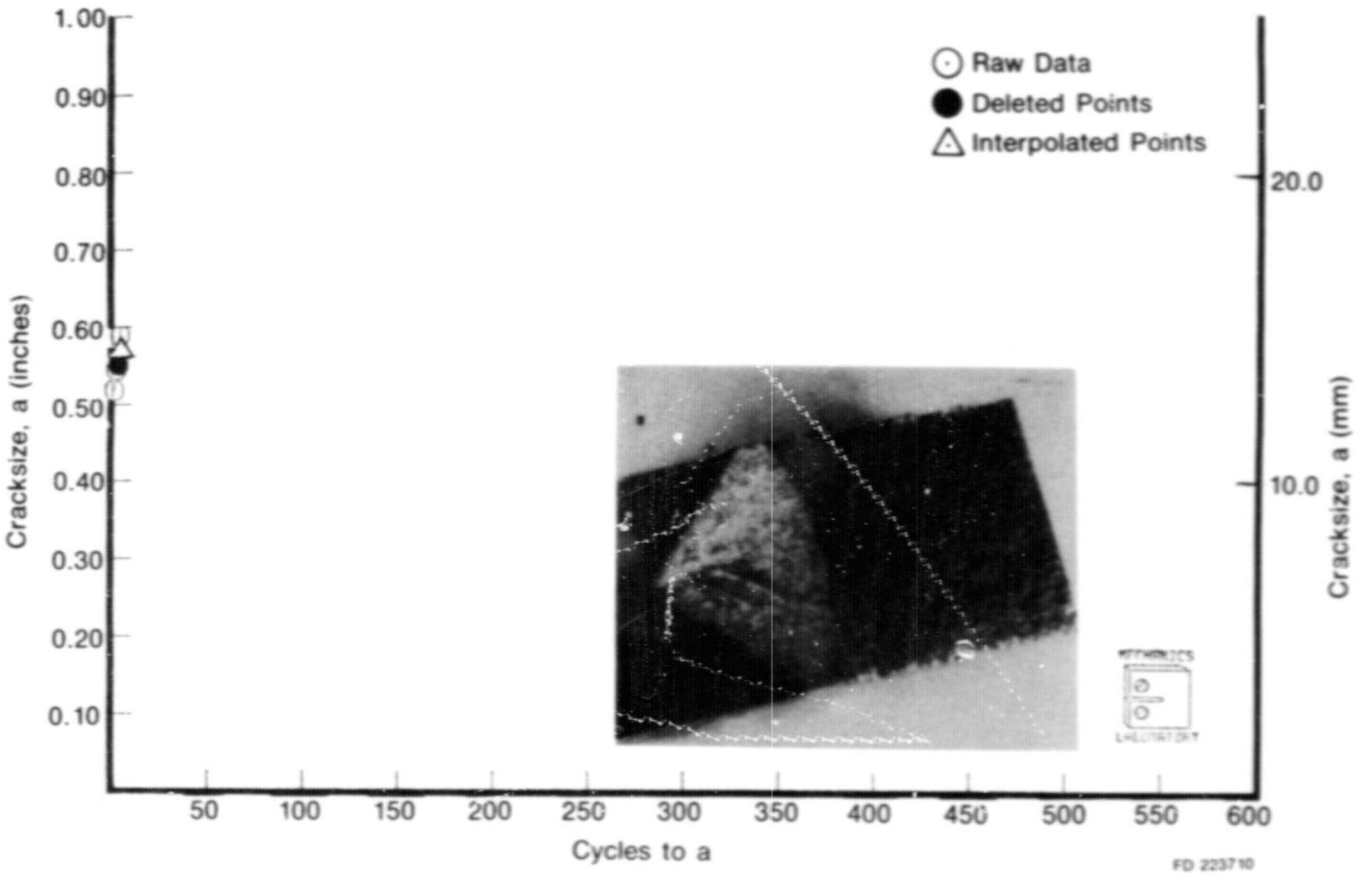

Figure 76. Crack Size vs Life for S.C. MAR-M-246 + Hf S/N 1 760°C (1400°F)

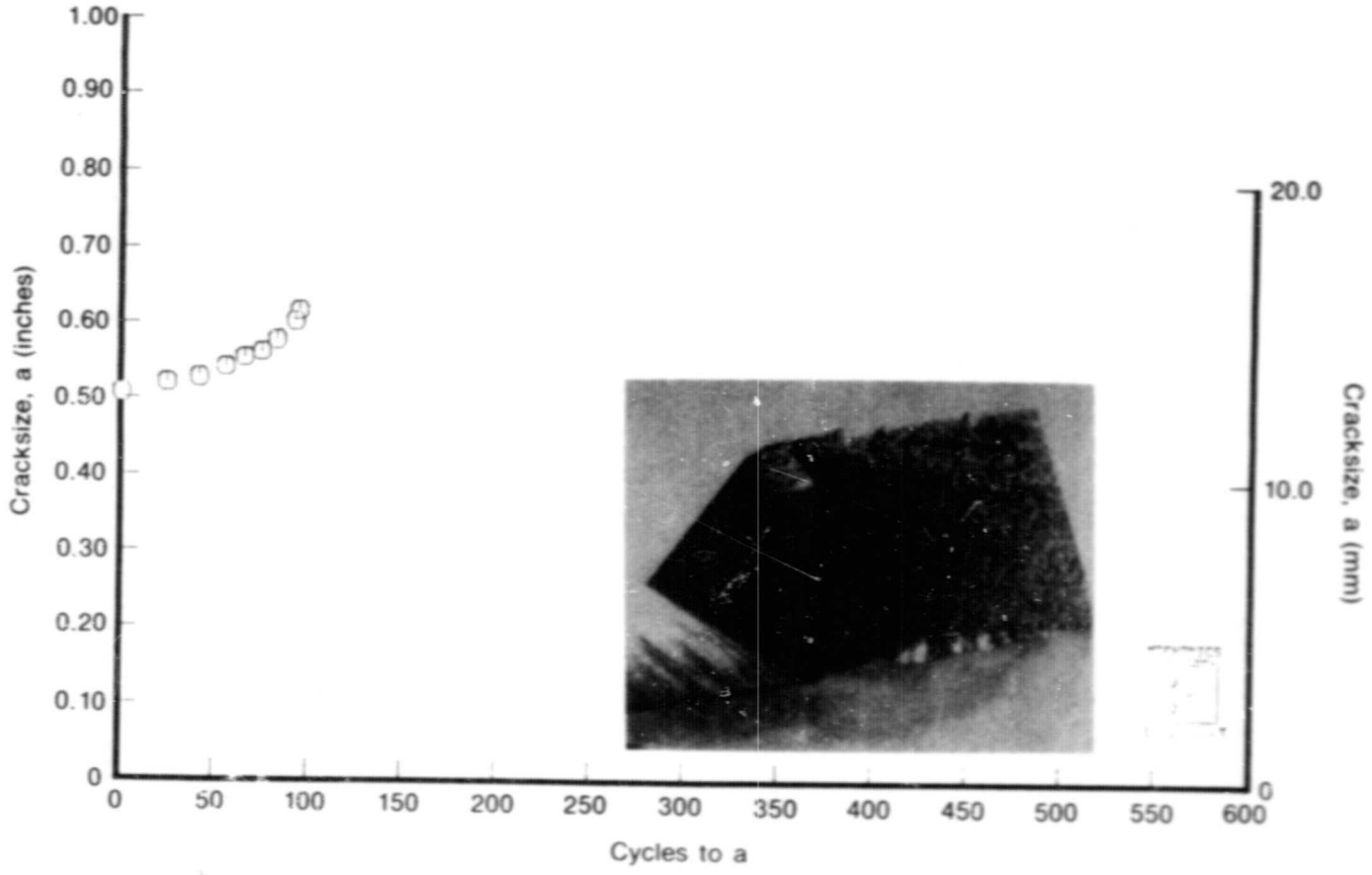

Figure 77. Crack Size vs Life for S.C. MAR-M-246 + Hf S/N 7 760°C (1400°F)

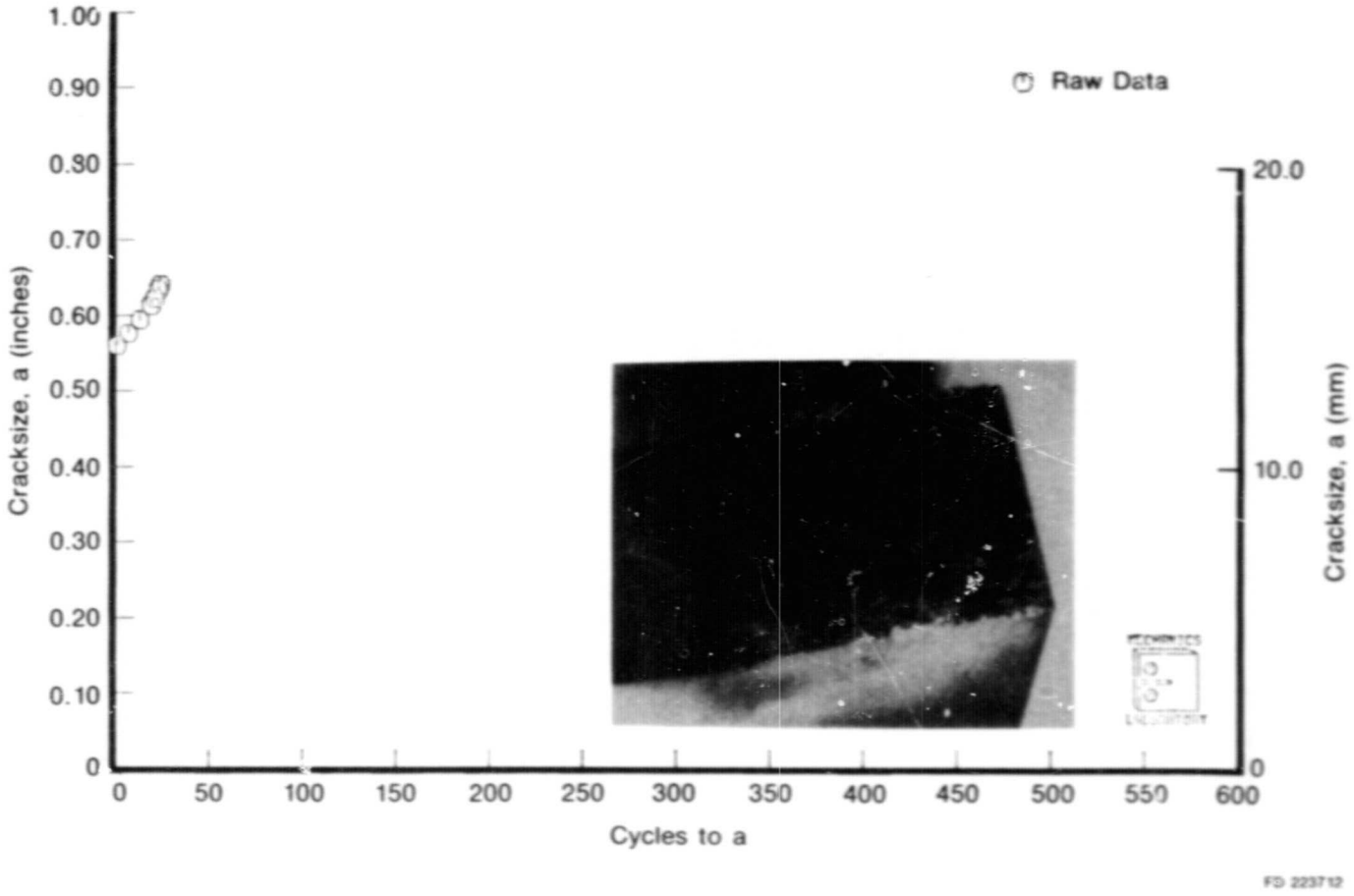

Figure 78. Crack Size vs Life for S.C. MAR-M-246 + Hf S/N 8 760°C (1400°F)

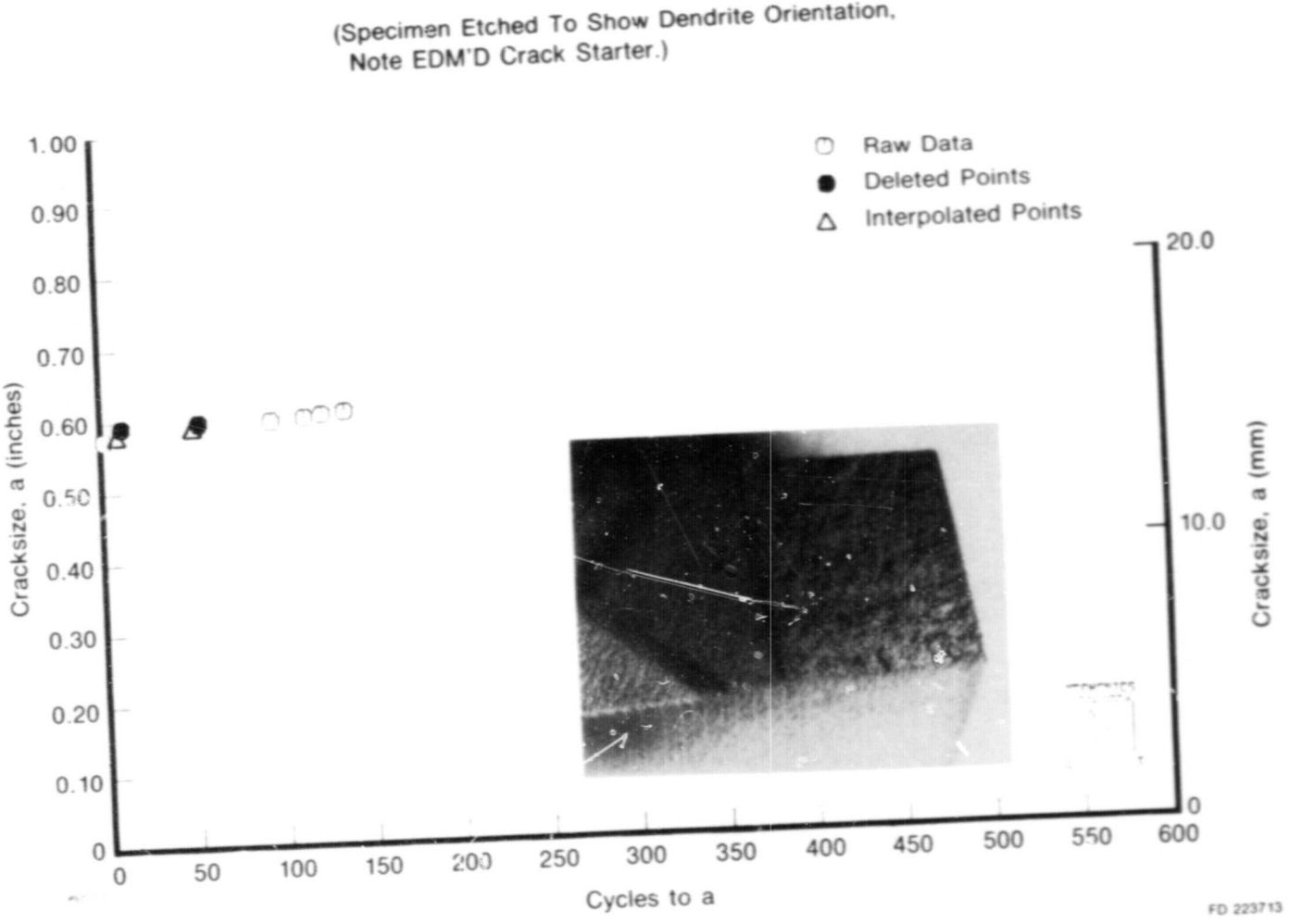

Figure 79. Crack Size vs Life for S.C. MAR-M-246 + Hf S/N 11 871°C (1600°F)

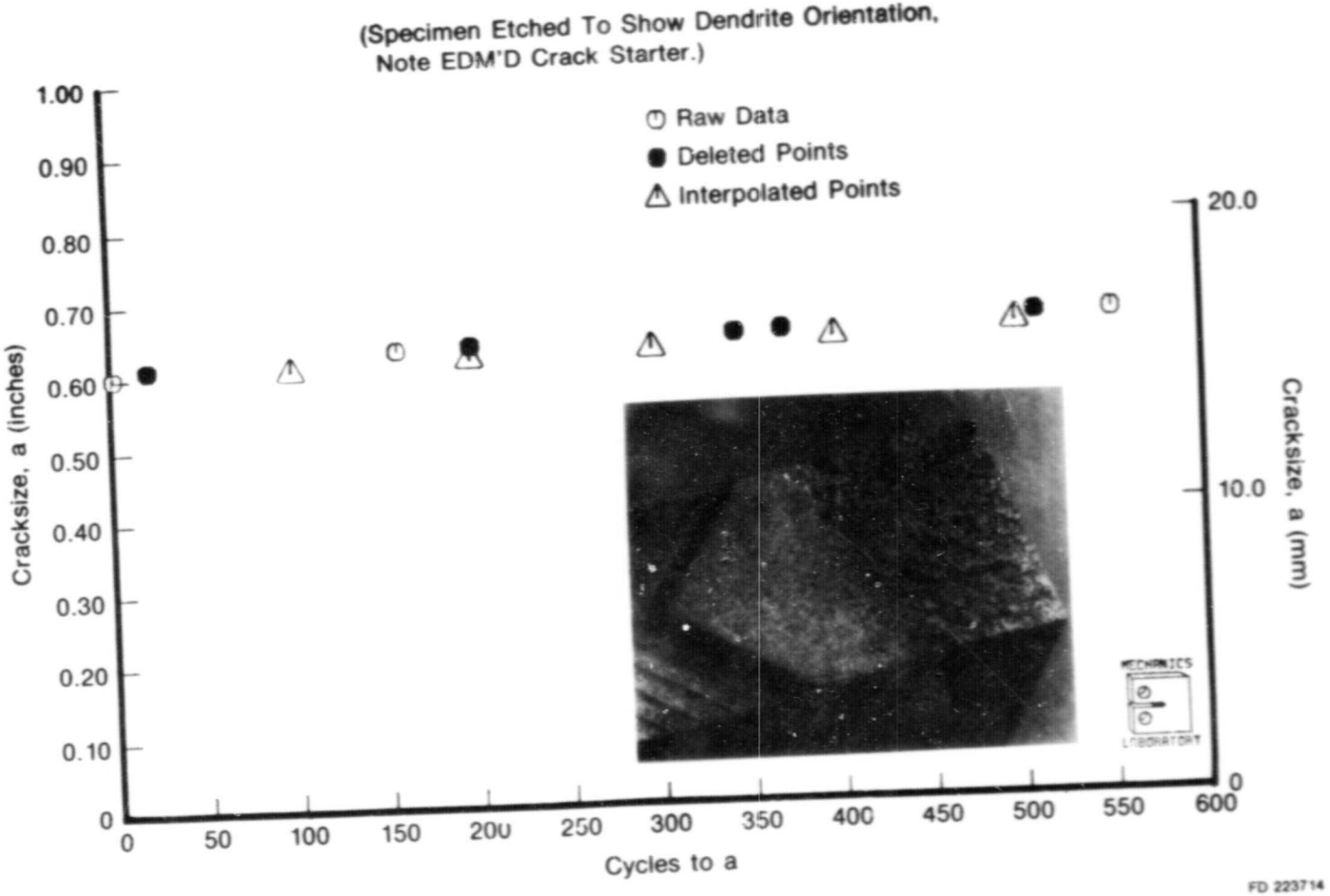

Figure 80. Crack Size vs Life for S.C. MAR-M-246 + Hf S/N 12 871°C (1600°F)

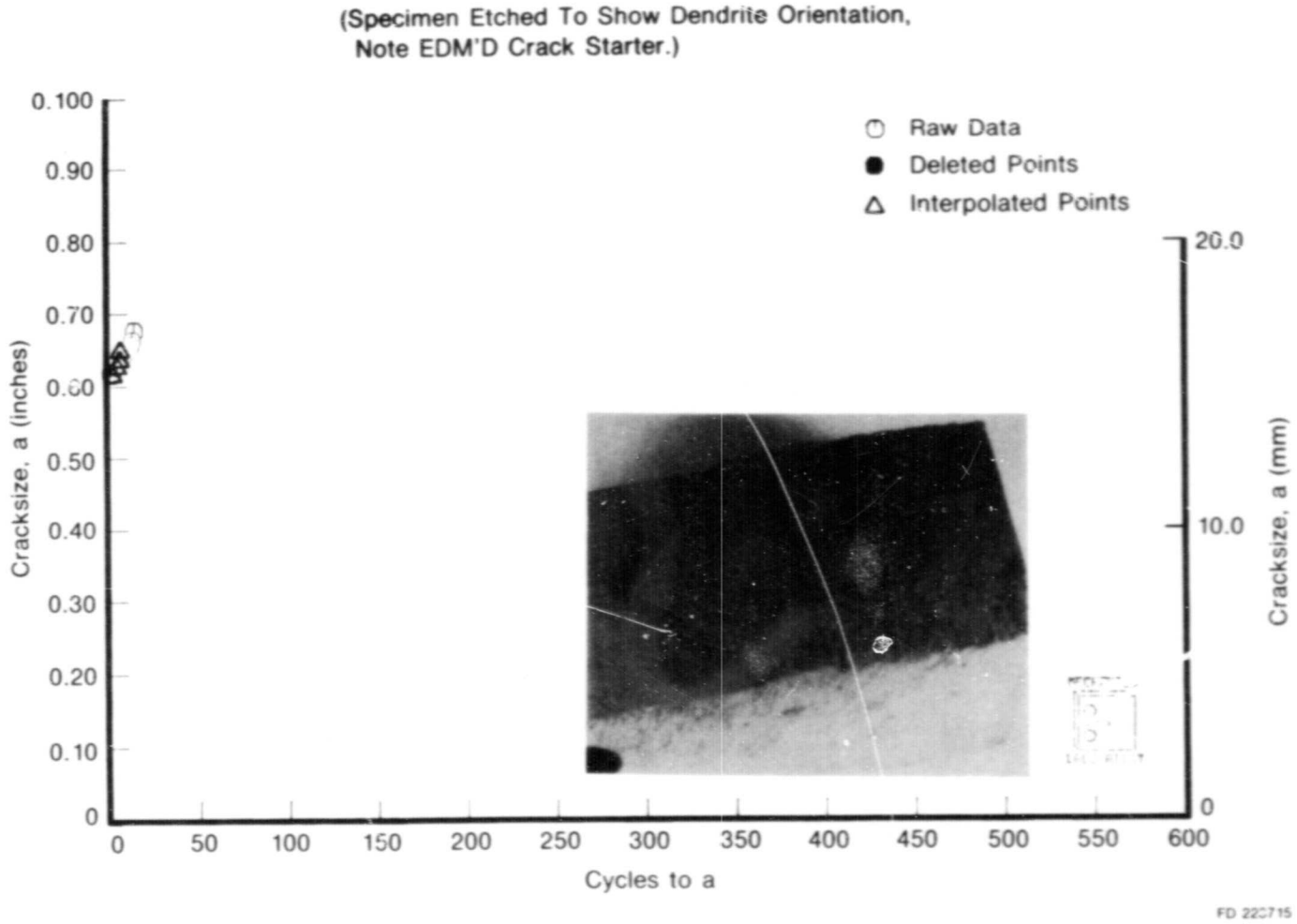

Figure 81. Crack Size vs Life for S.C. MAR-M-246 + Hf S/N 17 871°C (1600°F)

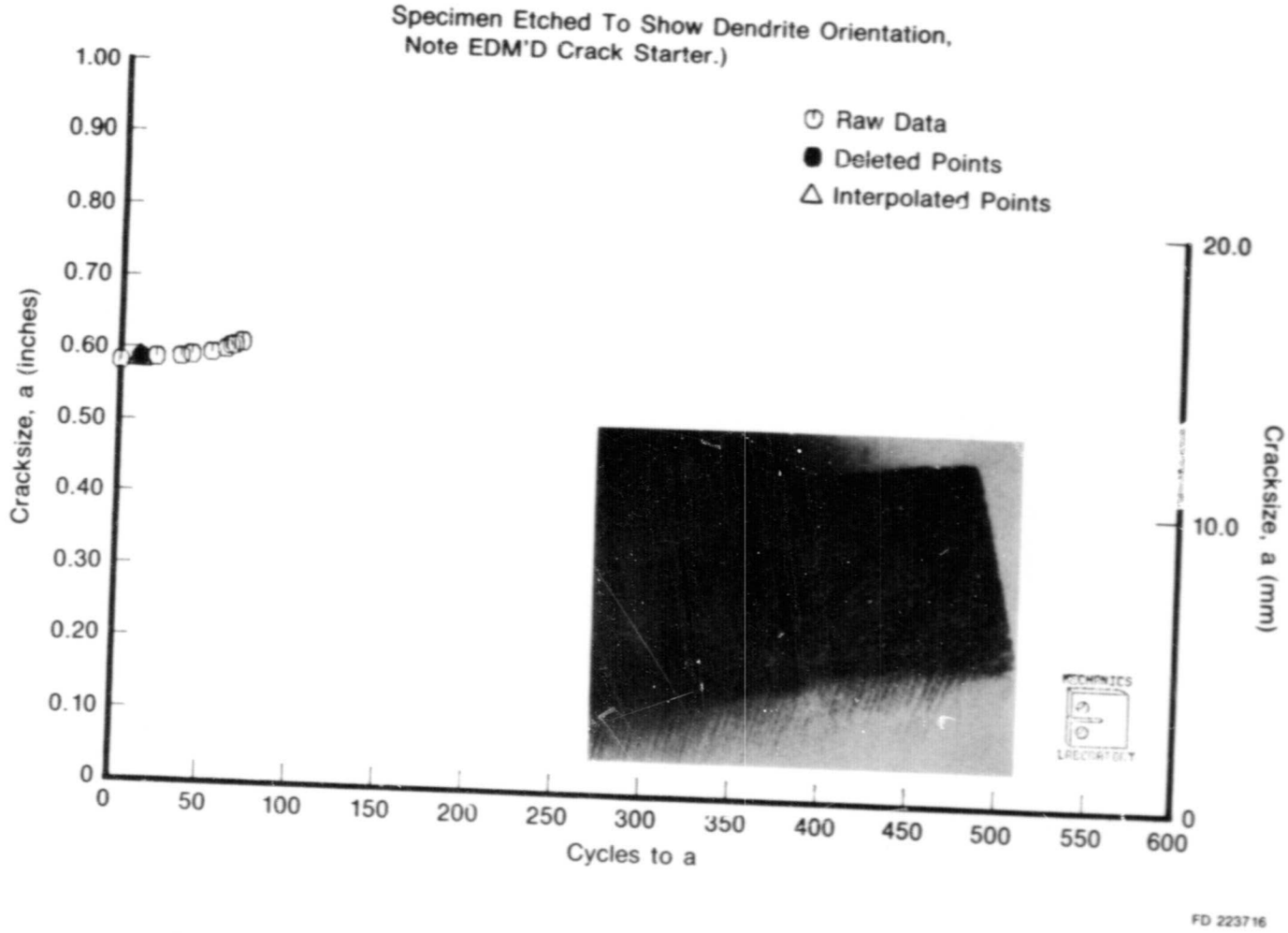

Figure 82. Crack Size vs Life for S.C. MAR-M-246 + Hf S/N 16 871°C (1600°F)

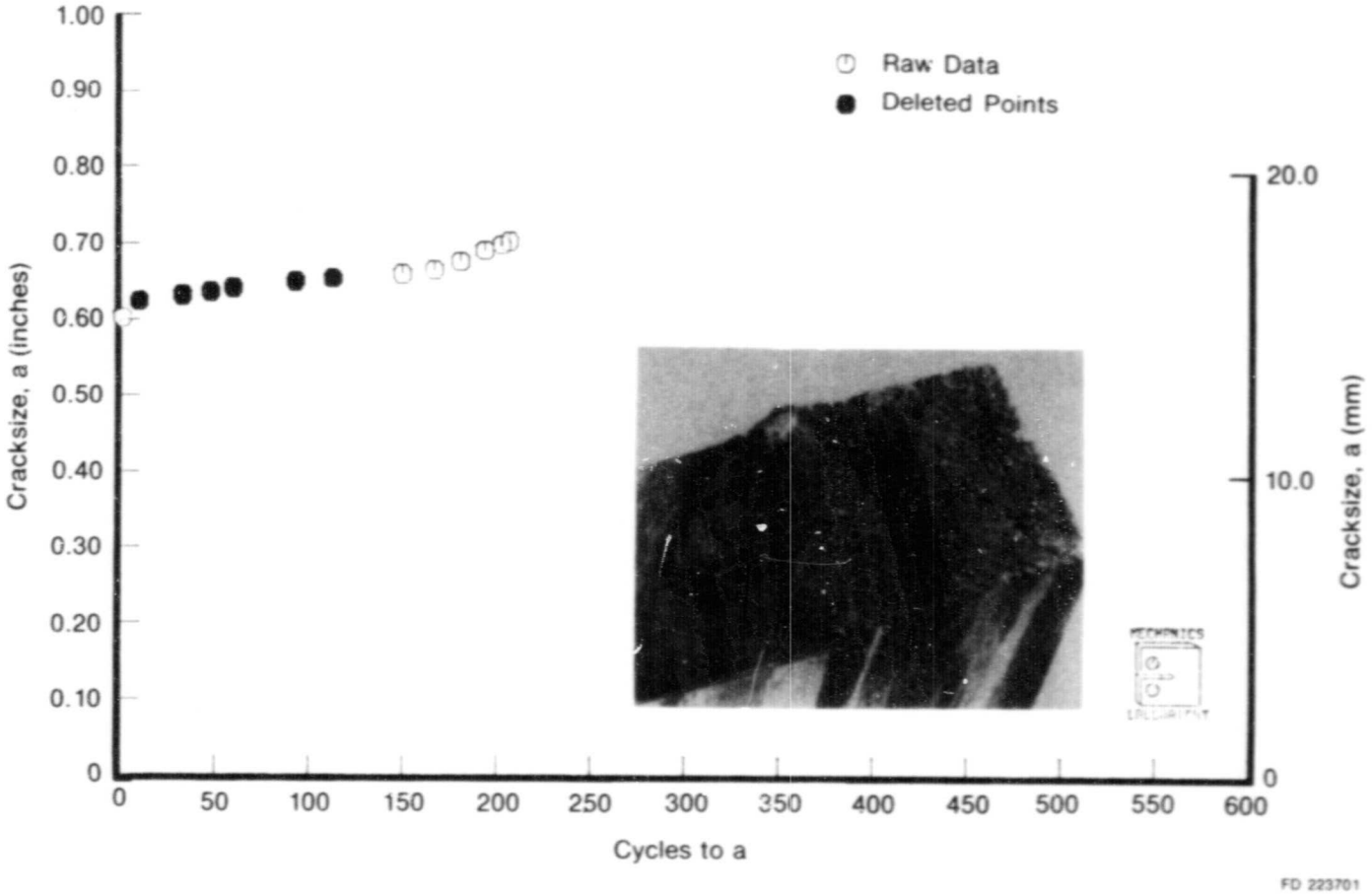

Figure 83. Crack Size vs Life for D.S. MAR-M-246 + Hf S/N 2 871°C (1600°F)

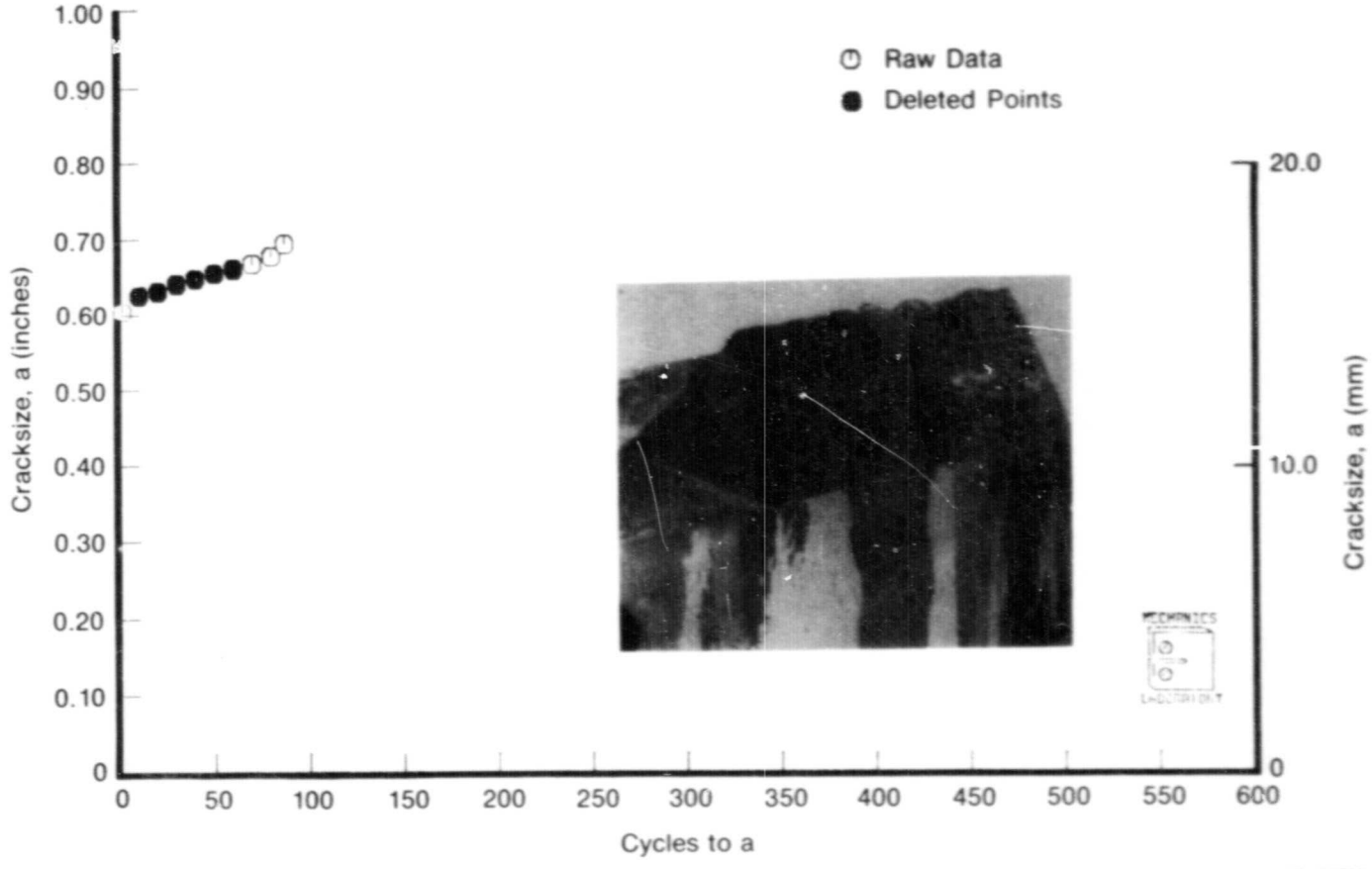

Figure 84. Crack Size vs Life for D.S. MAR-M-246 + Hf S/N 4 871°C (1600°F)

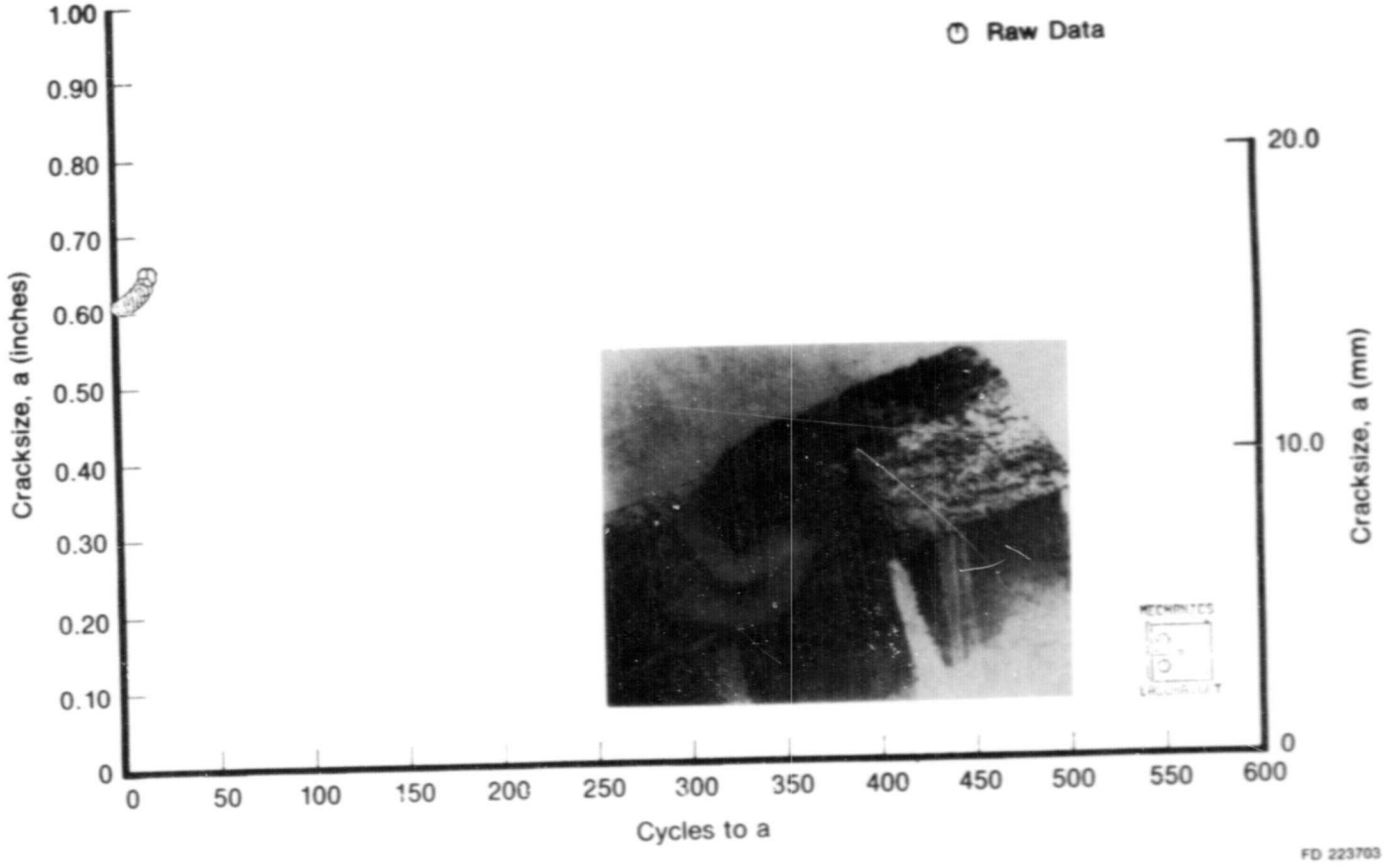

Figure 85. Crack Size vs Life for D.S. MAR-M-246 + Hf S/N 6 871°C (1600°F)

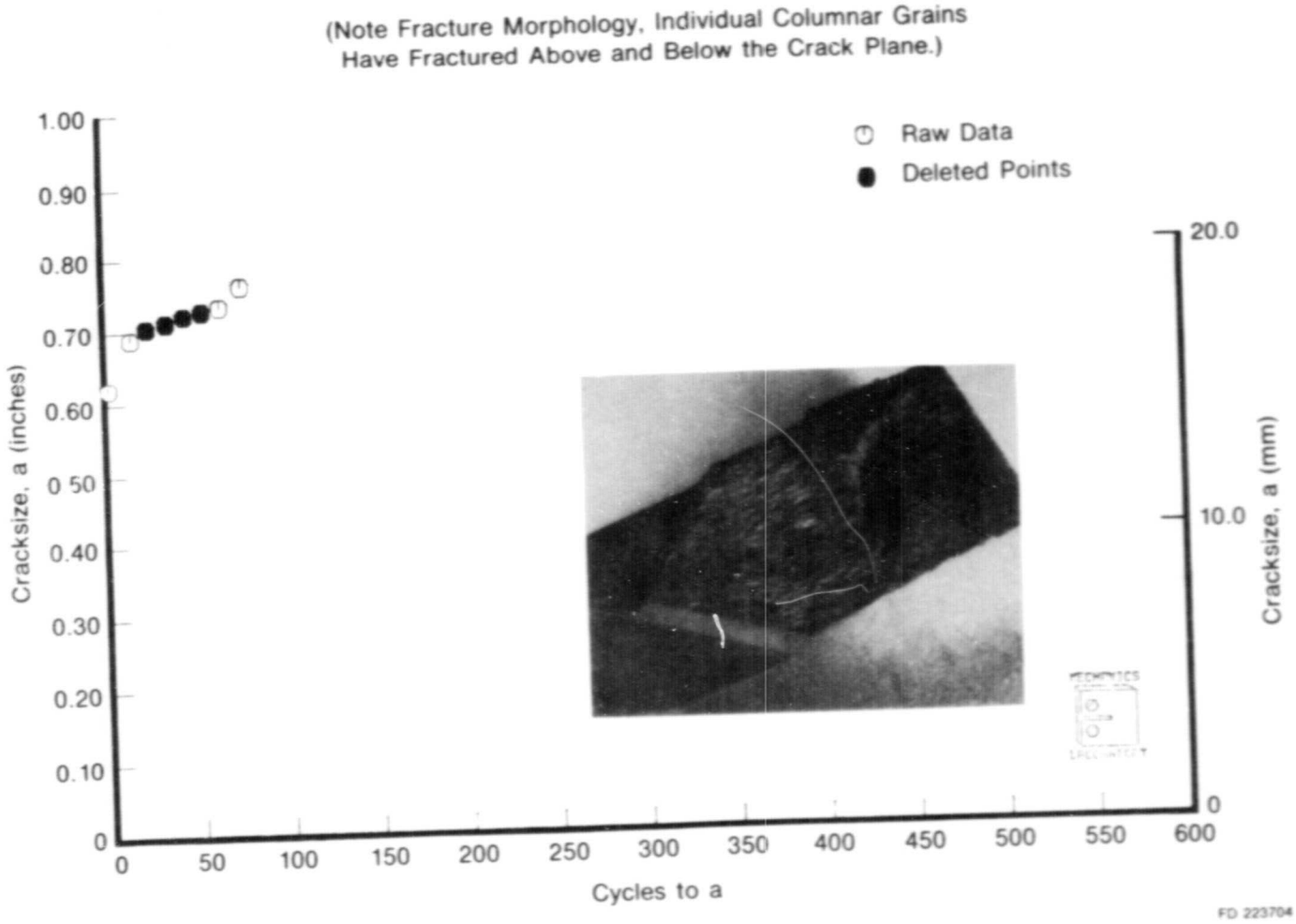

Figure 86. Crack Size vs Life for D.S. MAR-M-246 + Hf S/N 8 871°C (1600°F)

Based upon fracture surface examination which indicated mixed mode crack propagation (out of plane growth) and gross crack front shape, the assumptions of linear elastic fracture mechanics for these anisotropic materials were generally not met. Consequently, the equations for stress intensity K are invalid, and da/dn vs ΔK curves are presented for comparative purposes only.

C. TEST PROCEDURE

The specimen configuration used for crack growth testing was the lw compact specimen detailed in figure 11 . This specimen incorporated a chevron-type crack-starter notch and integrally machined knife edges for Crack Opening Displacement (COD) extensometry attachment as recommended by ASTN E399-74, "Plane-Strain Fracture Toughness of Metallic materials." Specimen thickness was chosen to conform to supplied raw material dimensions, and to the high pressure test vessel retort size.

The PWA 1480, MAR-M-246+Hf DS and SC material was machined such that crack growth properties could be determined perpendicular to the primary grain direction (see figure 7; L-T orientation per ASTM E399-74).

A compliance calibration was conducted to relate the COD measured by the test extensometry to the test specimen crack length. The compliance between the measured COD and the handbook* prediction was compared at various crack length, load, and temperature conditions. Results are presented in figure 87. The measured COD agreed with the handbook predictions, and the handbook relationship was used for all environmental testing. The PWA 1480 data points shown are calculated using values for both longitudinal and transverse elastic moduli as specimen orientations will vary in the x-y plane with respect to the [001] and [110] crystallographic planes. These points bracket the curve, consequently the effective E' values were taken from the curve.

*Tada, H., P.C. Paris, and G.R. Irwin, "The Stress Analysis of Cracks Handbook," Del Research Corporation, Hellertown, Pennsylvania, 1973.

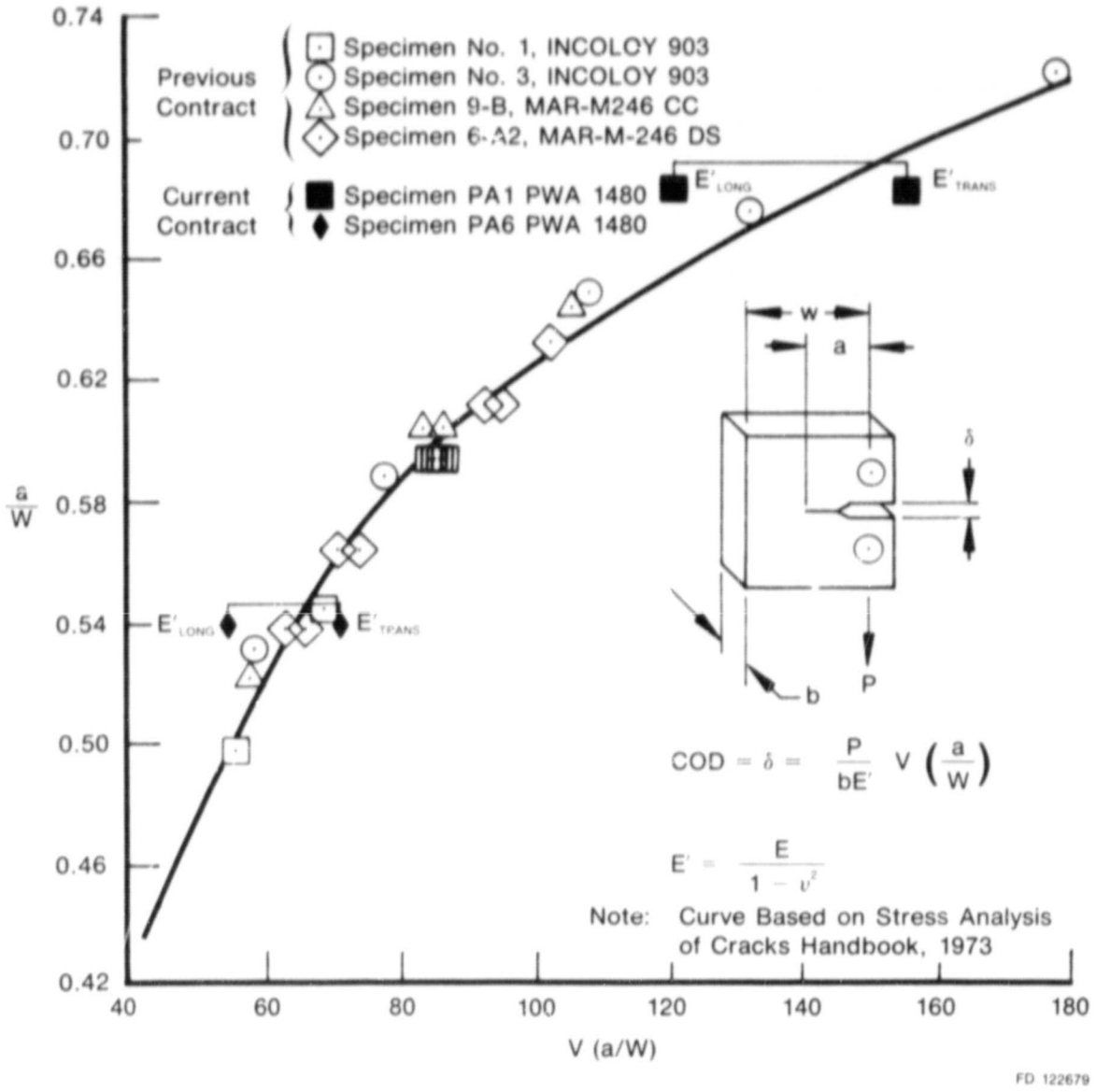

Figure 87. Crack Length vs Crack Opening Displacement (COD) Compliance Calibration Results for Incoloy 903, MAR-M-246 + Hf, and PWA 1480

Stress intensity values (K) were calculated from the equation:

$$K = \frac{P}{BW^{0.5}} \left[29.6 \left(\frac{a}{W} \right)^{0.5} - 185.5 \left(\frac{a}{W} \right)^{1.5} + 655.7 \left(\frac{a}{W} \right)^{2.5} - 10170.0 \left(\frac{a}{W} \right)^{3.5} + 638.9 \left(\frac{a}{W} \right)^{4.5} \right]$$

where

K = stress intensity (psi-in.$^{0.5}$)
P = applied load (pounds)
B = specimen thickness (inches)
W = specimen width (inches)
a = crack length (inches)

and cyclic stress intensity (ΔK) was calculated by the equation:

$$\Delta K = K_{max} - K_{min} = (1-R)\ K_{max} = 0.9K_{max}$$

where

ΔK = cyclic stress intensity (psi-in.$^{0.5}$)
K_{max} = stress intensity at max cyclic load
K_{min} = stress intensity at min cyclic load

with

R = 0.1 (R = minimum load/maximum load)

Test specimens were axial tension-tension fatigue precracked at 25°C (77°F) in air using a fatigue machine operating at a frequency of 30 Hz (1800 cpm) and R ratio = 0.1. Maximum precrack loads were approximately 80% of the maximum loads used during crack growth testing. Electric discharge machining was used to provide starter crack slits in SC MAR-M-246+Hf specimens due to difficulty in starting and propagating a crack transversly in this material (figure 88).

High-pressure environmental tests were conducted on a closed-loop, hydraulically actuated test machine located in an isolated test cell (figure 89). The pressure vessel with test frame and hydraulic actuator system are shown in figure 90. The pressure vessel was similar to the LCF vessel, and is shown in figures 91 and 92.

The test machine compensates for internal gas pressure loading of the test specimen through a pressure transducer feedback signal to the servosystem. The signal is used to control a steady force to the load linkage that is equal and opposite to the internal hydrogen pressure load against the load rod.

For elevated temperature testing, a two-zone resistance furnace with separate control systems for each zone was used. The furnace surrounds the specimen and fits within the frame of the pressure vessel (figure 92). Thermocouples attached to the specimen gage section were used to monitor and control temperature during test.

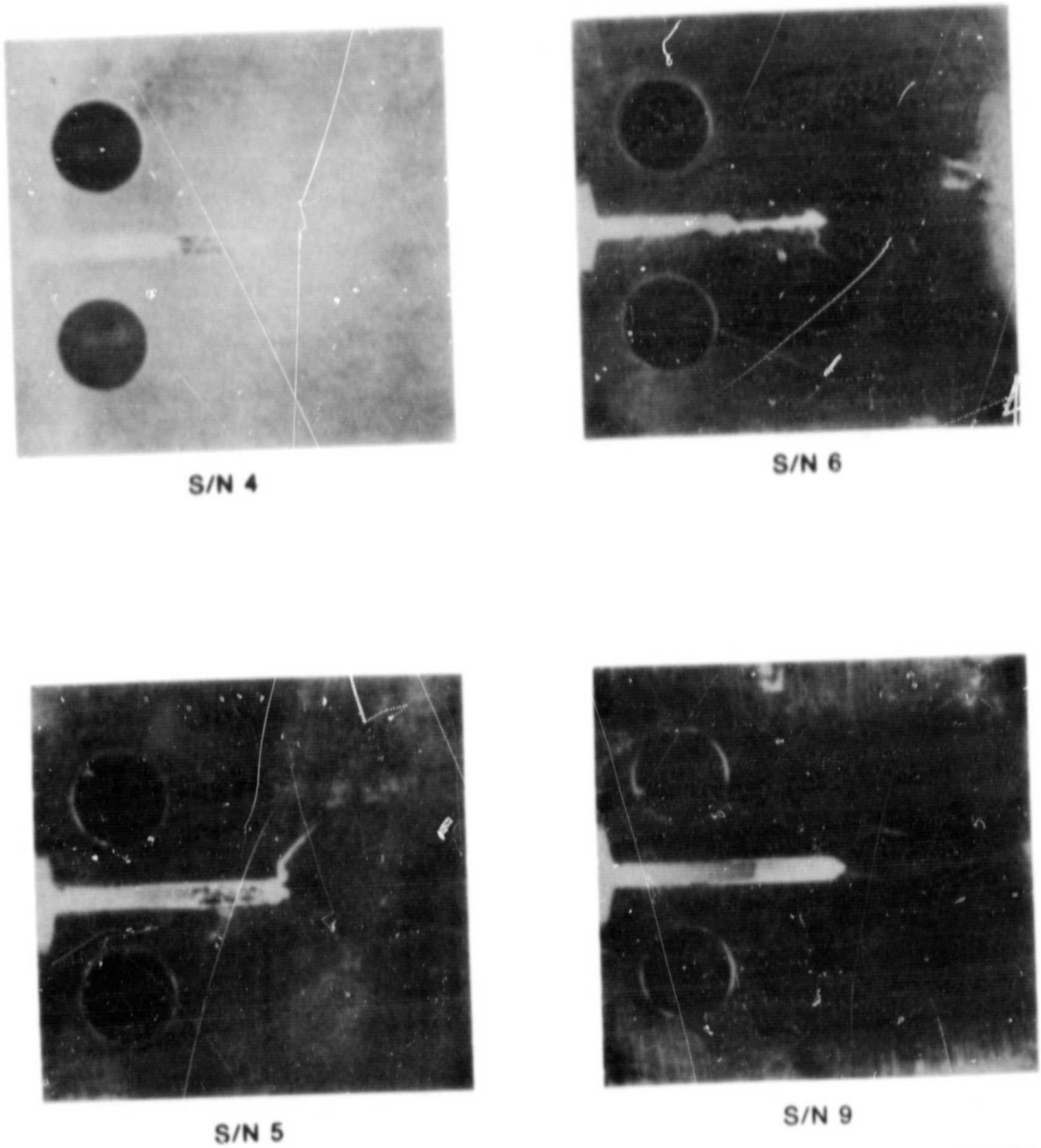

Figure 88. Single Crystal MAR-M-246 + Hf Crack Growth Specimens With Poor Starter Cracks

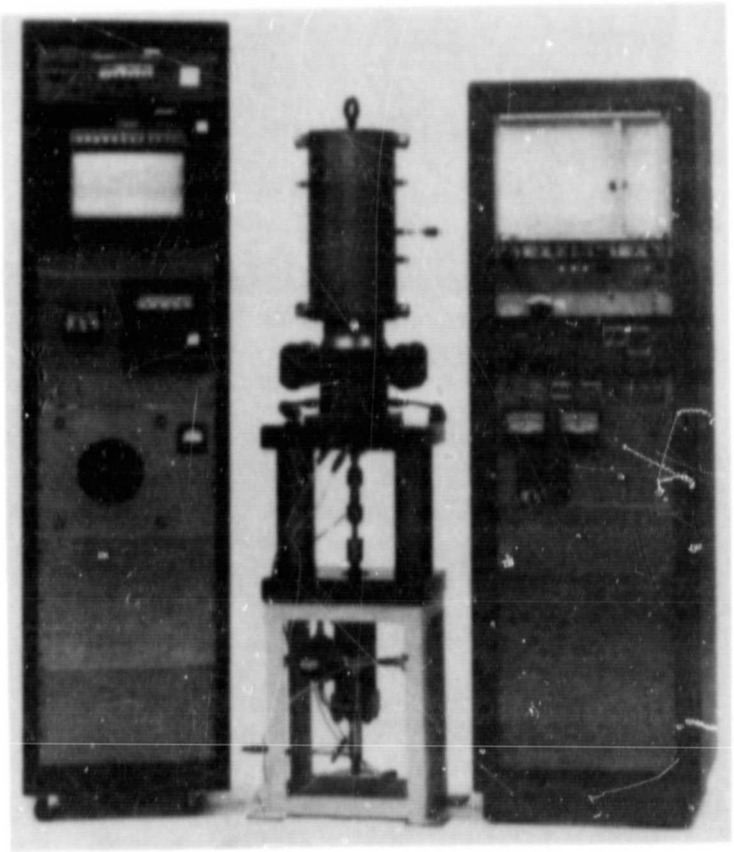

Figure 89. High-Pressure Environment Crack Growth Rate Testing Machine and Data Acquisition Equipment

The hydrogen and water vapor environment was obtained utilizing triple-distilled water in a pure hydrogen-containing retort system so the water was vaporized by furnace heat. The retort system, containing the test speciment and water, fits within the furnace and consists of a piston/tube type arrangement (figures 93 and 94). The piston, attached to the lower pull rod, incorporates an O-ring which provides a seal against the inner surface of a tube (cylinder), which is attached to the upper pull rod. During testing the tube remains basically stationary relative to the piston. The base of the piston incorporates an O-ring hole for passage of the extensometer tube, and check valves which allow hydrogen to enter the retort and prevent water from escaping. Pressure inside the retort and vessel was equalized; therefore, the retort contained the hydrogen-water vapor environment and was not subjected to any stresses due to differential (internal to external) pressure. Thermocouples also exit the retort via connectors installed in the base of the piston. They monitor and control specimen and water vapor temperature. By controlling the lower zone of the furnace, water was vaporized at a temperature which assured 50% by weight water vapor.

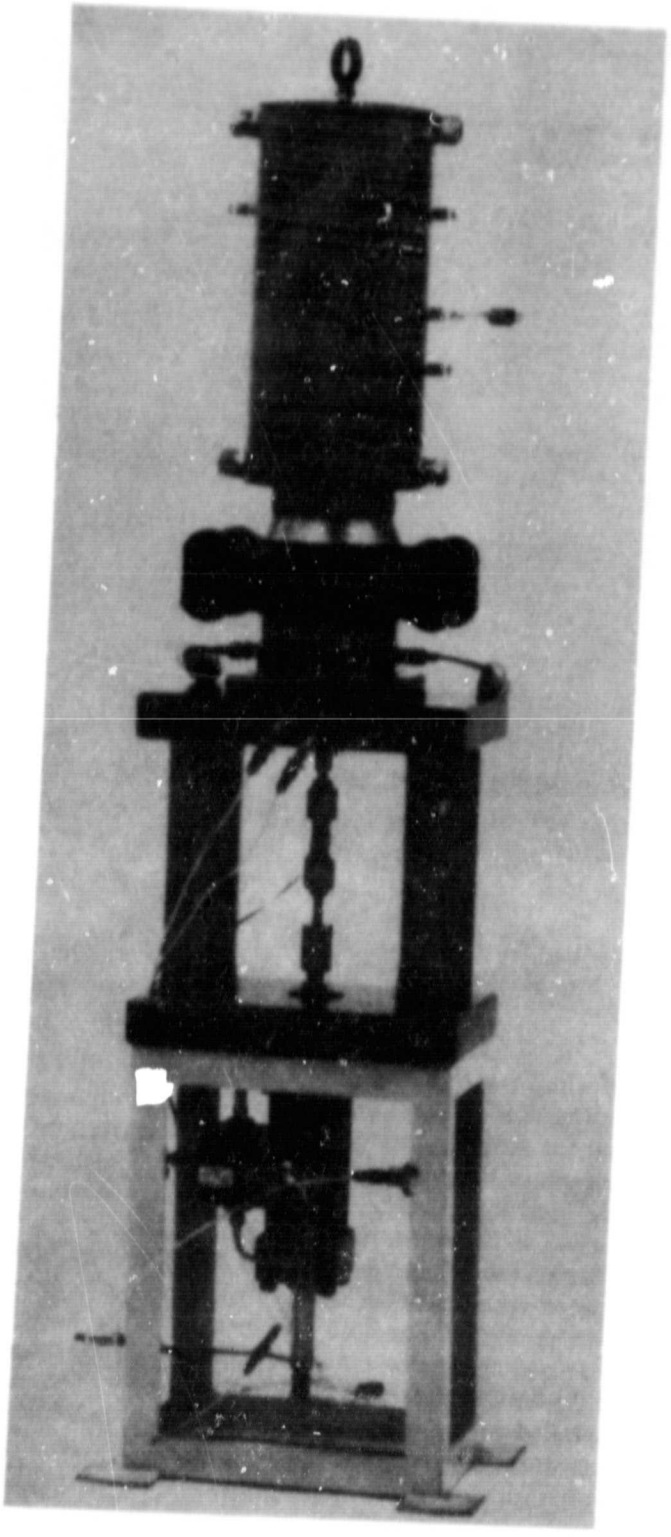

Figure 90. Crack Growth Rate Test Frame and Pressure Vessel

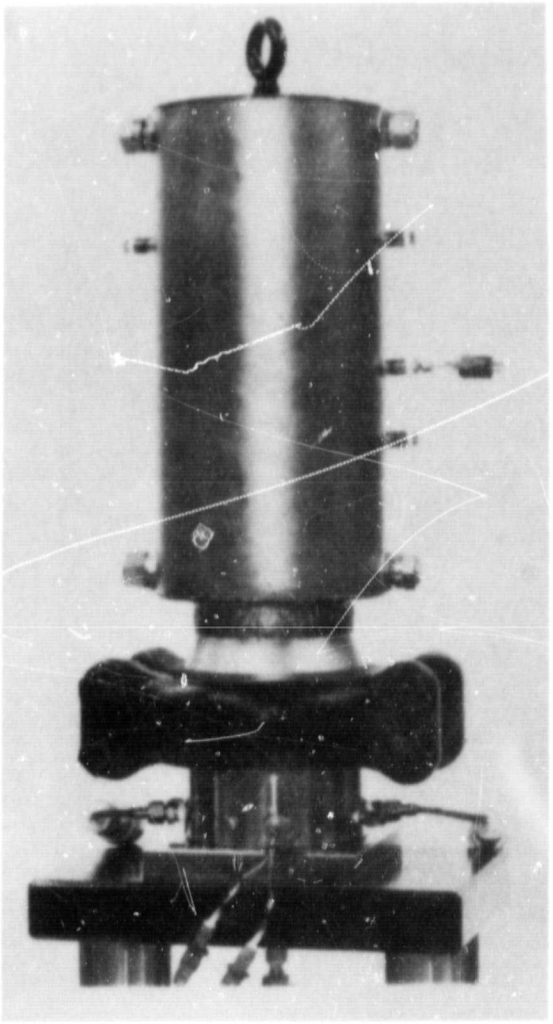

Figure 91. Crack Growth Rate Pressure Vessel, Closed

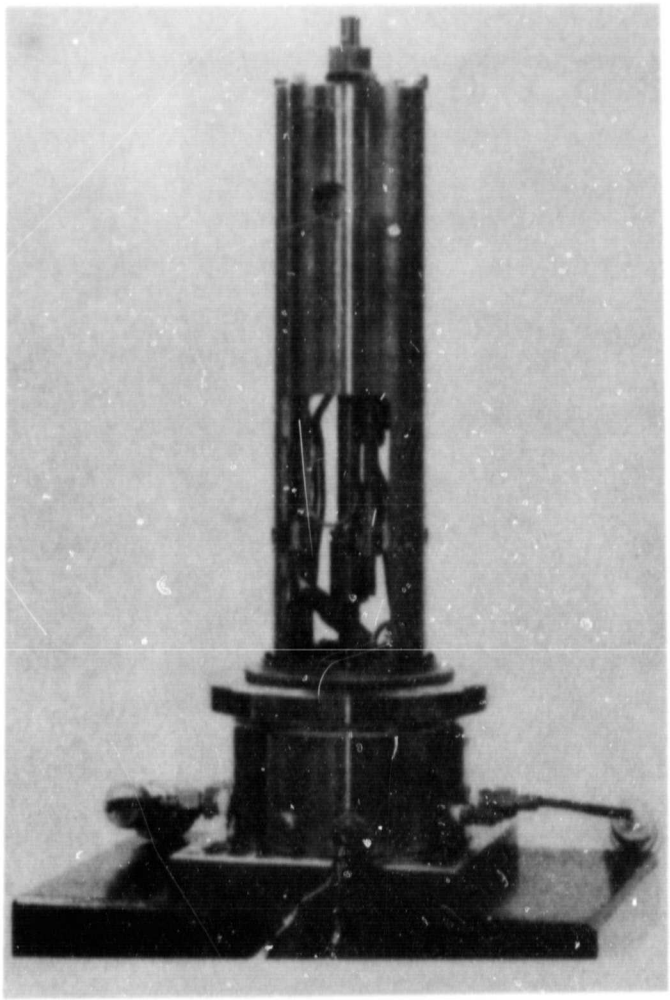

Figure 92. Crack Growth Rate Pressure Vessel, Opened

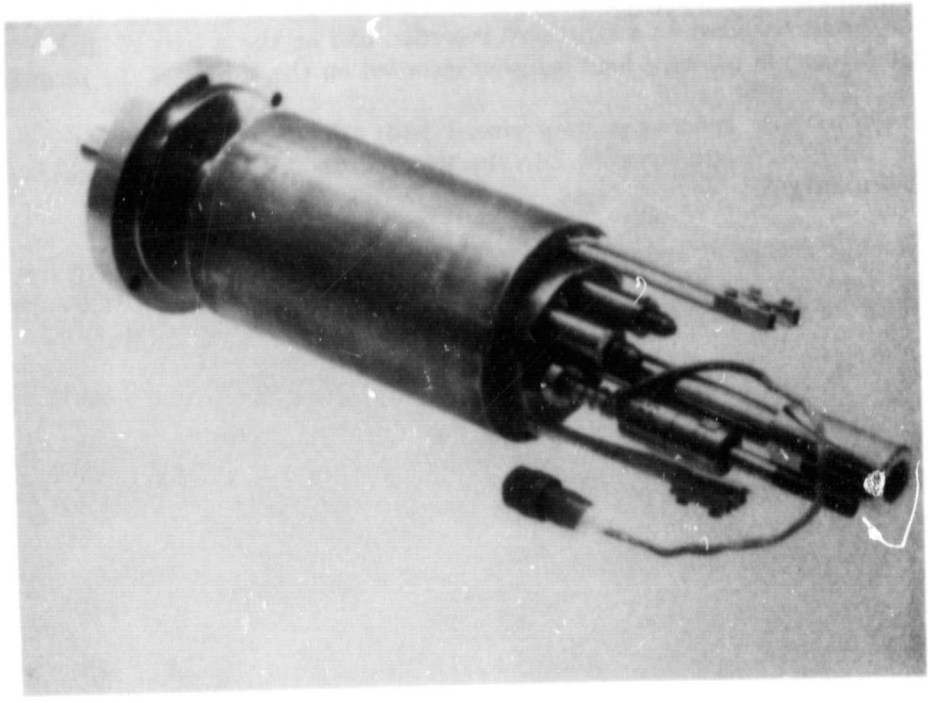

Figure 93. Crack Growth Rate Retort System With Furnace in Place

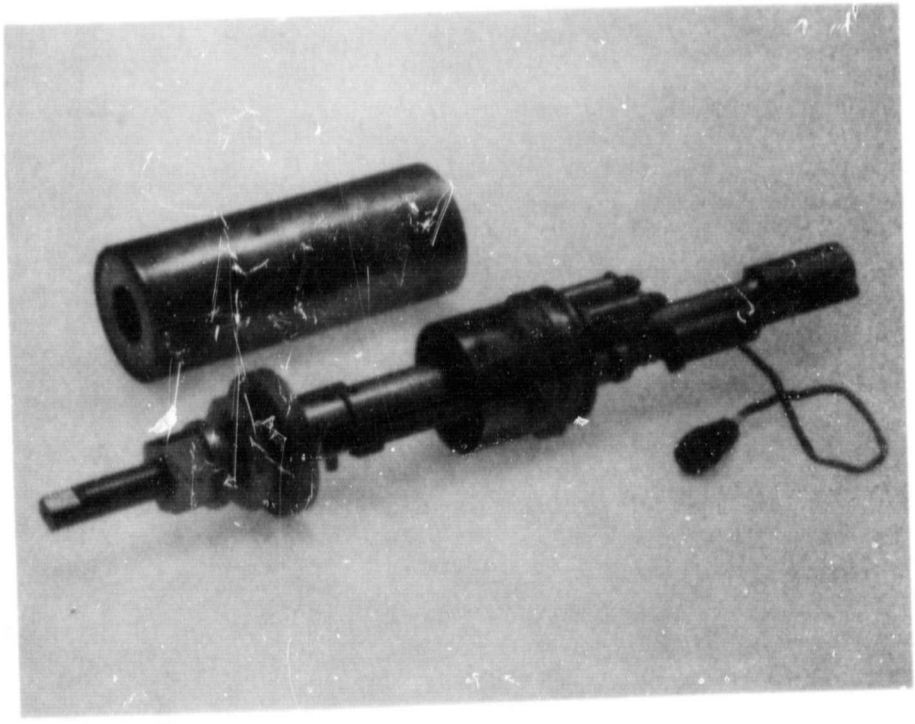

Figure 94. Crack Growth Rate Retort System and Extensometry

Specimen COD was measured and recorded throughout the test duration using a Linear Variable Displacement Transducer (LVDT) type extensometer system (figure 94). COD was monitored and recorded on a stripchart recorder, and on the X axis of an X-Y recorder. The load sensed by the external load cell was recorded on the Y axis of the recorder.

Prior to test, specimens were rinsed with trichlorethylene, wiped dry, rinsed with acetone, wiped dry, and inserted into the test fixture. All handling of specimens was done with clean gloves.

Periodic checks of hydrogen test environments revealed oxygen levels less than 1 ppm. The test and gas handling procedures used for Crack Growth rate testing were similar to those used for the tensile tests performed under this contract (Section IV-C).